A STUDY OF THE EFFECT OF SOME NON-LINEAR STABILITY DERIVATIVES ON THE LATERAL MOTIONS OF AIRCRAFT.

BY

Willard A. Pollard

A STUDY OF THE EFFECT OF SOME NON-LINEAR STABILITY DERIVATIVES ON THE LATERAL MOTIONS OF AIRCRAFT

A Thesis

Submitted to the Graduate Faculty of the

University of Minnesota

by

Willard A. Pollard

LT. U.S.N.

In Partial Fulfillment of the Requirements

for the Degree of

Master of Science in Aeronautical Engineering

August 1951

ACKNOWLEDGEMENTS

The author wishes to acknowledge the guidance in the aerodynamic aspects of the thesis given by Professor A. L. Cronk of the University of Minnesota, and the instruction in the use of the REAC given by H. E. Miller of the University of Minnesota.

TABLE OF CONTENTS

SUMMARY

This thesis is intended as a further investigation along the lines suggested by NACA TN 2233.

The effects of dead spot non-linearities in certain moment derivatives on the lateral motion responses of two airplanes are investigated. Dead spot non-linearities in moment derivatives occurring in the lateral equations are defined as non-linearities in which the moment derivatives in question are functions of sideslip angle, being zero over a certain range of sideslip angle on each side of zero sideslip, and outside this range of sideslip angle, known as the dead spot, having the constant value normally used in the solution of the lateral stability equations as based on the theory of small oscillations. Certain evidence has come to light in recent years which strongly suggests the possibility of the existence of such non-linearities.

The two airplanes whose lateral motions were investigated in this thesis were designated as Airplanes I and II, respectively. Airplane I is a conventional, slow speed, twin engine transport type aircraft. Airplane II is the high speed fighter type aircraft whose lateral motions were investigated in NACA TN 2233. Airplane I has very strong lateral dynamic

stability. Airplane II has marginal lateral dynamic stability.

The moment derivatives in which dead spot non-linearities were assumed in this investigation were: directional stability, damping in yaw, dihedral effect, and rolling moment due to yawing velocity derivatives. NACA TN 2233 considered the effects on the lateral motions of Airplane II only of dead spot non-linearities in only the first two of the preceding four lateral moment derivatives, when present simultaneously. This thesis investigates the effects of the four dead spot non-linearities listed above taken singly and in various combinations for both Airplanes I and II, respectively.

The dead spot range for all the non-linearities considered in this thesis was taken as extending from minus two degrees to plus two degrees of sideslip angle.

The lateral motions investigated were in response to disturbances in sideslip angle of five degrees and one degree, respectively.

The standard NACA lateral stability equations with controls fixed were used. These equations were solved for the lateral responses on the Reeves Electronic Analogue Computer, (REAC) at the University of Minnesota. Several cases were also

solved for response in sideslip angle by hand, using the method of the Laplace transform, as checks on the accuracy of the REAC.

It was found that the effects of the various dead spot non-linearities on the lateral responses showed, in general, the same trends for each of the two different aircraft. However, the effects on Airplane II were much more pronounced than the effects on Airplane I.

This thesis was completed in partial fulfillment of the requirements for a Master's Degree at the University of Minnesota.

INTRODUCTION

Up until the time of World War II, the longitudinal and lateral stability equations based strictly on the theory of small oscillations were considered satisfactory for practically all investigations and estimations of aircraft dynamic stability. Moreover, up until that time, a mere estimation of the general nature of an airplane's dynamic stability characteristics was considered to be all that was necessary for most design purposes, since it was only desired to insure that the airplane have satisfactory dynamic stability characteristics and it was not considered necessary to accurately predict the time histories of the motions in response to a disturbance or to control deflections. In order to estimate the longitudinal and lateral stability characteristics under these requirements, it was merely necessary to evaluate the longitudinal and lateral characteristic equations which were based, respectively, on the longitudinal and lateral stability equations, and then to find the roots of these equations. An examination of the coefficients of the longitudinal and lateral characteristic equations indicates whether or not the airplane has longitudinal and lateral dynamic stability, respectively. From the roots of the characteristic equations, the general nature of the modes of motion, longitudinal and lateral, respectively, can be estimated. This procedure

is simple and straightforward, and the required computations can be quickly made. The information on the stability characteristics thus obtained was practically always sufficient for design purposes. The background and further elaborations of these procedures is given in considerable detail in references (1) through (5).

Recent years have seen the advent of pilotless aircraft, guided missiles, aircraft rockets, and a greatly increased use of automatic pilot control of increasing complexity. All of these items frequently require that far more be known for design purposes concerning the dynamic characteristics of the airplane or missile than the mere fact that it is expected to be dynamically stable and a general knowledge of the nature of its predicted modes of motion in response to a small disturbance. In fact it is now considered necessary in many cases to accurately predict the time history of the motions in response to various control deflections and in response to various disturbances. The standard stability equations used for this purpose are generally the standard longitudinal and lateral stability equations as presented by the National Advisory Committee for Aeronautics, (NACA). These equations are essentially the dynamic stability equations which have been in use for the last forty years, reference (1). However, the equations have been modified to some

slight extent in recent years, and as previously stated, they were not generally used until recent years for the purpose of obtaining accurate time histories of the various aircraft motions.

Any method of hand solution of the stability equations for the time histories of motion responses will involve much computational labor and will be very tedious. However, the Laplace transform method of solution is perhaps the most readily applied and straightforward method of solution, especially since this method inherently permits the application of initial conditions as disturbances, a straightforward method of simulating actual disturbances on the airplane. Reference (6) describes the general application of the Laplace transform method of solution for time histories of the various motion responses. Reference (7) is a text giving the general background for the general application of the Laplace transform methods.

Due to considerable, tedious computational labor involved in solving the stability equations for time histories of motion responses by hand computation, it is far preferable to use an automatic computer for the solutions. Automatic digital computers give solutions of motion responses with a very high degree of accuracy and a fair degree of speed. Automatic elec-

tronic analogue computers do not give the degree of accuracy of automatic digital computers, but the analogue computers are much faster, solving for, and simultaneously plotting, the time histories of all motion responses in a matter of seconds, with satisfactory accuracy.

The longitudinal and lateral stability equations are based on the theory of small oscillations, which means that all disturbances and the amplitudes of all responses are fairly small, thus permitting the assumption that all force and moment derivatives are constants. The stability equations, including this assumption, give quite accurate time histories of motion responses for motion response amplitudes up to ten or fifteen degrees as is evidence by the investigations of reference (8). In this reference are reported the results of calculated motion responses for a swept wing fighter using force and moment derivatives constant with amplitude, as determined in the wind tunnel, and of comparing these calculated responses with responses for the actual full scale airplane in flight and subjected to the same disturbances. The agreement between the calculated and flight responses was in general very good, furnishing excellent justification for the use of the theory of small oscillations and force and moment derivatives constant with amplitude. However, in several cases reported in this reference fairly

large disturbances of the controls were used causing as a result motion responses which were large enough to fall outside the range of the theory of small oscillations. In these cases, there was, of course, a decrease in the accuracy of the calculated responses using derivatives constant with amplitude. However, the accuracy of the calculated responses for these cases was improved by assuming certain moment derivatives to be step function disturbances of angle of attack for longitudinal motions and angle of sideslip for lateral motions. These step functions were taken in such manner as to approximate the wind tunnel data over a wider range of angle of attack and angle of sideslip, respectively, than was the case when the derivatives were assumed constant with amplitude. Thus, reference (8) gives good justification for assuming longitudinal moment derivatives to be functions of angle of attack and lateral moment derivatives to be functions of angle of sideslip when motion responses are expected to exceed the range of small oscillations.

Reference (9) is an analytical lateral stability investigation which also assumes that certain moment derivatives are functions of angle of sideslip rather than being constant with angle of sideslip response amplitude. However, in this case the variation in the magnitude of the moment derivatives, as compared with the constant value normally assumed, is as-

sumed to occur near the value of zero sideslip rather than at the larger amplitudes of angle of sideslip as was the case in reference (8). Specifically, reference (9) assumes that the directional stability, C_{n_β}, and damping in yaw, C_{n_r}, derivatives are functions of the angle of sideslip for a high speed fighter type airplane. The nature of these variations of the above two moment derivatives with sideslip angle is shown in Figure 1. It will be noted that within a range of sideslip angles from minus two degrees to plus two degrees, the moment derivatives are zero, while outside this range the moment derivatives have the value which is normally considered constant with amplitude of sideslip angle. The range of sideslip from minus two degrees to plus two degrees is called the dead spot for the directional stability and damping in yaw derivatives. This type of variation of moment derivative with sideslip angle will be called a dead spot non-linearity, since it destroys the overall linear variation of $C_{n_\beta}\beta$ with β and of $C_{n_r}r$ with r. Note that in Figure 1, and henceforth at all times in this thesis, the dimensionless coefficient form for forces and moments is not used even though it is used in reference (9) and at practically all times by the NACA. Instead forces and moments in units of accelerations are used, since this makes the stability equations more straightforward and simpler to apply, especially in the case of

hand solutions. The list of symbols in Appendix A contains symbols and terminology used for force and moment derivatives when forces and moments are in units of acceleration.

The dead spots assumed in directional stability and damping in yaw derivatives in reference (9) are quite arbitrary. However, it is believed likely that under certain conditions such dead spots do exist, especially in high speed fighter type aircraft of the type analyzed in reference (9). These dead spots could be caused by poor fairing of the tail surfaces into the fuselage, by wing wake for low-set tail surfaces, or by anything which might interfere with flow over the tail surfaces in such a manner as to cause the dead spot effect assumed for these moment derivatives. Moreover, if these dead spot non-linearities do occur, they will quite possibly not be measured or indicated by wind tunnel data, due to the relatively small amplitude of the dead spot or due to the factors interfering with flow over the tail surfaces, such as poor fairing or filleting, not existing on the wind tunnel model at all. Therefore, it is of interest to determine the effect of such dead spot non-linearities on the lateral motions of aircraft in response to disturbances in an effort to account for unexplained lateral motion responses noted in actual aircraft in flight or in an effort to catalog the effect of various dead spot non-linearities on lateral motion responses for various types of aircraft in

order that the effect of such dead spot non-linearities may readily be predicted in future design work.

Reference (9) constitutes a preliminary analysis of the effects of dead spot non-linearities in moment derivatives on the lateral motions of aircraft. This thesis constitutes a further analysis of the effects of dead spot non-linearities on the lateral motions of aircraft.

Reference (9) considers the simultaneous effect of dead spot non-linearities in directional stability and damping in yaw derivatives on the lateral motions of a particular high speed fighter type airplane under certain flight conditions. This thesis considers the effect of the above two dead spot non-linearities plus the effect of a similar dead spot non-linearity in the dihedral effect derivative, l_β', on the airplane of reference (9) for a straight and level flight condition. The effects of these three dead spot non-linearities are considered individually and in various combinations with one another. Moreover, the effects on the lateral motion are considered for a two engine transport type aircraft in a straight and level flight condition at low speed. For the second airplane, the effects of the three preceding dead spot non-linearities are considered plus the effect of a similar dead spot in the rolling moment due

to yawing velocity derivative, l_r'. The effects of these four dead spot non-linearities on the lateral motions of the second airplane are considered individually and in various combinations. It is to be noted that l_r' is zero for the airplane of reference (9).

The dead spot non-linearities in l_β' and l_r' are arbitrarily assumed but they could possibly occur, and hence their effects are of interest. Anything which drastically interferes with the flow over the vertical surfaces would cause a tendency for dead spot non-linearities to occur in l_β' and l_r'.

As was the case in reference (9), the amplitude of all dead spots was arbitrarily assumed to extend from minus two degrees to plus two degrees of sideslip. Although this dead spot amplitude is arbitrary it is a value which could quite conceivably occur in the actual physical case, and moreover, it is a convenient value to use in calculations.

The disturbance which was used to cause lateral motion responses was in all cases a disturbance in sideslip alone. This procedure also corresponds to that of reference (9). For each case the effects of the dead spot non-linearities on the lateral motions was investigated for disturbances in sideslip of both five degrees and one degree, respectively. These dis-

turbances were chosen because they insured that the effects of the dead spot non-linearities on the lateral motions would be investigated for initial sideslip amplitudes both outside of and inside of the dead spot, respectively. Moreover, the lateral motions in response to sideslip disturbances furnish a good indication of the nature of the lateral motion responses of the airplane to small disturbances in general. A disturbance in sideslip alone is quite feasible from the physical point of view. If an airplane in straight and level flight is hit by a strong, sharp-edged gust with the result that it is practically instantaneously yawed through an angle of five degrees to the left of its flight path, the airplane has then experienced a disturbance in sideslip alone of plus five degrees. It should be noted that with the preceding definition of the disturbance, the airplane would have to be yawed through a yaw angle in the horizontal plane of plus five degrees to return the longitudinal axis to the direction of theflight path.

This thesis is a theoretical investigation, as was reference (9), and there are no results of actual flight cases with which to compare the results of the investigations comprising this thesis, although it was stated in a general way in reference (9) that undamped snaking motions had been noted in flight for high speed aircraft in response to small amplitude

sideslip disturbances and that this snaking motion might be attributable to dead spot non-linearities in n_β and n_r. However, in the absence of any detailed flight data on the lateral responses of airplanes having dead spot non-linearities, the results of the investigations of this thesis are intended to serve as a cataloging of the effects of the various dead spot non-linearities on the lateral motion responses of two different types of airplanes in straight and level flight.

The standard NACA lateral stability equations are used in computing the lateral motion responses to the sideslip disturbances. As previously stated, the accuracy of these equations in computing the time histories of lateral motions of small amplitude has been shown by reference (8) to be quite good. It should be noted, however, that the lateral stability equations as applied in this thesis are for "controls fixed".

The Reeves Electronic Analogue Computer (REAC), at the University of Minnesota was used to compute the lateral motion responses to the sideslip disturbances for the cases under investigation, since the solution for the time histories of the responses for all these cases would require a very prohibitively large amount of time.

DESCRIPTION OF AIRPLANES INVESTIGATED

The airplanes whose lateral motions were investigated in this thesis were designated as Airplanes I and II, respectively. Their characteristics are described below.

Airplane I is a conventional, slow speed twin engine transport. Its force and moment derivatives are given directly in units of acceleration and are tabulated in Table I. The equilibrium flight condition of Airplane I throughout these investigations is straight and level flight at an altitude of 7500 feet and a true airspeed of 242 feet per second, which is 165 miles per hour. It was expected that this airplane would have a very high degree of lateral dynamic stability. This expectation was borne out by the results of these investigations.

Airplane II is a high speed fighter type airplane which is used in the investigations of references (9). he force and moment derivatives of this airplane are given in reference (9) in the form of non-dimensional coefficients. These derivatives were converted to units of acceleration in Appendix B and are tabulated in Table II. The equilibrium flight condition of Airplane II throughout these investigations is straight and level flight at an altitude of 30,000 feet and a true airspeed of 753

feet per second, which is 513 miles per hour. It is evident from reference (9) that this airplane, although laterally dynamically stable, this airplane is moderately close to the lateral oscillatory instability boundary. This was borne from the results of the investigations of this thesis, which, in fact, showed that the lateral dynamic stability of Airplane II might be termed marginal when there are no non-linearities in the moment derivatives. It should be noted that the flight condition of Airplanes II in these investigations corresponded to the case where η was equal to zero degrees in reference (9). Moreover, the type of dead spot non-linearities assumed in the various moment derivatives corresponded to Case 2 of reference (9).

GENERAL PROCEDURE

Using the method of the Laplace transform as outlined by references (6), (7), and (9), the lateral response in sideslip was computed by hand for a disturbance in sideslip of plus five degrees for both Airplanes I and II, respectively, with no dead spot non-linearities in force or moment derivatives and for Airplane I with the dead spot non-linearity assumed in the dihedral effect derivative. These solutions were used primarily as checks on the accuracy of the REAC.

Then using the REAC, the lateral responses for sideslip and the lateral motions and rates of motion in response to disturbances in sideslip of five degrees and one degree, respectively, were determined for the various assumed dead spot non-linearities in moment derivatives, taken individually and in various combinations. These REAC solutions for the various lateral responses were then used to analyze the effects of the various dead spot non-linearities on the lateral responses as compared to the lateral responses for Airplanes I and II, respectively, with no dead spot non-linearities.

HAND SOLUTION OF THE LATERAL STABILITY EQUATIONS

In Appendix C are presented the stability equations and the Laplace transform of the lateral stability equations for initial condition disturbances. Equation C-2 of Appendix C are the standard NACA lateral stability equations in which forces and moments are in non-dimensional coefficient form and time appears as a non-dimensional parameter. These are the equations as used in reference (9). Equations C-2 are the same standard lateral stability equations but in which forces and moments appear in units of acceleration and time appears directly in seconds. These are the equations as used in this thesis, both for the hand solutions and for the REAC solutions.

Appendix C also contains the expansion of the determinants incident to the Laplace transform hand solution of equations C-2. These determinants were expanded in general form for initial condition types of disturbances. This corresponds to what was presented in reference (9) except that this reference presents only the expansion of the denominator determinant and the numerator determinant for angle of sideslip response, whereas Appendix C of this thesis presents in addition to the preceding expansions, the expansions of the numerator determinants for angle of roll and angle of yaw responses, respectively.

It will be noted that equations C-2 contain constant terms, y_c, n_c, and l_c', which are required for dead spot non-linearities in y_β, n_β, and l'_β, of the type illustrated in Figure 1, for dead spot non-linearities in n_β, and l'_β. In reference (9) only the constant C_{n_c}, corresponding to n_c, is included. It will be noted that this constant appears in different terms in the expansion of the numerator determinant for angle of sideslip in Appendix C of this thesis and in the expansion of reference (9). The author of reference (9) has acknowledged that reference (9) is in error in this respect and that Appendix C of this thesis is correct in this respect.

Using the equations and expansions of Appendix C the sideslip angle response was computed by hand for a disturbance in angle of sideslip of plus five degrees for Airplane I with no dead spot non-linearies and with the assumed dead spot in l_β' respectively. Sample calculations for these solutions are presented in Appendix D of this thesis. The responses in angle of sideslip for these two cases are plotted in Figure 2.

The response in angle of sideslip to a five degree disturbance in sideslip for Airplane II with no dead spot non-linearities was also computed by hand using the Laplace transform method outlined in Appendix C. This response solution is

plotted in Figure 3. It will be noted that this solution differs somewhat from the corresponding solution in reference (9), being very similar in general nature but lying closer to the solution for η equal to minus two degrees than to the solution for η equal to zero degrees, which was the actual case in this solution. It is believed, but not verified, that the sideslip response solution appearing in Figure 3 of this thesis is correct, rather than the sideslip response solution appearing in reference (9). Therefore, henceforth in this thesis the solution appearing in Figure 3 will be assumed to be correct.

REAC SOLUTION OF THE LATERAL STABILITY EQUATIONS

The Reeves Electronic Analogue Computer can solve the lateral stability equations directly and in very short time. Equations C-2 were used for the REAC solutions. Appendix E of this thesis presents equations C-2, the lateral stability equations and the various multiplying potentiometer settings used for Airplanes I and II, respectively.

A tabulation of the various REAC solutions which were made and their designations for purposes of this thesis is given in Table III.

It will be noted that in the case of each airplane, respectively, solutions were made for the airplanes with no dead spot non-linearities and a disturbance in sideslip of plus five degrees and for the airplanes with the various assumed dead spot non-linearities taken individually and in various combinations, as indicated by Table III, for disturbances in sideslip of plus five degrees and plus one degree, respectively. It will also be noted that by an integration process, indicated in Appendix E, angle of sideslip was made to appear as the abcissa in REAC solutions I-1 and II-1 rather than time, which is the usual abcissa. Thus, in these two solutions the various dead spot non-linearities for Airplanes I and II, respectively,

are presented by the REAC as functions of angle of sideslip in the manner in which the REAC applies them in the solution of the lateral stability equations. These two REAC solutions showed that as applied by the REAC, the dead spot non-linearities did not have precisely a dead spot range extending between plus and minus two degrees of sideslip angle and that the discontinuities were slightly rounded. However, these two solutions showed that the dead spot non-linearities as applied by the REAC were very nearly exactly as desired, comparing very favorably with desired dead spot non-linearities as illustrated by Figure 1.

All other REAC solutions were time histories of the various lateral responses for the various cases as tabulated in Table III. For each REAC solution the following lateral responses were recorded: angle of sideslip, angle of roll, angle of yaw, rate of roll, rate of yaw, and any dead spot non-linearities that were assumed for the case in question multiplied by the response with which they were associated in the lateral stability equations. This required that each REAC solution be recorded twice since the recorder which was used could record only four responses simultaneously. In order to insure that the two recordings of each solution were identical, angle of

sideslip response was recorded both times for each solution. It was found that for nearly all solutions the two recordings of angle of sideslip response matched one another very closely. The most marked exceptions to the above occurred in REAC solutions II-6 and II-9. In the case of REAC solutions II-6a and II-6b the two recordings of sideslip response matched exactly in period but showed a variation of about five per cent in their respective peak amplitudes. In the case of REAC solutions II-9a and II-9b, the two recordings of sideslip response matched very closely in amplitude but showed a variation of about five per cent in period. Since the general nature of sideslip response was the same in both recordings for both cases, the fairly small variations in amplitude and period, respectively, were not considered great enough to destroy the identity of the solution between the two recordings in either case. In nearly all other solutions variations between the two recordings of sideslip angle response were negligible.

The recording for each solution of the time history of the assumed dead spot non-linearities showed that for all cases the dead spot range of from plus to minus two degrees of sideslip angle was quite well maintained. Discontinuities for the non-linearities in n_β and l_β' were slightly rounded but were sufficiently sharp to represent the desired dead spot non-

linearities very closely. Discontinuities for the non-linearities in n_r and l_r' were quite sharp and thus represented the desired dead spot non-linearities very closely.

REAC solutions I-2 and II-2 represent the solutions for the lateral responses for Airplanes I and II respectively with no dead spot non-linearities and a sideslip disturbance of five degrees. These solutions were compared on the basis of peak amplitudes and periods with the hand solutions for sideslip angle response for the same cases, which are plotted in Figures 2 and 3, respectively, with the hand solutions being considered, of course, the more accurate. The results of these comparisons are tabulated in Table IV. Also tabulated in Table IV is the comparison of REAC solution I-3 with the corresponding hand solution for assumed dead spot non-linearity in l_β' for Airplane I with a sideslip disturbance of five degrees. It is evident that REAC solutions I-2 and I-3 compare very favorably with the corresponding hand solutions which are plotted in Figure 2. REAC solution II-2 does not compare as favorably with the corresponding hand solution for Airplane II, which is plotted in Figure 3. However, the main variation lies in a small consistent variation of peak amplitudes, and this variation is not considered sufficient to destroy the identity between the hand solution for sideslip response for Airplane II with no non-linearities and

the corresponding REAC solution. On the basis of the above comparisons the REAC is assumed to accurately solve the lateral equations of motion for lateral responses in the cases covered by this thesis.

Various characteristic values determined from the REAC solutions for the various lateral responses to a five degree sideslip response are tabulated in Tables V and VI for Airplanes I and II, respectively. Certain of the values from Tables V and VI are tabulated in Tables VII and VIII, respectively, as percentages of the corresponding values for the respective airplane with no dead spot non-linearities.

A number of REAC solutions were included in this thesis. The REAC solutions which were included and their figure numbers are indicated in Table III.

RESULTS AND DISCUSSION

The mathematical and physical background of these investigations have previously been covered elsewhere in this thesis. Moreover, the accuracy of the REAC computer, as checked by hand solutions for several cases has also been covered and found to be reasonably good. Therefore, it will now be assumed that the REAC solutions for the lateral responses are correct for each of the various cases investigated. This section of the thesis will be devoted to the analysis and discussion of the effects on the lateral aircraft responses of the various dead spot non-linearities as presented by the REAC solutions, that being the major purpose of the investigations comprising this thesis.

The REAC solutions corresponding to the various dead spot non-linearities are listed in Table III. Various quantities relating to the nature of the lateral responses for a sideslip angle disturbance of five degrees were determined from these solutions and tabulated in Tables V and VI for Airplanes I and II, respectively. Using the values in Tables V and VI, various quantities relating to the nature of the lateral responses were expressed as percentages of their values for the case with no non-linearities. These percentages were tabulated in Tables VII and VIII for Airplanes I and II, respectively.

Thus the various REAC solutions and Tables V, VI, VII, and VIII, were used as the basis for the following discussions. In the following discussions, the term "lateral responses" will, as before, indicate the aggregate of the time histories of angle of sideslip, angle of roll, angle of yaw, rate of roll, and rate of yaw, responses to the sideslip disturbances. It should also be noted that, except where noted otherwise, all discussions pertain to the first eighteen seconds following the disturbance.

Lateral responses for Airplanes I and II with no dead spot non-linearities:

Airplane I with no dead spot non-linearities in moment derivatives has a very stable response in all lateral responses to a five degree disturbance in sideslip angle. In less than 3.5 seconds and 1.0 cycle from the time of the first oscillation, each of the lateral responses is damped to one half amplitude. In less than 15.0 seconds and 4.0 cycles, each of the lateral responses is damped to 0.01 amplitude. Each of the lateral responses, except yaw angle, appear essentially as pure oscillations with negligible pure divergence from original trim conditions. Angle of roll, however, does show a slight spiral divergence after seven seconds, but at fifteen seconds from the original disturbance this pure divergence has increased only to

about 0.02 degree, a value which would not be noticed by the pilot.

The angle of yaw response shows the airplane's good directional stability, since within 2.5 seconds the angle of yaw has shown a pure divergence to the right of five degrees and has commenced a heavily damped oscillation about the value of five degrees, with an original amplitude of 2.5 degrees. Since at zero time the angle of yaw is zero and the relative wind is five degrees to the right of the longitudinal axis, the above yaw response is what would be expected of a stable airplane. Angle of yaw also shows a slight spiral instability after about ten seconds from zero time. However, at fifteen seconds, this spiral divergence is only 0.4 degree greater than the yaw angle of five degrees at which the airplane first stabilizes. Therefore, the airplane can be said to have negligible spiral instability for a disturbance in sideslip of five degrees.

As can be seen from Table V, the maximum amplitudes attained by all lateral responses are small, the maximum values attained by angles of sideslip, roll, and yaw, respectively, being: -2.65 degrees, -1.3 degrees, and -7.5 degrees. The maximum values attained by rate of roll and rate of yaw, respectively, are: -2.2 degrees/second, and 6.0 degrees/second. It is to be

noted that when the term maximum value of sideslip is used herein, it refers to the maximum value of sideslip angle oscillation amplitude attained following, but not including, the original disturbance.

The period for one cycle of all lateral responses is 4.15 seconds, which would probably be long enough to allow the pilot to take corrective action if he desired. However, the amplitudes of all lateral responses are so small, and their oscillations are so heavily damped that in less than fifteen seconds the airplane will have returned to an equilibrium straight and level flight condition with no discomfort to the pilot and no control action required.

Thus, it may be stated that the lateral motion responses of Airplane I with controls fixed are heavily damped oscillations of fairly long period with negligible spiral divergence in the first fifteen seconds.

The lateral motion of Airplane I, with no dead spot non-linearities in moment derivatives, in response to a disturbance in sideslip of one degree would be exactly the same as that for the five degree disturbance except that all amplitudes would be reduced by one fifth.

Airplane II with no dead spot non-linearities in moment derivatives has a stable response in all lateral motions to a five degree disturbance in sideslip. However, the stability characteristics of Airplane II are far less desirable than those of Airplane I. This is to be expected, however, since in a transport type aircraft, good stability characteristics are of prime importance since they insure smooth, comfortable straight and level flight, whereas in fighter type aircraft, on the other hand, although dynamic stability is required, some stability characteristics must be sacrificed in order to insure good maneuverability characteristics.

All lateral responses of Airplane II are pure oscillations with negligible spiral divergence. At 0.8 seconds following the disturbance, yawangle has attained a value of ten degrees and started oscillating about plus five degrees with an initial amplitude of fico degrees. Thus, Airplane II also has good directional stability, although its yaw oscillations are more lightly damped and of larger amplitude than those of Airplane I. The various lateral oscillations require over four seconds and about three cycles to damp to half amplitude. This can be seen from Tables V and VI to be about twice as many seconds and about five times as many cycles as required by Airplane I to damp to half amplitude. Moreover, at fifteen seconds fol-

lowing the disturbance, the lateral responses of Airplane II have just barely been damped to less than 0.1 amplitude and have oscillated through more than 9.5 cycles. This compares very unfavorably with Airplane I, whose lateral oscillations have completely damped out by fifteen seconds.

The maximum values attained by the lateral responses of Airplane II are relatively high. They are as follows: angles of sideslip, roll, and yaw, respectively are -4.6 degrees, -14.2 degrees, and 10.1 degrees; rate of roll and rate of yaw, respectively are 52 degrees/second and 21.5 degrees/second. All of these values are high enough to be quite noticeable to the pilot. The maximum roll angle of -14.2 degrees is on the verge of being too large to fit the assumptions of the theory of small oscillations on which the lateral equations are based, but it is not large enough to make an appreciable error in this solution. The large maximum rolling and yawing velocities occur within the first second after the disturbance and coupled with the shorter period, which is 1.5 seconds for all lateral responses, would make the motion very uncomfortable for the pilot who is trying to fly straight and level.

Thus the lateral responses of Airplane II, with controls fixed, are moderately damped oscillations with no spiral instability.

The lateral responses of Airplane II with no dead spot non-linearities in response to a disturbance in sideslip of one degree would be exactly the same as the response to the five degree disturbance in sideslip except that the amplitudes would be reduced by one fifth.

The difference in the nature of the lateral responses between Airplanes I and II in response to the same disturbance can be considered to conform to known theory. As can be seen from Tables I and II, the most marked difference between the characteristics of Airplanes I and II lies in the difference between their respective dihedral effects and directional stabilities, both being greater for Airplane II than for Airplane I. Moreover, the difference in the dihedral effects is greater than the difference in the directional stabilities. In non-dimensional coefficient form these differences would be even more marked since (qSb) would be smaller for Airplane II than for Airplane I. Now Figure 11-3 of reference (1) has been included in this thesis as Figure 4. From this figure it can be seen that there is a certain range for a particular airplane over which dihedral effect and directional stability may be varied which will give lateral dynamic stability. If a certain airplane lying in this stable region had its directional stability held constant and its effective wing dihedral varied so

that the dihedral effect becomes greater negatively, the oscillatory boundary is approached or crossed if the negative increase in dihedral effect is great enough. Conversely, if the dihedral effect is decreased negatively, the divergence boundary is approached or crossed. Reasoning on this basis in very general terms, if it were assumed that the main difference in the characteristics of Airplanes I and II were a moderate difference in directional stability derivative and a large difference in dihedral effect derivative, then Airplane II would be expected to be in the region of the oscillatory boundary and Airplane I in the region of the divergence boundary. Such is apparently the case, for as previously shown, Airplane II is in the stable region with no spiral divergence but with relatively lightly damped, short period oscillations, thus showing it to be relatively near the oscillatory boundary. Airplane I, on the other hand, is just barely on the unstable side of the divergence boundary, since it has a very mild spiral divergence and heavily damped, longer period oscillations. Thus, as previously stated, Airplane I has been permitted to have very mild, practically unnoticed spiral divergence in order that it may have very heavily damped, long period lateral oscillations, whereas Airplane II has been permitted to have only moderately well damped lateral oscillations in order that it may have good

maneuverability characteristics. However, in this case the combination of low period and high amplitudes make the lateral stability characteristics very desirable.

Predicted effects of dead spot non-linearities:

It would be very difficult to predict the effects of the various dead spot non-linearities with any accuracy without actually solving the stability equations with these non-linearities included, as was done in this investigation. However, by reasoning similar to that in the preceding paragraph, the effects which the non-linearities could be expected to have may be predicted in very general terms.

Following the line of reasoning of the preceding section, a decrease in dihedral effect to zero with all other airplane charactertistics held constant would, in accordance with Figure 4, be expected to increase the damping of the lateral oscillations and to cause spiral instability. In the case of the dead spot non-linearity, the dihedral effect is only zero when sideslip angle is between plus and minus two degrees. Nevertheless, the general effect would be expected to be that stated above.

Similarly, the reduction of directional stability deriv-

ative to zero when within the dead spot would be expected to have the general effect of modifying the lateral oscillations. However, since in this case dihedral effect would be held constant, the dead spot in directional stability derivative would be expected to primarily affect the lateral oscillations in a respect other than damping. Thus, the dead spot in directional stability derivative would be expected to primarily affect the period of the lateral oscillations. This agrees with the statement made in reference (9), stating that the directional stability derivative is similar to the spring constant in a spring-dashpot system.

The damping in yaw derivative, as can be seen from its name, is well known to affect primarily the damping of the lateral oscillations. Thus, the general effect of the dead spot non-linearity in the damping in yaw derivative would be expected to consist of a reduction in the damping of the lateral oscillations. This agrees with a statement made in reference (9) comparing the damping in yawing derivative with the damping constant of a spring-dashpot system.

The general effect of the dead spot in the rolling moment due to yawing velocity derivative would be difficult to predict.

Simultaneous combinations of the above dead spot non-linearities would also have effects which would be hard to predict except that it might be conjectured that the individual effects might be superimposed on one another.

The effects of the various dead spot non-linearities will now be described and discussed in very general terms. Except where stated otherwise, comparisons are made with the lateral responses of the airplanes for the case with no dead space non-linearities.

Effect of dead spot non-linearity in l_β':

The primary effects of the dead spot in l_β' were a marked decrease in amplitude for angle of roll and rate of roll for both airplanes for the five degree sideslip disturbance. For Airplane II, the damping of all lateral responses was moderately increased for the five degree sideslip disturbance, whereas for Airplane I the damping was essentially unchanged for all lateral responses. The effects on the period for the five degree disturbance were negligible for both airplanes. The effect of this dead spot for the one degree disturbance in sideslip was negligible for both airplanes except that both angle of roll and rate of roll remained zero for Airplane II throughout the solution.

Effect of dead spot non-linearity in n_{β}:

This non-linearity had the effect on Airplane I of considerably lengthening the periods of the oscillations of the lateral responses for the five degree sideslip disturbance. In addition the maximum amplitudes were, in general, increased somewhat and the damping was somewhat decreased. The effect for the one degree sideslip disturbance on Airplane I was similar to the above except that all amplitudes remained small, less than one degree or one degree per second, respectively. No spiral divergence was evident for either of the disturbances.

The effects of this non-linearity on Airplane II for the disturbances in sideslip of both five degrees and one degree were the same as for Airplane I with the sideslip disturbance of five degrees with the very major exception that Airplane II had a rapidly developing and extremely large spiral divergence which made the airplane's lateral stability characteristics extremely unsatisfactory for both the five degree and one degree sideslip disturbances.

Effect of dead spot non-linearity in l_r':

The effect of the dead spot in l_r' on Airplane I for the sideslip disturbance of five degrees were very small. The

Effect of dead spot non-linearity in L_β'.

This non-linearity had the effect on airplane I of considerably lengthening the periods of the oscillations of the lateral responses for the five degree sideslip disturbance. In addition the maximum amplitudes were, in general, increased somewhat and the damping was somewhat decreased. The effect for the one degree sideslip disturbances on airplane I was similar to the above except that all amplitudes remained small, less than one degree or one degree per second, respectively. No spiral divergence was noticed for either of the disturbances.

The effects of this non-linearity on airplane II for the disturbances in sideslip of both five degrees and one degree were the same as for airplane I with the sideslip disturbance of five degrees with the very large amplitudes that airplane II had a rapidly developing and extremely large spiral divergence which made the airplane's lateral stability characteristics extremely unsatisfactory for both the five degree and one degree sideslip disturbances.

Effect of dead spot non-linearity in L_β'.

The effect of the dead spot in L_β' on airplane I for the sideslip disturbance of five degrees were very small. The periods and maximum amplitudes of all lateral responses were essentially unchanged. The time to damp to half amplitude of angle of roll and rate of roll responses was somewhat decreased, whereas it was slightly increased for the other responses. The time to damp to 0.1 amplitude was slightly increased for all lateral responses. A small spiral divergence was evident which was somewhat greater than that for the case with no non-linearities.

For the case of Airplane I with a one degree disturbance in sideslip, this non-linearity had the primary effect of producing a spiral divergence which, though small, was appreciably greater than the spiral divergence encountered in Airplane I with no non-linearities. All lateral response oscillations were of small amplitude and heavily damped.

Effect of dead spot non-linearity in n_r:

This non-linearity had the effect for both Airplanes I and II for disturbances in sideslip of both five degrees and one degree of reducing the damping and leaving the period unchanged. However, the reduction in damping for Airplane I, although appreciable did not make the stability characteristics of Airplane I unsatisfactory, whereas the response oscillations

for Airplane II became neutrally damped for the five degree disturbance unstable for the one degree disturbance, thus making the stability characteristics of Airplane II unsatisfactory for this case.

Combined dead spot non-linearities in l_β' and l_r':

The primary effect of this set of non-linearities on the lateral responses of Airplane I was to reduce the oscillations of angle of roll and rate of roll responses to such an extent that angle of roll response was a pure divergence by three seconds following the disturbance for the five degree sideslip disturbance and by one second following the disturbance for the one degree disturbance. This divergence was not pronounced enough to be objectionable.

Combined dead spot non-linearities in n_β and n_r:

The primary effects of this set of non-linearities on both airplanes for both sideslip disturbances were to reduce the damping, lengthen the period, and in most cases increase the maximum amplitude for all lateral responses. For Airplane I the magnitude of these effects was not objectionable. For Airplane II the lateral stability characteristics were made unsatisfactory.

for airplane II became directionally [illegible] for the five-degree aileron [illegible] for the one-degree disturbance, thus making the stability characteristics of airplane II unsatisfactory for this case.

Combined dead spot non-linearities in δ_a and δ_r.

The primary effect of this set of non-linearities on the lateral responses of airplane I was to reduce the oscillations of angle of roll and rate of roll responses to such an extent that angle of roll resembled a pure divergence by three seconds following the disturbance for the five-degree aileron disturbance and by two seconds following the disturbance for the one-degree disturbance. This divergence was not pronounced enough to be objectionable.

Combined dead spot non-linearities in δ_a and δ_r.

The primary effects of this set of non-linearities on both airplanes for both aileron disturbances were to reduce the damping, lengthen the period, and in both cases increase the maximum amplitude for all lateral responses. For airplane I the magnitude of these effects was not objectionable. For airplane II the lateral stability characteristics were made unsatisfactory.

For the five degree disturbance in sideslip of Airplane II all lateral responses became neutrally damped at from 0.7 to 0.8 of their initial amplitudes. For the one degree disturbance in sideslip of Airplane II, all lateral responses became unstable.

Combined effect of dead spot non-linearities in l_{β}', l_r', n_{β}, and n_r:

The primary effect of this set of non-linearities on the lateral responses of Airplane I for sideslip disturbances of both five degrees and one degree was to lengthen the period and reduce the damping, each by a moderate amount. However, the tendency also was to reduce the oscillations of angle of roll and rate of roll responses making angle of roll response nearly a small, pure divergence throughout the major portion of the solution for both the five degree and one degree disturbances, respectively. For the one degree sideslip disturbance, the directional stability is very poor with angle of sideslip oscillating about 1.3 degrees.

Combined effect of dead spot non-linearities in l_{β}', n_{β}, and n_r:

The major effects of this set of non-linearities on Airplane II for both the five degree and one degree sideslip

disturbances, respectively, were to increase the period and reduce the damping of the lateral response oscillations. However, the stability characteristics for this case, although marginal, could be considered satisfactory and are much improved over the case with dead spot non-linearities in both n_β and n_r. Thus the dead spot non-linearity in l_β' showed a very strong damping effect on the combined dead spot non-linearities in n_β and n_r. This is the effect which would be predicted if the results for the dead spot for l_β' alone were superimposed on the results for the combined dead spots in n_β and n_r.

Although the results presented in this section show some agreement with the simple predictions attempted earlier in the section, it is obvious that for any sort of accurate indication of the effects of various dead spot non-linearities, the actual responses must be solved for as was done in the investigations of this thesis. As an extreme example of this it may be noted that the violent spiral instability caused for Airplane II by the dead spot non-linearity in n_β would be completely unexpected in a mere general qualitative analysis of the situation.

However, inasmuch as the results of this thesis show a general similarity in the trends of the effects of the dead spot non-linearities on the lateral responses of Airplanes I and II,

which differed widely in their characteristics, it is believed that the general results of this thesis for each of the airplanes could be applied, respectively to airplanes of very similar characteristics. Interpolation of the results for Airplanes I and II, respectively, for an airplane whose characteristics differ significantly from either of these would probably lead to incorrect conclusions in many cases. It is believed that if an accurate estimation of the effects of any dead spot non-linearities are desired for a particular airplane, then the lateral responses to disturbances of interest should be solved for that airplane, as was done in the investigations of this thesis.

CONCLUSIONS

The major effects of the dead spot non-linearities investigated in this thesis were found to be as follows:

Dead spot in l_β': Exercised a moderate increased damping action on the lateral response oscillations.

Dead spot in n_β: Acted to lengthen the period of the lateral response oscillations.

Dead spot in l_r': This derivative was zero for Airplane II. The effect on the lateral responses of Airplane I were negligible.

Dead spot in n_r: Acted very markedly to reduce the damping of the lateral response oscillations.

The effects of combinations of the above non-linearities appeared, in general to be a superposition of the effects of the non-linearities acting individually.

The general trend of the effects of the various dead spot non-linearities were, in general, the same for Airplanes I

and II. However, the magnitude of the effects was much greater for Airplane II, the less stable airplane.

Dead spot non-linearities in n_β and n_r caused some extremely unstable and dangerous lateral responses in Airplane II.

If an accurate appraisal of the effects of any dead spot non-linearities in moment derivatives on a particular airplane are desired, the lateral responses of that airplane with the non-linearity included must be solved as was done in this thesis for Airplane I and II.

REFERENCES

(1) G. H. Bryan, Stability in Aviation, London, Macmillan and Co. Ltd., 1911.

(2) Leonard Bairstow, Applied Aerodynamics, London, New York, Longmans Green and Co., 1939.

(3) W. F. Durand, Aerodynamic Theory, Volume V. Berlin Julius Springer Publisher, 1935.

(4) NACA TR 521: An Analysis of Longitudinal Stability in Power-Off Flight with Charts for Use in Design, C. H. Zimmerman, 1935.

(5) NACA TR 589: An Analysis of Lateral Stability in Power-Off Flight with Charts for Use in Design, by Charles H. Zimmerman, Langley Memorial Aeronautical Laboratory, 1937.

(6) NACA TN 2002: Applications of the Laplace Transformation to the Solution of the Lateral and Longitudinal Stability Equations, by F. A. Mokrzycki, Ryan Aeronautical Co., January 1950.

(7) R. V. Churchill, Modern Operational Mathematics in Engineering, New York and London, Mc-Graw-Hill Book Co., Inc., 1944.

(8) NACA TN 2013: A Study of the Use of Experimental Stability Derivatives in the Calculation of the Lateral Disturbed Motions of a Swept Wing Airplane and Comparison with Flight Results, by John D. Bird and Byron M. Jaquet, Langley Aeronautical Laboratory, Langley Air Force Bawe, Virginia, January 1950.

(9) NACA TN 2233: Some Effects of Non-Linear Variation in the Directional Stability and Damping in Yawing Derivatives on the Lateral Stability of an Airplane, by Leonard Sternfield, Langley Aeronautical Laboratory, Langley Airforce Base, Virginia, November 1950.

(10) C. D. Perkins and R. E. Hage, Airplane Performance Stability and Control, New York, John Wiley and Sons, Inc. London, Chapman and Hall, Limited, 1949.

TABLE I

Characteristics of Airplane I.

Type of Airplane:- Conventional, twin engine, slow speed transport type aircraft.

Mass and Inertia characteristics:-

W	23,600 lbs.
I_{x_0}	62,000 slug ft.^{2}
I_{z_0}	140,000 slug ft.^{2}

Flight Condition for the Thesis Investigations:-
Straight and Level Flight.

IAS	125 knots. / 211 ft./sec.
TAS	143 knots. / 165 mph. / 242 ft./sec.
η	0
γ	0
I_{xz}	0
Altitude	7500 ft.

Force and Moment Derivatives in units of acceleration:-

y_β	-28.556	ft/sec.^{2}
y_p	0	
y_r	0	
l'_β	-5.0336	sec^{-2}
l'_p	-8.3	sec^{-1}
l'_r	$+1.65$	sec^{-1}
n_β	$+2.2264$	sec^{-2}
n_p	-0.212	sec^{-1}
n_r	-0.493	sec^{-1}

TABLE II

Characteristics of Airplane II.

Type of Airplane:- High speed fighter type aircraft.

Mass and Inertia Characteristics:-

W/S	80 lbs./ft.^{2}
$K_{x_0}^2$	0.0573
$K_{z_0}^2$	0.0069

Flight condition for the Thesis Investigations.-

Straight and Level Flight.

TAS	753 ft./sec. 513 mph
η	0
γ	0
K_{xz}	0
Altitude	30,000 ft.

Force and Moment Derivatives:-

Non-Dimensional Form		Units of Acceleration		
C_{Y_β}	0	y_β	0	
C_{Y_p}	0	y_p	0	
C_{Y_r}	0	y_r	0	
C_{l_β}	-0.126	l'_β	-66.9	sec^{-2}
C_{l_p}	-0.462	l'_p	-4.52	sec^{-1}
C_{l_r}	0	l'_r	0	
C_{n_β}	+0.28	n_β	+17.91	sec^{-2}
C_{n_p}	-0.0155	n_p	-0.01827	sec^{-1}
C_{n_r}	-0.392	n_r	-0.461	sec^{-1}

TABLE III A

Descriptions of the Various REAC Solutions

Airplane I

REAC Solution No.	Non Linearities	Quantities Recorded 1	2	3	4	Disturbance	Figure No.
I-1	Recording of Non-Linearities as functions of β	$(l')_\beta$	$(n)_\beta$	l'_z	n_z		5
I-2a	None	$l'_\beta \beta$	β	ϕ	ψ	$\beta_0 = 5.0°$	6
I-2b	None	$n_\beta \beta$	β	$\Delta\phi$	$\Delta\psi$	$\beta_0 = 5.0°$	7
I-3a	l'_β	$(l')_\beta$	β	ϕ	ψ	$\beta_0 = 5.0°$	8
I-3b	l'_β	$(l')_\beta$	β	$\Delta\phi$	$\Delta\psi$	$\beta_0 = 5.0°$	9
I-103a	l'_β	$(l')_\beta$	β	ϕ	ψ	$\beta_0 = 1.0°$	10
I-103b	l'_β	$(l')_\beta$	β	$\Delta\phi$	$\Delta\psi$	$\beta_0 = 1.0°$	11
I-4a	n_β	$(n)_\beta$	β	ϕ	ψ	$\beta_0 = 5.0°$	12
I-4b	n_β	$(n)_\beta$	β	$\Delta\phi$	$\Delta\psi$	$\beta_0 = 5.0°$	
I-104a	n_β	$(n)_\beta$	β	ϕ	ψ	$\beta_0 = 1.0°$	
I-104b	n_β	$(n)_\beta$	β	$\Delta\phi$	$\Delta\psi$	$\beta_0 = 1.0°$	
I-5a	l'_z	$\frac{l'_z \Delta\psi}{10}$	β	ϕ	ψ	$\beta_0 = 5.0°$	13
I-5b	l'_z	$\frac{l'_z \Delta\psi}{10}$	β	$\Delta\phi$	$\Delta\psi$	$\beta_0 = 5.0°$	
I-105a	l'_z	$\frac{l'_z \Delta\psi}{10}$	β	ϕ	ψ	$\beta_0 = 1.0°$	
I-105b	l'_z	$\frac{l'_z \Delta\psi}{10}$	β	$\Delta\phi$	$\Delta\psi$	$\beta_0 = 1.0°$	
I-6a	n_z	$n_z \Delta\psi$	β	ϕ	ψ	$\beta_0 = 5.0°$	14
I-6b	n_z	$n_z \Delta\psi$	β	$\Delta\phi$	$\Delta\psi$	$\beta_0 = 5.0°$	
I-106a	n_z	$n_z \Delta\psi$	β	ϕ	ψ	$\beta_0 = 1.0°$	
I-106b	n_z	$n_z \Delta\psi$	β	$\Delta\phi$	$\Delta\psi$	$\beta_0 = 1.0°$	
I-7a	l'_β and l'_z	$\frac{l'_z \Delta\psi}{10}$	β	ϕ	ψ	$\beta_0 = 5.0°$	15a
I-7b	l'_β and l'_z	$(l')_\beta$	β	$\Delta\phi$	$\Delta\psi$	$\beta_0 = 5.0°$	15b
I-107a	l'_β and l'_z	$\frac{l'_z \Delta\psi}{10}$	β	ϕ	ψ	$\beta_0 = 1.0°$	15c
I-107b	l'_β and l'_z	$(l')_\beta$	β	$\Delta\phi$	$\Delta\psi$	$\beta_0 = 1.0°$	
I-8a	n_β and n_z	$n_z \Delta\psi$	β	ϕ	ψ	$\beta_0 = 5.0°$	16a
I-8b	n_β and n_z	$(n)_\beta$	β	$\Delta\phi$	$\Delta\psi$	$\beta_0 = 5.0°$	16b
I-108a	n_β and n_z	$n_z \Delta\psi$	β	ϕ	ψ	$\beta_0 = 1.0°$	
I-108b	n_β and n_z	$(n)_\beta$	β	$\Delta\phi$	$\Delta\psi$	$\beta_0 =$ [illegible].0°	

TABLE III A (continued)

Airplane I

REAC Solution No.	Non Linearities	Quantities Recorded 1	2	3	4	Disturbance	Figure No.*
I-9a	n_β, n_z, ℓ'_β, and ℓ'_z	$n_z D\psi$	β	ϕ	ψ	$\beta_0 = 5.0°$	17
I-9b **	n_β, n_z, ℓ'_β, and ℓ'_z	$(n)_\beta$	β	$D\phi$	$D\psi$	$\beta_0 = 5.0°$	18
I-109a	n_β, n_z, ℓ'_β, and ℓ'_z	$n_z D\psi$	β	ϕ	ψ	$\beta_0 = 1.0°$	20.
I-109b	n_β, n_z, ℓ'_β, and ℓ'_z	$(n)_\beta$	β	$D\phi$	$D\psi$	$\beta_0 = 1.0°$	
I-109c	n_β, n_z, ℓ'_β, and ℓ'_z	$n_z D\psi$	β	$(\ell')_\beta$	$\frac{\ell'_z D\psi}{10}$	$\beta_0 = 1.0°$	
*I-9c	n_β, n_z, ℓ'_β, and ℓ'_z	$n_z D\psi$	β	$(\ell')_\beta$	$\frac{\ell'_z D\psi}{10}$	$\beta_0 = 5.0°$	19

Note * ~ Indicates figure numbers of REAC solutions which were included in this thesis presentation. REAC solutions without figure numbers were not included in this thesis presentation

TABLE III B

Descriptions of the Various REAC Solutions

Airplane II

REAC Solution No.	Non Linearities	Quantities Recorded 1	2	3	4	Disturbance	Figure No.*
II-1	Recording of Non-Linearities	$\frac{(l')_\beta}{10}$	$\frac{(n_\beta)}{10}$	l'_r	n_r		21
II-2a	None	$\frac{(l')_\beta}{10}$	β	ϕ	ψ	$\beta_0 = 5.0°$	22
II-2b	None	$\frac{(n)_\beta}{10}$	β	$D\phi$	$D\psi$	$\beta_0 = 5.0°$	23
II-3a	l'_β	$\frac{(l')_\beta}{10}$	β	ϕ	ψ	$\beta_0 = 5.0°$	24
II-3b	l'_β	$\frac{(l')_\beta}{10}$	β	$D\phi$	$D\psi$	$\beta_0 = 5.0°$	
II-103a	l'_β	$\frac{(l')_\beta}{10}$	β	ϕ	ψ	$\beta_0 = 1.0°$	25
II-103b	l'_β	$\frac{(l')_\beta}{10}$	β	$D\phi$	$D\psi$	$\beta_0 = 1.0°$	
II-4a	n_β	$\frac{(n)_\beta}{10}$	β	ϕ	ψ	$\beta_0 = 5.0°$	26
II-4b	n_β	$\frac{(n)_\beta}{10}$	β	$D\phi$	$D\psi$	$\beta_0 = 5.0°$	
II-104a	n_β	$\frac{(n)_\beta}{10}$	β	ϕ	ψ	$\beta_0 = 1.0°$	27
II-104b	n_β	$\frac{(n)_\beta}{10}$	β	$D\phi$	$D\psi$	$\beta_0 = 1.0°$	
II-6a	n_r	$n_r D\psi$	β	ϕ	ψ	$\beta_0 = 5.0°$	28
II-6b	n_r	$n_r D\psi$	β	$D\phi$	$D\psi$	$\beta_0 = 5.0°$	
II-106a	n_r	$n_r D\psi$	β	ϕ	ψ	$\beta_0 = 1.0°$	29

TABLE III B (continued)

REAC Solution No	Non Linearities	Quantities Recorded 1	2	3	4	Disturbance	Figure No.*
II - 106B	n_z	$n_z \Delta\psi$	β	$\Delta\phi$	$\Delta\psi$	$\beta_0 = 1.0°$	
II - 8a	n_z and n_β	$n_z \Delta\psi$	β	ϕ	ψ	$\beta_0 = 5.0°$	30
II - 8b	n_z and n_β	$\frac{(n)_\beta}{10}$	β	$\Delta\phi$	$\Delta\psi$	$\beta_0 = 5.0°$	31
II - 108a	n_z and n_β	$n_z \Delta\psi$	β	ϕ	ψ	$\beta_0 = 1.0°$	32
II - 108b	n_z and n_β	$\frac{(n)_\beta}{10}$	β	$\Delta\phi$	$\Delta\psi$	$\beta_0 = 1.0°$	33
II - 9a	n_z, n_β, and l'_β	$n_z \Delta\psi$	β	ϕ	ψ	$\beta_0 = 5.0°$	34
II - 9b	n_z, n_β, and l'_β	$\frac{(l')_\beta}{10}$	β	$\Delta\phi$	$\Delta\psi$	$\beta_0 = 5.0°$	35
II - 9c	n_z, n_β, and l'_β	$\frac{(n)_\beta}{10}$	β			$\beta_0 = 5.0°$	36
II - 109a	n_z, n_β, and l'_β	$n_z \Delta\psi$	β	ϕ	ψ	$\beta_0 = 1.0°$	37.
II - 109b	n_z, n_β, and l'_β	$\frac{(l'')_\beta}{10}$	β	$\Delta\phi$	$\Delta\psi$	$\beta_0 = 1.0°$	38
II - 109c	n_z, n_β, and l'_β	$\frac{(n)_\beta}{10}$	β			$\beta_0 = 1.0°$	39

* ~ Indicates figure numbers of REAC solutions which were included in this thesis presentation. REAC solutions without figure numbers were not included in this thesis presentation

TABLE IV

Comparison of REAC Solutions I-2a, I-3b, I-3a, and II-2a, with the Corresponding Hand Solutions of Figures 2 and 3, respectively, as regards β.

		REAC Sol. #I-2a			REAC Sol. #I-3a			REAC Sol. #II-2a		
		REAC Sol	Hand Sol	%	REAC Sol.	Hand Sol.	%	REAC Sol.	Hand Sol	%
Period		4.15	4.045	102.4	4.3	4.205	102.3	1.50	1.47	102.0
Peak amp. of β response for successive oscillations (Numbers 1 through 10 refer to the number of each respective oscillation)	1	-2.65°	-2.61°	101.6	-2.62°	-2.49°	105.1	-4.6°	-4.36°	105.2
	2	+1.42°	+1.37°	103.6	+1.25°	+1.24°	100.8	+4.0°	+3.84°	104.1
	3							-3.65°	-3.40°	107.2
	4							+3.015°	+2.98°	101.1
	5							-2.87°	-2.67°	107.5
	6							+2.45°	+2.32°	105.6
	7							-2.25°	-2.01°	112.1
	8							+1.92°	+1.80°	106.7
	9							-1.78°	-1.60°	111.1
	10							+1.50°	+1.40°	107.1

Note: "%" in the column headings of the above TABLE refers to the respective REAC solution values expressed as percentages of the corresponding hand solution values.

TABLE V

Lateral Response Data for Airplane I As Determined from REAC Solutions for $\beta_0 = 5.0°$

Dead Spot Non-L.n.	REAC Solution No.	Response	Period (sec.)	Max Value Attained (° or °/sec)	Time to Attain Max. Value (sec.)	Time to Damp to 1/2 Amp (sec.)	Cycles to Damp to 1/2 Amp	Time to Damp to 0.1 Amp (sec.)	Time to Damp to 0.01 Amp (sec.)	Divergence at 5 sec. (° or °/sec.)	Divergence at 10 sec. (° or °/sec.)	Divergence at 15 sec. (° or °/sec.)	
None	I-2a	β	4.15	-2.65	2.05	2.3	0.56	8.0	15.0	0	0	0.02	
		ϕ	4.15	-1.3	0.95	3.05	0.77	7.75	14.35	0.1	0.2	0.25	
		ψ	4.15	7.5, 2.3*	2.1, 2.1	2.0	0.50	6.3	12.5	5.0	5.2	5.4	
	I-2b	$D\phi$	4.10	-2.2	0.33	3.27	0.91	7.94	16.0	0	0	0.02	
		$D\psi$	4.15	6.0	0.95	2.05	0.5	7.05	14.55	0	0	0.05	
l'_β	I-3a	β	4.3	-2.62	2.1	2.4	0.57	7.0	15.0	0	0	0.02	
		ϕ	4.1	0.8, 0.4*	2.6, 2.6	3.75	1.0	7.95	14.3	0.4	0.44	0.6	
		ψ	4.4	7.9, 2.9*	2.2, 2.2	1.8	0.4	5.8	13.8	5.5	5.9	6.1	
	I-3b	$D\phi$	4.3	1.1	1.15	2.95	1.0	7.25	14.8	0	0	0.05	
		$D\psi$	4.3	6.0	0.9	2.10	0.5	6.4	14.1	0	0	0.2	
n_β	I-4a	β	12.3	-2.5	3.45	3.45	0.5	14.0	>18.0	0	0	0	
		ϕ	18.0	2.2	6.5	10.4	0.8	18.0	>18.0	0	0	0	
		ψ	14.0	{7.0, ‡1.0}*	3.7, 3.7	8.3	0.75	10.8	12.3	0	0	0	0
	I-4b	$D\phi$	12.4	-2.5	0.35	5.65	0.7	11.65	>18.0	0	0	0	
		$D\psi$	8.0	3.5	1.0	2.0	0.30	4.0	17.0	0	0	0	
l'_r	I-5a	β	4.17	-2.87	2.08	2.8	0.671	8.1	16.6	0	0	0	
		ϕ	4.1	-1.37	1.2	2.4	0.6	8.3	17.0	0.4	0.7	1.18	
		ψ	4.2	7.8, 2.8*	2.1, 2.1	2.1	0.5	9.4	16.0	0	0.4	6.0	
	I-5b	$D\phi$	4.2	-2.2	0.28	3.2	0.8	8.2	15.2	0	0.1	0.1	
		$D\psi$	4.15	6.0	0.9	2.7	0.6	8.4	16.1	0	0.1	0.1	
n_r	I-6a	β	4.1	-3.7	2.05	4.5	1.1	>18	>18	0	0	0	
		ϕ	4.1	1.85	3.0	4.15	1.0	>18	>18	0.2	0.4	0.6	
		ψ	4.15	8.5, 3.5*	2.1, 2.1	6.2	1.5	>18	>18	5.2	5.9	6.1	
	I-6b	$D\phi$	4.15	2.45	1.8	7.78	2.0	>18	>18	0	0	0	
		$D\psi$	4.1	6.5	1.05	5.05	1.23	>18	>18	0	0	0	
l'_β and l'_r	I-7a	β	4.3	-2.75	2.15	2.6	0.605	8.0	15.0	0	0	0.03	
		ϕ	3.70	-6.44	0.65	(2)	(2)	(2)	(2)	0.40	0.88	1.36	
		ψ	4.3	7.8, 2.8*	2.2, 2.2	2.1	0.5	8.9	13.0	5.1	5.4	5.7	
	I-7b	$D\phi$	1.0	-0.98	0.1	(3)	(3)	(3)	0.1	0.1	0.1		
		$D\psi$	4.3	5.9	0.85	2.15	0.5	8.65	15.15	0	0	0.1	
n_β and n_r	I-8a	β	7.1, 12.3	-3.25	3.1	6.1	0.86	>23	>23	0	0	0	
		ϕ	11.1	2.53, 2.33*	5.1, 5.1	>23	>2	>23	>23	0.2	0.6	0.85	
		ψ	10.55	8.0, 3.0*	{3.25, 3.25}	4.05	0.5	>23	>23	5.2	5.6	6.0	
	I-8b	$D\phi$	9.7, 3.6	-2.45	0.3	9.9	1.3	>28	>28	0	0	0	
		$D\psi$	8.2, 13.3	3.3	1.5	3.5	0.45	14.9	>28	0	0	0	
l'_β, l'_r, and n_β, n_r	I-9a	β	8.2, 23.0	-3.25	3.35	7.5	0.9	>30	>30	0	0	0	
		ϕ	6.6	0.9 (4)	7.4	(4)	(4)	(4)	(4)	0.2	0.65	1.2	
		ψ	21.5	8.3, 8.3*	3.5, 3.5	12.7	0.75	>30	>30	5.1	5.4	6.0	
	I-9b	$D\phi$	9.6 (5)	-1.2	0.3	(5)	(5)	(5)	(5)	0.1	0.1	0.1	
		$D\psi$	8.5	3.3	0.9	4.7	0.4	>18	>18	0	0	0	

> Indicates "greater than".

* Indicates max. oscillatory value when different from max. total value.

‡ All values from here on to the right are displaced one column to the right for I-4a ψ.

(1) Maximum value while oscillating. This value exceeded by a pure divergence in 5.5 seconds.

(2) Oscillates for 1/2 cycle only. Oscillations abruptly and completely damped out at 2.8 seconds.

(3) Shape of oscillation very irregular. Plane oscillates through two complete cycles of $D\phi$. At 3 seconds oscillations abruptly oscillations and completely damped out.

(4) Maximum value occurs while oscillating. At nine seconds oscillations are completely and abruptly damped out.

(5) Oscillations consist of two disjointed pulses.

Note that time to damp to 1/2 amp. measured from time of first oscillation, [illegible] time to damp to 1/2 amp. is measured [illegible]

NOTES on TABLE I

> Indicates "greater than".

* Indicates max. oscillatory value when different from total val..

+ All values from here on to the right are displaced one column to the right for ψ response in RI solution I-4a.

(1) Maximum value while oscillating. This value exceeded by a pure divergence in 5.5 seconds.

(2) Oscillates for 1/2 cycle only. Oscillations abruptly and completely damped out at 2.8 seconds.

(3) Shape of oscillation very irregular. Plane oscillates through two complete cycles of ΔΦ. At 3 seconds [redacted] oscillations abruptly and completely damped out.

(4) Maximum value occurs while oscillating. At nine seconds, after 1.5 oscillations, oscillations are completely and abruptly damped out.

(5) Oscillations consist of two disjointed pulses

Additional Notes:

Time to damp 1/2 amplitude measured from time of first oscillation, except in the case of β response, where time to damp to 1/2 amplitude is measured from zero time.

In any case where 2 periods are given, the first period given is the period for the first portion of the solution; the second, for the latter portion of the solution.

TABLE VI

Lateral Response Data for Airplane II

As Determined from REAC Solutions for $\beta_0 = 5.0°$

Non Linearities	REAC Solution No.	Quantity	Period	Max. Value Attained 1st 10 sec.	Time to Attain Max Value	Time to Damp to 1/2 Amp	Cycles to Damp to 1/2 Amp	Time to Damp to 0.1 Amp	Divergence at 5 sec.	Divergence at 10 sec.	Divergence at 15 sec	Portion of Amp at 15 sec
None	II-2a	β	1.50	−4.6	0.75	4.5	3.0	14.5	0	0	0	0.084
		ϕ	1.50	−14.2	0.6	4.6	3.0	13.7	0	0	−0.8°	0.095
		ψ	1.5	11.1, 5.1*	0.8, 0.8	13.7	2.4	12.9	5.0	5.0	4.8°	0.088
	II-2b	$D\phi$	1.5	52	0.95	4.45	3.0	13.6	0	0	0	0.089
		$D\psi$	1.5	21.5	0.37	4.4	2.9	14.2	0	0	0	0.0913
l'_β	II-3a	β	1.55	−4.45°	0.18	3.7	2.4	10.8	0	0	0	[illegible].140
		ϕ	1.55	−6.7°	0.65	(1)	(1)	(1)	−1.0	−1.0	−1.1	0.180
		ψ	1.55	10.0, 5.0*	0.8, 0.8	3.1	2.0	9.2	5.0	5.0	4.9	0.040
	II-3b	$D\phi$	1.50	18.0	1.0	(2)	(2)	(2)	0	0	0	0
		$D\psi$	1.55	21.0	0.43	3.4	7.2	108	0	0.1	0.9	0.043
n_β	II-4a	β	2.4, 4.55	−5.0	1.15	8.7	3.0	>18.0	−0.5	−0.5	−0.5	0.26
		ϕ	2.5, 4.7	52.0, 23.0*	8.1, 0.8	14.7	4.7	>18.5	17.0	42.0	70.0	0.50
		ψ	2.65, 4.0	140, 5.0*	1.15	7.55	2.5	15	7.5	13.6	24.0	0.2
	II-4b	$D\phi$	2.60, 4.2	67.0	1.45	8.7	3.0	>30	5.0	5.0	5.0	0.418
		$D\psi$	2.70, 4.1	12.3	0.5	4.5	1.7	27	1.1	2.0	3.0	0.145
+ n_z	II-6a	β	1.50	−4.8	0.85		↑		0	0	0	0.68
		ϕ	1.50	−19.0, −12.8*	2.2, 2.2				−6.5	−7.0	−6.5	0.708
		ψ	1.50	10.2, 5.2*	0.85, 0.85				4.0	2.5	1.0	0.664
+	II-6b	$D\phi$	1.50	56.0	1.0		lightly damped		0	0	1.5	0.669
		$D\psi$	1.50	22.4	0.4				0	0	0	0.605
n_β and n_z	II-8a	β	2.45, 2.65	−5.0°	1.25				0	0	0	0.76
		ϕ	2.5, 2.6	−33.0, −24.0*	33, 0.9				−5°	+2.0°	+5.0°	0.835
		ψ	2.5, 2.6	0.0, 5.0*	1.25, 1.25				3.5	3.5	4.5	[illegible]
	II-8b	$D\phi$	2.5, 2.65	−60.0	0.45				0	0	0	0.867
		$D\psi$	2.5, 2.6	−11.0	2.0		↓		0	0	0.5	0.727
‡ l'_β, n_β, and n_z	II-9a	β	2.6, 3.8	−5.0	1.2	17.0	5.0	>26	−0.3	−0.3	−0.3	0.56
		ϕ	2.65, 3.8	−11.2	0.9	5.4	2.0	21.4	3.8	7.5	10.0	0.134
		ψ	2.65, 3.8	10.2, 5.2*	1.2, 1.2	15.8	5.0	>5.8	5.9	7.0	9.0	0.576
	II-9b	$D\phi$	2.70, 4.10	33.0	1.45	5.3	2.0	>18	0	0	0	0.1513
		$D\psi$	2.80, 4.20	11.1	0.7	7.3	2.5	>18	0	0	0	0.279

(1) After 2 cycles at 4.5 seconds, oscillations are completely damped out. ϕ is constant at −1.0° after 4.5 seconds.

(2) After 2.5 cycles at 4.5 seconds, oscillations are completely damped out.

\+ Matching in β somewhat off in amplitude; o.k. in period.

‡ Matching in β, of about 0.1 second in period; o.k. in amplitude.

Note: In any case where 2 periods are given, the first period given, is the period for the first portion of the solution; the second, for the latter portion of the solution.

TABLE VII

Lateral Response Data for Airplane I Expressed as Percent of Value for Airplane I with No Non-Linearities ($\beta_0 = 5.0°$)

Non-Linearities	REAC Solution Number	Quantity	Period	Max. Value Attained	Time to Damp to 1/2 Amp	Time to Damp to 0.1 Amp.
None	I-2a	β	100	100	100	100
		ϕ	100	100	100	100
		ψ	100	1,00 100	100	100
	I-2b	$\Delta\phi$	100	100	100	100
		$\Delta\psi$	100	100	100	100
l'_β	I-3a	β	103.6	98.9	104.2	87.5
		ϕ	98.9	61.5 *30.75	123.0	102.7
		ψ	106.0	105.2 *116.0	90.0	92.1
	I-3b	$\Delta\phi$	104.8	50.0	90.2	94.4
		$\Delta\psi$	103.6	100.0	102.3	90.8
n_β	I-4a	β	296.5	94.4	150.0	175.0
		ϕ	434	169.2	341	232.5
		ψ	337.5	93.4 *40.0%	415	171.5
	I-4b	$\Delta\phi$	302.5	113.5	172.8	151.9
		$\Delta\psi$	192.7	58.3	97.6	56.8
l'_r	I-5a	β	100.4	108.3	121.7	101.1
		ϕ	98.9	105.3	78.7	107.0
		ψ	101.1	103.9 *112.0	105.0	[illegible]
	I-5b	$\Delta\phi$	102.3	100.0	97.9	106.9
		$\Delta\psi$	100	100.0	131.7	110.0
n_r	I-6a	β	98.9	139.6	195.6	> 225.0
		ϕ	98.9	142.2	136.0	> 232.5
		ψ	100	113.2 *140.0	310	> 286
	I-6b	$\Delta\phi$	101.1	111.2	238	> 235
		$\Delta\psi$	98.9	108.2	246.0	> 255.5

TABLE VII continued (page 2)

Non-Linearities	REAC Solution Number	Quantity	Period	Max Value Attained	Time to Damp to 1/2 Amp	Time to Damp to 0.1 Amp
l'_β and l'_r	I-7a	β	103.6	103.7	113.0	100
		ϕ	84.2	33.8	(1)(2) 91.8	(2) 91.8
		ψ	103.6	104.0 *112.0	105.0	141.0
	I-7b	$\Delta\phi$	24.4	44.5	(4) 91.8	(4)
		$\Delta\psi$	103.6	98.4	104.9	122.5
n_β and n_r	I-8a	β	⊛ 171.1 296.5	122.6	265	* 287.5
		ϕ	267.5	194.7 *79.1	> 754	> 754
		ψ	254.3	166.7 120.0	202.5	> 365
	I-8b	$\Delta\phi$	⊛ 236.5 332	111.2	302.5	> 3.65
		$\Delta\psi$	⊛ 197.5 320.5	55.0	170.7	211.5
l'_β, l'_r, n_β, n_r	I-9a	β	⊛ 197.5 554	122.6	326	> 375
		ϕ	159.0	69.2	(3) 295	(3) 295
		ψ	518	110.6 *132.0	635	> 476
	I-9b	$\Delta\phi$	234	54.5	(5) 290.5	(5)
		$\Delta\psi$	204.5	55.0	229.0	> 255.5

(1) Max. value while oscillating
Exceeded by pure divergence in 5.5 seconds.
(2) Oscillations completely damped out at this percentage.
(3) Oscillations completely damped out at this percentage.
(4) Oscillations completely damped out at this percentage.
(5) Oscillations completely damped out at this percentage

* Indicates max. oscillatory value when different from max total value.

⊛ In any case where two periods are given, the first period given, is the period for the first portion of the solution; the second, for the latter portion of the solution.

TABLE VIII

Lateral Response Data for Airplane II Expressed as Percent of Value for Airplane II with No Non-Linearities ($\beta_0 = 5.0°$)

Non-Linearities	REAC Solution Number	Quantity	Period	Max Value Attained in 1st 10 sec.	Time to Damp to 1/2 Amp	Portion of Original Amplitude at 15 sec
None	II-2a	β	100	100	100	100
		ϕ	100	100	100	100
		ψ	100	100 / *100	100	100
	II-2b	$D\phi$	100	100	100	100
		$D\psi$	100	100	100	100
l'_β	II-3a	β	103.2	96.8	82.2	47.6
		ϕ	103.2	42.9	(1) 97.8	(2)
		ψ	103.2	99.11 / *98.1	83.8	45.4
	II-3b	$D\phi$	100	34.6	(1) 101.0	0
		$D\psi$	103.2	97.7	77.3	46.3
n_β	II-4a	β	160.0 / ⊛303.5	108.5	193.2	310
		ϕ	166.7 / ⊛313.5	366 / *161.9	308.5	526
		ψ	173.7 / ⊛266.5	138.5 / * 98.1	204.0	227
	II-4b	$D\phi$	173.2 / ⊛280	128.8	195.4	469
		$D\psi$	180 / ⊛273.5	57.3	102.2	158.5
n_r	II-6a	β	100	104.2	↑	810
		ϕ	100	133.8 / * 84.6	↑	745
		ψ	100	101 / *101.9	↑	754
	II-6b	$D\phi$	100	107.7	Lightly Damped	752
		$D\psi$	100	104.2	↓	715
n_β and n_r	II-8a	β	163.2 / ⊛176.7	108.6	↓	905
		ϕ	166.7 / ⊛173.2	232 / *169.0	↓	879
		ψ	166.7 / ⊛173.2	99.1 / * 98.1	↓	796
	II-8b	$D\phi$	166.7 / ⊛173.6	115.2	↓	975
		$D\psi$	166.7 / ⊛173.2	51.2	↓	782

TABLE VIII continued (page 2)

Nonlinearities	REAC Solution Number	Quantities	Period	Max. Value Attained 1st 10 sec	Time to damp to 1/2 Amp	Portion of Original Amplitude at 15 sec
l'_β, n_β, and n_r	II - Aa	β	⊛ 173.2 253	108.6	377.5	666
		ϕ	⊛ 176.7 253.5	78.9	117.2	141.0
		ψ	⊛ 176.7 253.5	101.0 102.0	42.7	65.5
	II - Ab	$D\phi$	⊛ 180.0 273.0	63.4	119.0	170.0
		$D\psi$	186.6 280.0	51.6	165.8	300.0

(1) Oscillations completely damped out at this percentage.

(2) Constant amplitude; oscillations completely damped out prior to 15.0 seconds.

(3) Oscillations completely damped out prior to 15.0 seconds.

* Indicates max. oscillatory value when different from max. total value.

⊛ In any case where two periods are given, the first period given, is the period for the first portion of the solution; the second for the latter portion of the solution.

Appendix A.

Terminology.

All terminology, in general, corresponded to standard NACA terminology.

The airplane axis system was the right-handed stability axis, (wind axis), system, commonly used by the NACA.

The positive directions of all forces and moments corresponded to the right hand rule system used by the NACA.

The symbols used in this thesis are as listed below:- [For forces and moments expressed as non-dimensional coefficients, see reference (9)].

β	Angle of sideslip, degrees or radians.
ϕ	Angle of roll, degrees or radians.
ψ	Angle of yaw, degrees or radians.
D	Differential operator, (d/dt)
t	Time, seconds.
$D\phi$, p	Rate of roll, degrees/second or radians/second.
$D\psi$, r	Rate of yaw, degrees/second or radians/second.
γ_0	Angle between relative wind and horizontal in longitudinal plane of aircraft, degrees or radians, (assumed constant throughout all solutions).
u_0	[redacted] Forward velocity of airplane, ft./sec., (assumed constant throughout all solutions.)
Subscript "0"	Refers to initial condition.
L'	Rolling moment, ft. lbs.
N	Yawing moment, ft. lbs.
Y	Side Force, lbs.
l'	L'/I_x, rolling moment, sec^{-2}.
n	N/I_z, yawing moment, sec^{-2}
y	Y/m, side force, $ft./sec.^2$
$l'_\beta, n_\beta, y_\beta$	$\partial l'/\partial\beta$; $\partial n/\partial\beta$; and $\partial y/\partial\beta$; respectively, $sec^{-2} radian^{-1} = sec^{-2}$
For Dead Spots in l'_β and n_β only. $(l')_\beta$, $(n)_\beta$	For positive and negative β, respectively:- $(l'_\beta\beta \pm l'_c)$, $(n_\beta\beta \mp n_c)$, outside dead spot, but zero inside dead spot, i.e.:- rolling and yawing moments due to β.
l'_c, n_c	$(2.0/57.3) \times l'_\beta$, and $(2.0/57.3) \times n_\beta$, respectively, sec^{-2}.
l'_p, n_p	$\partial l'/\partial p$ and $\partial n/\partial p$, respectively, sec^{-1}.
l'_r, n_r	$\partial l'/\partial r$ and $\partial n/\partial r$, respectively, sec^{-1}
	Angle between principal longitudinal axis and relative wind.

Appendix B.

Conversion of Stability Derivatives from Non-Dimensional Form to Dimensionsal Form with Units of Acceleration, for Airplane II.

The stability derivatives of Airplane II were converted from non-dimensional coefficient form to dimensional form with units of acceleration as indicated by the following sample calculation:- (Note that in addition to the data for Airplane II in TABLE II :- b = wing span = 27.7 ft. :- From Ref. (9)).

The damping in roll derivative in non-dimensional coefficient form is:- $C_{l_p} = -0.462$, (See TABLE II).
To convert to damping in roll derivative, with C_l in units of acceleration:-

$$l'_p = \left(\frac{\partial C_l}{\partial \frac{pb}{2u_0}}\right) \times (qSb)\left(\frac{b}{2u_0}\right)\left(\frac{1}{I_x}\right) = C_{l_p}\left(\frac{qSb}{I_x}\right)\left(\frac{b}{2u_0}\right)$$

$$q = \rho\frac{V^2}{2} = \frac{0.00089 \times 753^2}{2} = 252.0 \text{ lbs./ft.}^2$$

$$k_x^2 = K_{x_0}^2 \times b^2 = (0.0069) \times (27.7)^2 = 5.29 \text{ ft.}^2$$

$$\frac{qSb}{I_x} = \frac{qSb}{mk_x^2} = \frac{qSb}{\frac{W}{g}k_x^2} = \left[\frac{qg}{\left(\frac{W}{S}\right)}\right]\left(\frac{b}{k_x^2}\right) = \frac{(252.0)(32.2)}{80} \times \frac{27.7}{5.29}$$

$\frac{qSb}{I_x} = 531$ [redacted] sec.^{-2}

$$\frac{b}{2u_0} = \frac{27.7}{2 \times 753} = 0.01840 \text{ sec.}$$

Therefore:- $l'_p = (-0.462)(531)(0.01840) = -4.52 \text{ sec.}^{-1}$

Appendix C.

Lateral Stability Equations and the Laplace Transform Thereof.

The standard lateral stability equations as used by the NACA, in form suitable for applying the Laplace Transform are as follows:-

C-1
$$\begin{cases} (2\mu_b D_b - C_{y_\beta})\beta - (\tfrac{1}{2} C_{y_p} D_b + C_L)\phi + [(2\mu_b - \tfrac{1}{2} C_{y_r})D_b - C_L \tan\gamma_0]\psi = C_{y_\delta}\delta + C_{y_c} \\ -(C_{l_\beta})\beta + (2\mu_b K_x^2 D_b^2 - \tfrac{1}{2} C_{l_p} D_b)\phi - (2\mu_b K_{xz}^2 D_b^2 + \tfrac{1}{2} C_{l_r} D_b)\psi = C_{l_\delta}\delta + C_{l_c} \\ -(C_{n_\beta})\beta - (2\mu_b K_{xz}^2 D_b^2 + \tfrac{1}{2} C_{n_p} D_b)\phi + (2\mu_b K_z^2 D_b^2 - \tfrac{1}{2} C_{n_r} D_b)\psi = C_{n_\delta}\delta + C_{n_c} \end{cases}$$

When forces and moments are converted to units of acceleration, the above equations become:-

[redacted]

C-2
$$\begin{cases} (u_0 D - y_\beta)\beta - (y_p D + g\cos\gamma_0)\phi + [(u_0 - y_r)D - g\sin\gamma_0]\psi = y_\delta\delta + y_c \\ -(l'_\beta)\beta + (D^2 - L'_p D)\phi - (\frac{k_{xz}^2}{k_x^2} D^2 + L'_r D)\psi = l'_\delta\delta + l'_c \\ -(n_\beta)\beta - (\frac{k_{xz}^2}{k_z^2} D^2 + n_p D)\phi + (D^2 - n_r D)\psi = n_\delta\delta + n_c \end{cases}$$

If the controls are considered fixed, the Laplace transform of the above equations becomes as given on the following page:-

where:- $\bar{\beta}$, $\bar{\phi}$, and $\bar{\psi}$, are the transformed variables.
σ is the Laplace operator.
Subscript "o" refers to initial conditions.

C-3

$$\left\{\begin{aligned}
&(u_0\sigma - y_\beta)\bar{\beta} - (y_p\sigma + g\cos\gamma_0)\bar{\phi} + [(u_0 - y_r)\sigma - g\sin\gamma_0]\bar{\psi} \\
&\qquad = u_0\beta_0 - y_p\phi_0 + (u_0 - y_r)\psi_0 + \frac{y_c}{\sigma} \\
&-(l'_\beta)\bar{\beta} + (\sigma^2 - l'_p\sigma)\bar{\phi} - \left(\frac{k_{xz}^2}{k_x^2}\sigma^2 + l'_r\sigma\right)\bar{\psi} \\
&\qquad = \sigma\phi_0 + (D\phi)_0 - l'_p\phi_0 - \frac{k_{xz}^2}{k_x^2}[\sigma\psi_0 + (D\psi)_0] \\
&\qquad\quad - l'_r\psi_0 + \frac{l'_c}{\sigma} \\
&-(n_\beta)\bar{\beta} - \left(\frac{k_{xz}^2}{k_z^2}\sigma^2 + n_p\sigma\right)\bar{\phi} + (\sigma^2 - n_r\sigma)\bar{\psi} \\
&\qquad = -\frac{k_{xz}^2}{k_z^2}[\sigma\phi_0 + (D\phi)_0] - n_p\phi_0 + \sigma\psi_0 + (D\psi)_0 - n_r\psi_0 + \frac{n_c}{\sigma}.
\end{aligned}\right.$$

Equations C-3 may be solved simultaneously and algebraically, by the method of determinants for $\bar{\beta}$, $\bar{\phi}$, and $\bar{\psi}$.

Thus:-

$$\bar{\beta} = \frac{\bar{\Delta}_1}{\Delta}$$

$$\bar{\phi} = \frac{\bar{\Delta}_2}{\Delta}$$

$$\bar{\psi} = \frac{\bar{\Delta}_3}{\Delta}.$$

The determinants, when expanded, are polynomials, as follows:-

$$\bar{\Delta}_1 = f_1(\sigma) = A_1\sigma^4 + B_1\sigma^3 + C_1\sigma^2 + D_1\sigma + E_1$$

$$\bar{\Delta}_2 = f_2(\sigma) = A_2\sigma^4 + B_2\sigma^3 + C_2\sigma^2 + D_2\sigma + E_2 + \frac{F_2}{\sigma}$$

$$\bar{\Delta}_3 = f_3(\sigma) = A_3\sigma^4 + B_3\sigma^3 + C_3\sigma^2 + D_3\sigma + E_3 + \frac{F_3}{\sigma}$$

$$\bar{\Delta} = \sigma[F(\sigma)]$$

where:- $F(\sigma) = A\sigma^4 + B\sigma^3 + C\sigma^2 + D\sigma + E$.

By Heaviside's expansion theorem the solutions for β, ϕ, and ψ respectively, as functions of time are found to be:-

$$\beta = \frac{E_1}{E} + \sum_{n=1}^{4} \frac{f_1(\lambda_n)}{\lambda_n [F'(\lambda_n)]} e^{\lambda_n t}$$

$$\phi = \frac{E E_2 - F_2 D}{E^2} + \frac{F_2}{E} \times t + \sum_{n=1}^{4} \frac{f_{(2)}(\lambda_n)}{\lambda_n^2 [F'(\lambda_n)]} e^{\lambda_n t}.$$

$$\psi = \frac{E E_3 - F_3 D}{E^2} + \frac{F_3}{E} \times t + \sum_{n=1}^{4} \frac{f_{(3)}(\lambda_n)}{\lambda_n^2 [F'(\lambda_n)]} e^{\lambda_n t}.$$

(Note that in many cases, F_i and/or E_i are zero, making the first terms zero and enabling λ_n or λ_n^2, as the case may be, to be cancelled in the last term.)

Where:- λ_n are the four roots of $[F(\sigma)]$, respectively.

$$f_{(2)}(\lambda_n) = A_2\lambda_n^5 + B_2\lambda_n^4 + C_2\lambda_n^3 + D_2\lambda_n^2 + E_2\lambda_n + F_2$$

$$f_{(3)}(\lambda_n) = A_3\lambda_n^5 + B_3\lambda_n^4 + C_3\lambda_n^3 + D_3\lambda_n^2 + E_3\lambda_n + F_3$$

The general expressions for the coefficients of $F(\sigma)$, $f_1(\sigma)$, $f_2(\sigma)$, and $f_3(\sigma)$, are given on the following pages.

Note:- Simplification of Heaviside Expansion for the two complex roots:-

Let:- $\lambda_3 = c + id$, and $\lambda_4 = c - id$.

[redacted] $\frac{f_1(\lambda_3)}{\lambda_3[F'(\lambda_3)]} = ae^{ib}$; $\frac{f_1(\lambda_4)}{\lambda_4[F'(\lambda_4)]} = ae^{-ib}$

Then:- $$\frac{f_1(\lambda_3)}{\lambda_3[F'(\lambda_3)]} e^{\lambda_3 t} + \frac{f_1(\lambda_4)}{\lambda_4[F'(\lambda_4)]} e^{\lambda_4 t} = [ae^{ib}]e^{(c+id)t} + [ae^{-ib}]e^{(c-id)t}$$

$$= ae^{ct}[e^{i(b+dt)} + e^{-i(b+dt)}] = ae^{ct}[\cos(b+dt) + i\sin(b+dt) + \cos(b+dt) - i\sin(b+dt)]$$

$$= 2ae^{ct}\cos(b+dt).$$

(The above applies also to ϕ and ψ.)

Expansion of $\bar{\Delta} = \sigma[F(\sigma)] = \sigma(A\sigma^4 + B\sigma^3 + C\sigma^2 + D\sigma + E)$:-

$$A = u_0(1 - k_{xz}^4/k_x^2 k_z^2).$$

$$B = -[(y_\beta + u_0 n_r) + u_0 l'_p + (k_{xz}^2/k_x^2)(u_0 n_p) + (k_{xz}^2/k_z^2)(u_0 l'_r) - (k_{xz}^4/k_x^2 k_z^2)(y_\beta)]$$

$$C = [(y_\beta n_r + u_0 n_\beta - y_r n_\beta) + (l'_p y_\beta - l'_\beta y_p) + (k_{xz}^2/k_x^2)(n_p y_\beta - n_\beta y_p) + (k_{xz}^2/k_z^2)(l'_r y_\beta + u_0 l'_\beta - y_r l'_\beta) + u_0(l'_p n_r - l'_r n_p)].$$

$$D = -g[\cos\gamma_0(l'_\beta + \frac{k_{xz}^2}{k_x^2} n_\beta) + \sin\gamma_0(\frac{k_{xz}^2}{k_z^2} l'_\beta + n_\beta)] + y_\beta(l'_r n_p - l'_p n_r) + l'_\beta(y_p n_r - y_r n_p) + n_\beta(y_r l'_p - y_p l'_r) + u_0(l'_\beta n_p - n_\beta l'_p)$$

$$E = g[\cos\gamma_0(l'_\beta n_r - n_\beta l'_r) - \sin\gamma_0(l'_\beta n_p - n_\beta l'_p)].$$

Expansion of $\bar{\Delta}_1 = f_1(\sigma) = A_1\sigma^4 + B_1\sigma^3 + C_1\sigma^2 + D_1\sigma + E_1$:-

$$A_1 = \beta_0[u_0(1 - k_{xz}^4/k_x^2 k_z^2)]$$

$$B_1 = \beta_0[u_0(-\frac{k_{xz}^2}{k_z^2} l'_r - n_r - \frac{k_{xz}^2}{k_x^2} n_p - l'_p)] + \phi_0[g\cos\gamma_0(1 - k_{xz}^4/k_x^2 k_z^2)] + (D\phi)_0[y_p(1 - k_{xz}^4/k_x^2 k_z^2)] + \psi_0[g\sin\gamma_0(1 - k_{xz}^4/k_x^2 k_z^2)] + (D\psi)_0[(y_r - u_0)(1 - k_{xz}^4/k_x^2 k_z^2)] + y_c(1 - k_{xz}^4/k_x^2 k_z^2).$$

$$C_1 = \beta_0[u_0(l'_p n_r - l'_r n_p)] + \phi_0[g\cos\gamma_0(-\frac{k_{xz}^2}{k_z^2} l'_r - n_r - \frac{k_{xz}^2}{k_x^2} n_p - l'_p)] + (D\phi)_0[(n_p y_r - y_p n_r) + (g\cos\gamma_0 - n_p u_0) + \frac{k_{xz}^2}{k_z^2}(-l'_p u_0 - l'_r y_p + l'_p y_r) - g\cos\gamma_0 k_{xz}^4/k_x^2 k_z^2]$$
$$+ \psi_0[g\sin\gamma_0(-\frac{k_{xz}^2}{k_z^2} l'_r - n_r - \frac{k_{xz}^2}{k_x^2} n_p - l'_p)]$$
$$+ (D\psi)_0[\frac{k_{xz}^2}{k_x^2}(y_p n_r - n_p y_r) + (l'_r y_p - l'_p y_r) + g\sin\gamma_0(1 - k_{xz}^4/k_x^2 k_z^2) + u_0(l'_p + k_{xz}^2/k_x^2 n_p)]$$
$$- y_c[l'_p + n_r + \frac{k_{xz}^2}{k_z^2} l'_r + \frac{k_{xz}^2}{k_x^2} n_p] - l'_c[\frac{k_{xz}^2}{k_z^2}(u_0 - y_r) - y_p] + n_c[\frac{k_{xz}^2}{k_x^2} y_p - (u_0 - y_r)].$$

$$D_1 = \phi_0[g\cos\gamma_0(l'_p n_r - n_p l'_r)] + (D\phi)_0[g\sin\gamma_0(n_p + \frac{k_{xz}^2}{k_z^2} l'_p) + g\cos\gamma_0(-\frac{k_{xz}^2}{k_z^2} l'_r - n_r)]$$
$$+ \psi_0[g\sin\gamma_0(l'_p n_r - l'_r n_p)] + (D\psi)_0[g\cos\gamma_0(l'_r + \frac{k_{xz}^2}{k_x^2} n_r) + g\sin\gamma_0(-\frac{k_{xz}^2}{k_x^2} n_p - l'_p)]$$

$+ y_c[l'_p n_r - l'_r n_p]$ [redacted] $- l'_c[y_p n_r - g\cos\gamma_0 + n_p(u_0 - y_r) - (k_{xz}^2/k_z^2)(g\sin\gamma_0)]$

$$+ n_c[(k_{xz}^2/k_x^2)(g\cos\gamma_0) + l'_r y_p + g\sin\gamma_0 + l'_p(u_0 - y_r)].$$

$$E_1 = g(l'_c)(n_p\sin\gamma_0 - n_r\cos\gamma_0) + g(n_c)(l'_r\cos\gamma_0 - l'_p\sin\gamma_0).$$

Expansion of $\bar{\Delta}_2 = f_2(\sigma) = A_2\sigma^4 + B_2\sigma^3 + C_2\sigma^2 + D_2\sigma + E_2 + F_2/\sigma$:-

$$A_2 \doteq \phi_0\left[u_0(1 - k_{xz}^4/k_x^2 k_z^2)\right]$$

$$B_2 = \phi_0\left[-y_\beta - u_0 n_r - u_0 l'_p - (k_{xz}^2/k_z^2)u_0 l'_r - n_p u_0 k_{xz}^2/k_x^2 + y_\beta k_{xz}^4/k_x^2 k_z^2\right]$$
$$+ (D\phi)_0\left[u_0(1 - k_{xz}^4/k_x^2 k_z^2)\right].$$

$$C_2 = \phi_0\left[-y_p l'_\beta - n_p u_0 l'_r + y_\beta n_r + u_0 n_\beta - n_\beta y_r + l'_p y_\beta + l'_p u_0 n_r + k_{xz}^2/k_z^2(l'_\beta u_0 - l'_\beta y_r + y_\beta l'_r) + k_{xz}^2/k_x^2(-y_p n_\beta + n_p y_\beta)\right].$$
$$+ (D\phi)_0\left[-y_\beta - u_0 n_r - (k_{xz}^2/k_z^2)u_0 l'_r + (k_{xz}^4/k_x^2 k_z^2)y_\beta\right] + (D\psi)_0\left[u_0 l'_r + u_0 n_r k_{xz}^2/k_x^2\right]$$
$$+ \beta_0\left[u_0 l'_\beta + u_0 n_\beta k_{xz}^2/k_x^2\right] + l'_c(u_0) + n_c(u_0 k_{xz}^2/k_x^2).$$

$$D_2 = \phi_0\left[y_p l'_\beta n_r - y_p n_\beta l'_r - n_\beta g\sin\gamma_0 - l'_p y_\beta n_r - l'_p n_\beta u_0 + l'_p n_\beta y_r + n_p l'_\beta u_0 - n_p l'_\beta y_r + n_p y_\beta l'_r - l'_\beta g\sin\gamma_0 k_{xz}^2/k_z^2\right].$$
$$+ (D\phi)_0\left[y_\beta n_r + u_0 n_\beta - n_\beta y_r + (k_{xz}^2/k_z^2)(l'_\beta u_0 - l'_\beta y_r + y_\beta l'_r)\right].$$
$$+ \psi_0\left[l'_\beta g\sin\gamma_0 + n_\beta g\sin\gamma_0 k_{xz}^2/k_x^2\right] + (D\psi)_0\left[l'_\beta y_r - l'_\beta u_0 - y_\beta l'_r + k_{xz}^2/k_x^2(-y_\beta n_r - n_\beta u_0 + n_\beta y_r)\right].$$
$$+ \beta_0\left[-u_0 l'_\beta n_r + u_0 n_\beta l'_r\right] + y_c(l'_\beta + n_\beta k_{xz}^2/k_x^2) - l'_c(y_\beta + u_0 n_r)$$
$$+ n_c(u_0 l'_r - y_\beta k_{xz}^2/k_x^2).$$

$$E_2 = \phi_0\left[g\sin\gamma_0(l'_p n_\beta - n_p l'_\beta)\right] + (D\phi)_0\left[g\sin\gamma_0(-n_\beta - l'_\beta k_{xz}^2/k_z^2)\right]$$
$$+ \psi_0\left[g\sin\gamma_0(l'_r n_\beta - n_r l'_\beta)\right] + (D\psi)_0\left[g\sin\gamma_0(l'_\beta + n_\beta k_{xz}^2/k_x^2)\right]$$
$$- y_c(l'_\beta n_r - n_\beta l'_r) + l'_c\left[y_\beta n_r + n_\beta(u_0 - y_r)\right] - n_c\left[l'_\beta(u_0 - y_r) + y_\beta l'_r\right].$$

$$F_2 = -l'_c(n_\beta g\sin\gamma_0) + n_c(l'_\beta g\sin\gamma_0).$$

Expansion of $\Delta_3 = f_3(\sigma) = A_3\sigma^4 + B_3\sigma^3 + C_3\sigma^2 + D_3\sigma + E_3 + F_3/\sigma$:-

$$A_3 = \psi_0[u_0(1 - k_{xz}^4/k_x^2 k_z^2)]$$

$$B_3 = \psi_0[-y_\beta - u_0 l'_p - u_0 n_r - u_0 n_p k_{xz}^2/k_x^2 - u_0 l'_r k_{xz}^2/k_z^2 + y_\beta k_{xz}^4/k_x^2 k_z^2] + (D\psi)_0[u_0(1 - k_{xz}^4/k_x^2 k_z^2)]$$

$$C_3 = \psi_0[u_0 n_\beta - y_r n_\beta - u_0 l'_r n_p + y_\beta l'_p - l'_\beta y_p + n_r y_\beta + u_0 n_r l'_p + k_{xz}^2/k_z^2(u_0 l'_\beta - y_r l'_\beta + l'_r y_\beta) + k_{xz}^2/k_x^2(y_\beta n_p - n_\beta y_p)]$$

$+ (D\psi)_0[$ [redacted] $- y_\beta - u_0 l'_p - u_0 n_p k_{xz}^2/k_x^2 + y_\beta k_{xz}^4/k_x^2 k_z^2]$

$$+ (D\phi)_0[u_0 n_p + u_0 l'_p k_{xz}^2/k_z^2] + \beta_0[u_0 n_\beta + u_0 l'_\beta k_{xz}^2/k_z^2]$$

$$+ l'_c(u_0 k_{xz}^2/k_z^2) + n_c(u_0)$$

$D_3 = \psi_0[u_0 l'_\beta n_p - u_0 n_\beta l'_p - y_r l'_\beta$ [redacted] $n_p + y_r n_\beta l'_p - l'_r n_\beta y_p + l'_r y_\beta n_p - l'_\beta g\cos\gamma_0 - n_r y_\beta l'_p + n_r l'_\beta y_p - n_\beta g\cos\gamma_0 k_{xz}^2/k_x^2]$

$$+ (D\psi)_0[y_\beta l'_p - l'_\beta y_p + (k_{xz}^2/k_x^2)(y_\beta n_p - n_\beta y_p)] + \phi_0[n_\beta g\cos\gamma_0 + l'_\beta g\cos\gamma_0 k_{xz}^2/k_z^2]$$

$$+ (D\phi)_0[n_\beta y_p - y_\beta n_p + (k_{xz}^2/k_z^2)(l'_\beta y_p - y_\beta l'_p)] + \beta_0[u_0 l'_\beta n_p - u_0 n_\beta l'_p]$$

$$+ y_c(n_\beta + l'_\beta k_{xz}^2/k_z^2) + l'_c(u_0 n_p - y_\beta k_{xz}^2/k_z^2) - n_c(y_\beta + u_0 l'_p)$$

$$E_3 = \psi_0[n_r l'_\beta g\cos\gamma_0 - l'_r n_\beta g\cos\gamma_0] + (D\psi)_0[-l'_\beta g\cos\gamma_0 - n_\beta g\cos\gamma_0 k_{xz}^2/k_x^2]$$

$$+ \phi_0[n_p l'_\beta g\cos\gamma_0 - n_\beta l'_p g\cos\gamma_0] + (D\phi)_0[n_\beta g\cos\gamma_0 + l'_\beta g\cos\gamma_0 k_{xz}^2/k_z^2]$$

$$+ y_c(l'_\beta n_p - n_\beta l'_p) + l'_c(n_\beta y_p - y_\beta n_p) + n_c(y_\beta l'_p - l'_\beta y_p)$$

$$F_3 = l'_c(n_\beta g\cos\gamma_0) - n_c(l'_\beta g\cos\gamma_0).$$

Appendix D.

Sample Calculations for Hand Solutions for Response in β, Using Method of Laplace Transform.

Airplane I with dead spot non-linearity in l'_β.
Disturbance :- Disturbance in sideslip angle only of 5.0°.
i.e.:- $\beta_0 = 5.0° = 0.0872667$ radians.
(The results of this computation are plotted in Fig. 2).
Using the determinant expansions of Appendix C and the characteristics of Airplane I from TABLE I. :-

Outside the dead spot, ($l'_\beta = -5.0336$ sec.$^{-2}$, $l'_c = \pm\frac{2.0}{57.2957} \times l'_\beta = \mp 0.1757062$ sec.$^{-2}$, when β is +, l'_c is +; when β is −, l'_c is −):-
(Note that throughout the following, all coefficients are divided by $u_0 = 242$).

$$F(\sigma) = \sigma^4 + 8.911\sigma^3 + 7.705673\sigma^2 + 20.740123\sigma - 0.15860429.$$

$$F'(\sigma) = 4.0\sigma^3 + 26.733\sigma^2 + 15.411346\sigma + 20.740123$$

$$f_1(\sigma) = (\beta_0)\sigma^4 + [8.793\beta_0 + 0.13305785\phi_0 - (D\psi)_0]\sigma^3 + [4.4417\beta_0 + 1.1699776\phi_0 + 0.34505785(D\phi)_0 - 8.3(D\psi)_0]\sigma^2 + [0.5910030\phi_0 + 0.06559752(D\phi)_0 + 0.21954545(D\psi)_0 \pm 0.06062878]\sigma \pm 0.011525888$$ *

$f_2(\sigma) =$ [redacted] $(\phi_0)\sigma^5 + [8.911\phi_0 + (D\phi)_0]\sigma^4 + [7.705674\phi_0 + 0.611(D\phi)_0 + 1.65(D\psi)_0 - 5.0336\beta_0 \pm 0.17570616]\sigma^3 + [20.070363\phi_0 + 2.284574(D\phi)_0 + (5.22830)(D\psi)_0 + 1.1919952\beta_0 \pm 0.10735646]\sigma^2 \pm (0.04014372)\sigma.$

$$f_3(\sigma) = (\psi_0)\sigma^5 + [8.911\psi_0 + (D\psi)_0]\sigma^4 + [7.705674\psi_0 + 8.418(D\psi)_0 - 0.212(D\phi)_0 + 2.2264\beta_0]\sigma^3 + [20.740123\psi_0 + 0.9794(D\psi)_0 + 0.29624\phi_0 - 0.0250160(D\phi)_0 + 19.5462432\beta_0 \mp 0.0372497059\,2]\sigma^2 [-0.15860431\psi_0 + 0.66976(D\psi)_0 + 2.6007811\phi_0 + 0.29624(D\phi)_0 \mp 0.004395465]\sigma \pm 0.05205119.$$

Inside the dead spot, ($l'_\beta = 0$, $l'_c = 0$):-

$$F(\sigma) = \sigma^4 + 8.911\sigma^3 + 7.705673\sigma^2 + 19.003240\sigma - 0.4887959.$$

$$F'(\sigma) = 4.0\sigma^3 + 26.733\sigma^2 + 15.411346\sigma + 19.00324$$

$$f_1(\sigma) = (\beta_0)\sigma^4 + [8.793\beta_0 + 0.13305785\phi_0 - (D\psi)_0]\sigma^3 + [4.4417\beta_0 + 1.1699776\phi_0 + 0.34505785(D\phi)_0 - 8.3(D\psi)_0]\sigma^2 + [0.5910030\phi_0 + 0.06559752(D\phi)_0 + 0.21954545(D\psi)_0]\sigma$$

$$f_2(\sigma) = (\phi_0)\sigma^5 + [8.911\phi_0 + (D\phi)_0]\sigma^4 + [7.705674\phi_0 + 0.6110(D\phi)_0 + 1.65(D\psi)_0]\sigma^3 + [19.0032398\phi_0 + 2.284574(D\phi)_0 + 0.19470(D\psi)_0 + 3.67356\beta_0]\sigma^2.$$

$$f_3(\sigma) = (\psi_0)\sigma^5 + [8.9110\psi_0 + (D\psi)_0]\sigma^4 + [7.705674\psi_0 + 8.418(D\psi)_0 - 0.212(D\phi)_0 + 2.2264\beta_0]\sigma^3 + [19.0032406\psi_0 + 0.9794(D\psi)_0 + 0.29624\phi_0 - 0.025016(D\phi)_0 + 18.47912\beta_0]\sigma^2 + [0.4887956\psi_0 + 2.458792\phi_0 + 0.296240(D\phi)_0]\sigma.$$

* wherever two signs occur in these determinant evaluations, the upper sign corresponds to positive β, and the lower to negative β. This is due to l'_c.

The two real roots of $F(\sigma)$ were found by "Horner's Method". Using these roots, $F(\sigma)$ was then reduced to a quadratic. This quadratic was then solved for the conjugate pair of complex roots.

The roots of $F(\sigma)$ were thus found to be :-

Outside the Dead Spot.
$$\begin{cases} \lambda_1 = 0.007625426 \\ \lambda_2 = -8.2832892 \\ \lambda_3 = -0.317668113 + i\,1.5524477 = 1.5846157e^{i101.564375^\circ} \\ \lambda_4 = -0.317668113 - i\,1.5524477 = 1.5846157e^{-i101.564375^\circ} \end{cases}$$

Inside the Dead Spot.
$$\begin{cases} \lambda_1 = 0.0254513 \\ \lambda_2 = -8.2573862 \\ \lambda_3 = -0.33953255 + i\,1.4867857 = 1.5250620e^{i102.86400^\circ} \\ \lambda_4 = -0.33953255 - i\,1.4867857 = 1.5250620e^{-i102.86400^\circ} \end{cases}$$

Using the above roots, $F'(\lambda_n)$ was evaluated with the following results:-

Outside the Dead Spot.
$$\begin{cases} F'(\lambda_1) = 20.8591974 \\ F'(\lambda_2) = -546.049712 \\ F'(\lambda_3) = 39.967591e^{-i157.138197^\circ} \\ F'(\lambda_4) = 39.967591e^{i157.138197^\circ} \end{cases}$$

Inside the Dead Spot
$$\begin{cases} F'(\lambda_1) = 19.412862 \\ F'(\lambda_2) = -537.5805088 \\ F'(\lambda_3) = 36.674265e^{-i155.57267^\circ} \\ F'(\lambda_4) = 36.674265e^{i155.57267^\circ} \end{cases}$$

Using initial conditions, $\beta_0 = 0.0872667$ radians, and the above roots for $F(\sigma)$, outside the dead spot; $f_1(\lambda_n)$, $f_2(\lambda_n)$, and $f_3(\lambda_n)$, were evaluated for the first portion of the solution, (until the dead spot boundary, $\beta = 2.0^\circ$, is reached). The results were as follows:-

$f_1(\lambda_1) = 0.01201109$ $f_2(\lambda_1) = 0.04173789$ $f_3(\lambda_1) = 0.05211478$

$f_1(\lambda_2) = 0.82431$ $f_2(\lambda_2) = -19.79434$ $f_3(\lambda_2) = 4.144945$

$f_1(\lambda_3) = 2.6911748e^{-i63.150628^\circ}$ $f_2(\lambda_3) = 0.8271191e^{i45.318817^\circ}$ $f_3(\lambda_3) = 4.0645748e^{-i145.74047^\circ}$

$f_1(\lambda_4) = 2.6911748e^{i63.150628^\circ}$ $f_2(\lambda_4) = 0.8271191e^{-i45.318817^\circ}$ $f_3(\lambda_4) = 4.0645748e^{i145.74047^\circ}$

(Note that before evaluating the preceding functions, λ_n was cancelled out wherever possible between the numerator and denominator of the respective Heaviside Expansions as given on page C-3 of Appendix C.)

Using the above values in the Heaviside Expansions on page C-3, the following equations were found for the lateral responses as functions of time:- (t = time in seconds).

$$\beta = -0.07267072 + 0.07551282e^{0.007625426\times t} + 0.00018224497e^{-8.2832892\times t} + 0.084984454e^{-0.317668113\times t}\cos(-7.576808^\circ + t\times 88.94850^\circ);\ \text{radians}$$

$$\phi = -0.25309133 + 0.26240300e^{0.007625426\times t} - 0.004376289e^{-8.2832892\times t} + 0.026119574e^{-0.317668113\times t}\cos(100.89637^\circ + t\times 88.9485^\circ);\ \text{radians}$$

$$\psi = -42.88758 - 0.32818273\times t + 42.967005e^{0.007625426\times t} - 0.0001063204e^{-8.2832892\times t} + 0.081000784e^{-0.317668113\times t}\cos(168.26897^\circ + t\times 88.9485^\circ),\ \text{radians}$$

Differentiation of ϕ and ψ yields, respectively rate of roll and rate of yaw which are found to be as follows:-

$$D\phi = 0.0020009347e^{0.007625426\times t} + 0.036250067e^{-8.2832892\times t} - 0.0082973557e^{-0.317766811\times t}\cos(100.892637^\circ + t\times 88.9485^\circ) - 0.040549273e^{-0.317766811\times t}\sin(100.892637^\circ + t\times 88.9485^\circ);\ \text{rad./sec.}$$

$$D\psi = -0.32818273 + 0.32764172e^{0.007625426\times t} + 0.0009163 9718e^{-8.2832892\times t} - 0.025731366e^{-0.317766811\times t}\cos(168.26897^\circ + t\times 88.9485^\circ) - 0.12574948e^{-0.317766811\times t}\sin(168.26897^\circ + t\times 88.9485^\circ);\ \text{rad./sec.}$$

The preceding expressions for the lateral responses are valid only until the dead spot boundary, $\beta = +2.0^\circ$, is first crossed. As the dead spot boundary is crossed another set of solutions for the lateral responses must be found, as the airplane is then within the dead spot.

The procedure is as follows, and is the procedure given in reference (9):-

β as given on the bottom of page D-2 was evaluated in degrees every 0.2 second starting at zero time until a value of β less than $+2.0^\circ$ was reached. The resulting curve was plotted on Fig. 2. From Fig. 2 the approximate time at which the dead spot boundary was crossed was found to be 0.78 seconds.

This time, ($t = 0.78$ seconds), was substituted in the preceding equations for the lateral responses. This gave the exact values of all the lateral responses at 0.78 seconds, which was now assumed to be the time at which the dead spot boundary was first crossed. The resulting values for the lateral responses were used as the initial conditions for the next section of the solution, which was, of course, inside the the dead spot. Using these initial conditions, this second portion of the solution was formulated exactly as was done for the first portion except that the various values pertaining to inside the dead spot were used. All lateral responses were found for this second portion of the solution. For purposes of computation, time was taken as zero at the beginning of this second portion of the solution. Thus, this time was added to 0.78 seconds, to give time with respect to the beginning of the entire solution. The time for the second crossing of the dead spot boundary, $\beta = -2.0^\circ$, was found as outlined above for the first crossing. The values of the lateral responses at the second dead

spot crossing were used as the initial conditions for the third portion of the solution which was outside the dead spot. This procedure must be repeated each time the dead spot boundaries are crossed. As can be seen from Fig. 2, the dead spot boundaries were crossed three times, and thus there were four portions of the total solution, the response in β, remaining within the dead spot throughout the fourth portion.

The initial conditions and the equation for β response for each portion of the solution are given below.

First Portion of Solution.

Begins at 0 seconds.

Initial Conditions:- $\beta_0 = 5.0° = 0.0872667$ radians.

$$\beta = -0.07267072 + 0.07551282 e^{0.007625426 \times t} + 0.00018224497 e^{-8.2832892 \times t} + 0.08498454 e^{-0.31766811 \times t} \cos(-7.576808° + t \times 88.9485°), \text{radians.}$$

Second Portion of Solution.

Begins at 0.78 seconds.

Initial Conditions:- $\beta_0 = 0.03463540$ rad.; $\phi_0 = -0.00922383$; $(D\phi)_0 = 0.00310512$ rad./sec.
$\psi_0 = 0.045931$ radians; $(D\psi)_0 = 0.09507922$ rad./sec..

$$\beta = -0.000033740516 e^{0.0254513 \times t} - 0.00007487250 e^{-8.2573862 \times t} + 0.06933834 e^{-0.33953255 \times t} \cos(59.92845° + t \times 85.186353°); \text{radians}$$

Third Portion of Solution.

Begins at 1.63 seconds.

Initial Conditions:- $\beta_0 = -0.03502612$ radians; $\phi_0 = 0.00354795$ radians;
$(D\phi)_0 = 0.012185$ rad/sec.; $\psi_0 = 0.11568017$ rad.; $(D\psi)_0 = 0.04782584$ rad/sec.

$$\beta = 0.07267072 - 0.07492669 e^{0.007625426 \times t} + 0.00014120221 e^{-8.2832892 \times t} + 0.04736394 e^{-0.31766811 \times t} \cos(134.016815° + t \times 88.94850°); \text{radians.}$$

Fourth Portion of Solution.

Begins at 2.46 seconds

Initial Conditions:- $\beta_0 = -0.03490522$ radians; $\phi_0 = 0.01138474$ radians;
$(D\phi)_0 = 0.00637316$ rad/sec.; $\psi_0 = 0.120284$ rad.; [redacted]
$(D\psi)_0 = -0.03056453$ rad./sec..

$$\beta = 0.00016294609 e^{0.0254513 \times t} + 0.00005528660 e^{-8.2573862 \times t} + 0.03886165 8 e^{-0.33953255 \times t} \cos(-154.67431° + t \times 85.186353°); \text{radians}$$

The response in β, for $\beta_0 = 5.0°$, for Airplanes I and II with no non-linearities require only the calculations as outlined to obtain β for the first portion of this solution, (except that $\zeta_c' = 0$), and of course no other lateral responses need be calculated in this case. Thus, the calculations for the case with no non-linearities are much shorter than those for the case where a dead spot is involved.

Appendix E

The lateral dynamic stability equations (Equations, C-2), were transposed to the following form for solution by the REAC computer:-

$$
\left.
\begin{aligned}
D\beta &= y_\beta/u_0\,\beta + \frac{y_p}{u_0} D\phi + \frac{g\cos\gamma_0}{u_0}\phi - \frac{(u_0 - y_r)}{u_0} D\psi + \frac{g\sin\gamma_0}{u_0}\psi \\
D^2\phi &= l'_\beta \beta + l'_p D\phi + \frac{k_{xz}^2}{k_x^2} D^2\psi + l'_r D\psi \\
D^2\psi &= n_\beta \beta + \frac{k_{xz}^2}{k_z^2} D^2\phi + n_p D\phi + n_r D\psi
\end{aligned}
\right\} \quad \text{E-1.}
$$

The schematic wiring diagram of the REAC with no non-linearities in force or moment derivatives is given below:-

(◫▷ ~ Integrating amplifiers.) , (I).
(▷ ~ Summing and phase inverter amplifiers.) , (S).
(○ ~ Multiplying potentiometers.) , (P).

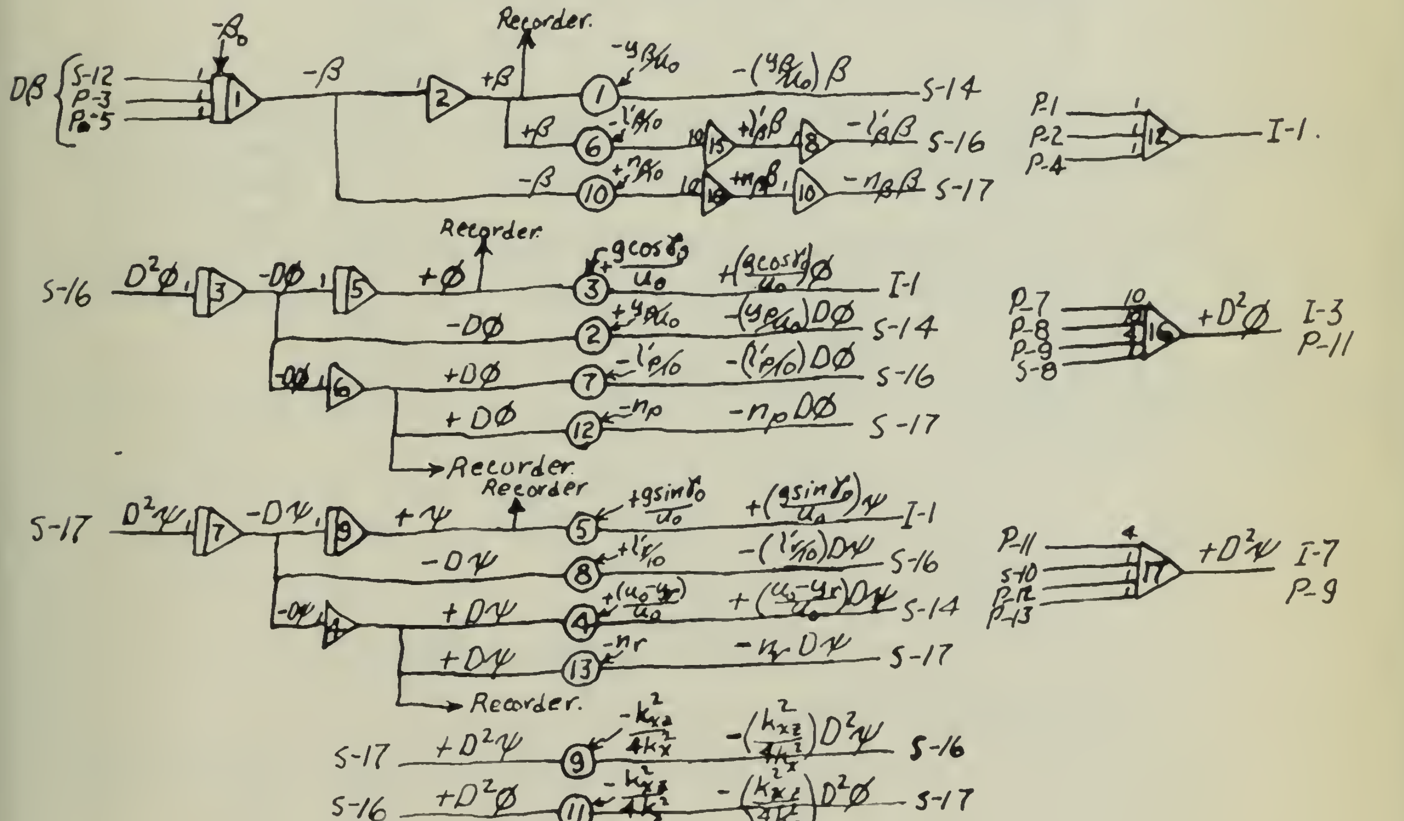

Notes:- Above diagram is for Airplane I

For Airplane II following changes are made:-

Remove P-8 from circuit; connect S-8 output to S-16, Gain 10, instead of S-16, Gain 1; connect S-10 output to S-17, Gain 10, instead of S-17, Gain 1; (These notes continued on next page.)

Continuation of "Notes" for REAC wiring diagram on the preceding page:-

For Airplane II, P-6 and P-10 settings are, respectively, $-l'_\beta/100$ and $+n_\beta/100$.

Outputs of S-15 and S-18 are, respectively, $+l'_\beta\beta/10$ and $+n_\beta\beta/10$.

For Airplane I, 1 volt = 1.0°.

For Airplane II, 1 volt = 5.0°.

Therefore, for the 5° disturbance:-

For Airplane I ~ $-\beta_0 = -5.0$ volts.

For Airplane II ~ $-\beta_0 = -1.0$ volt.

Schematic REAC Wiring Diagram for Dead Spot in l'_β:-

Notes:- $l'_\beta = \partial l'/\partial\beta$

$(l')_\beta = l'$ due to $\beta = l'_\beta\beta$ for no dead spot in l'_β.

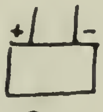

~ Limiters, (L).

Primed numbers refer to elements of computer #2, unprimed numbers to elements of computer #1, i.e.:-

(10) indicates summing amplifier 10 for REAC computer #1, (actually phase inverter 10).

(10') indicates summing amplifier 10 for REAC computer #2, (actually phase inverter 10).

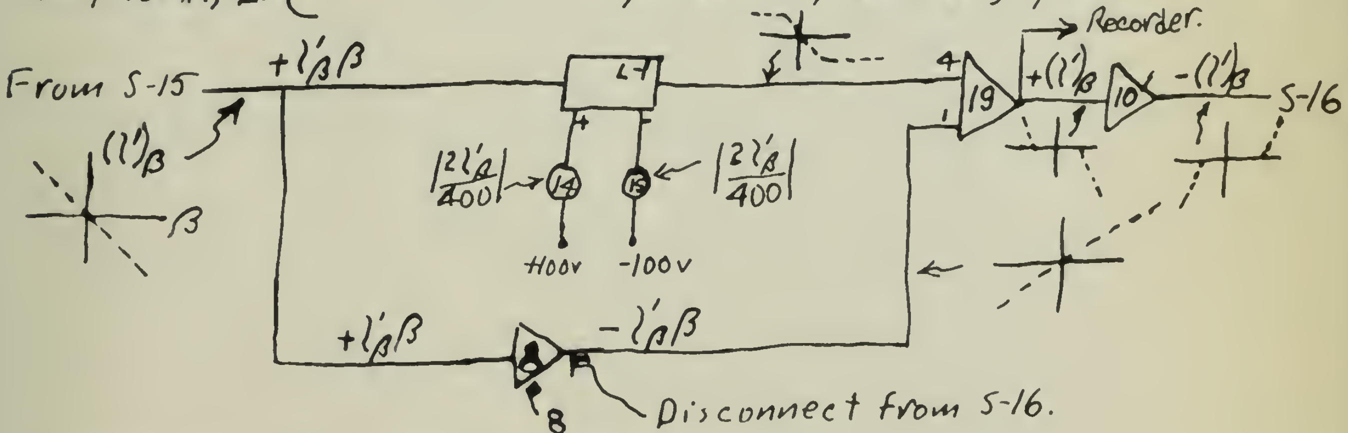

To simulate $l'_\beta\beta$ for REAC solution I-1:-

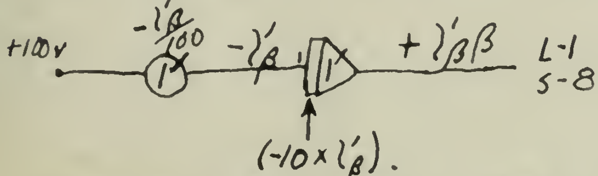

i.e.:- t in seconds is equivalent to β in degrees.

Above wiring is for Airplane I; Wiring is similar for Airplane II.

Schematic REAC Wiring Diagram for Dead Spot in n_β :-

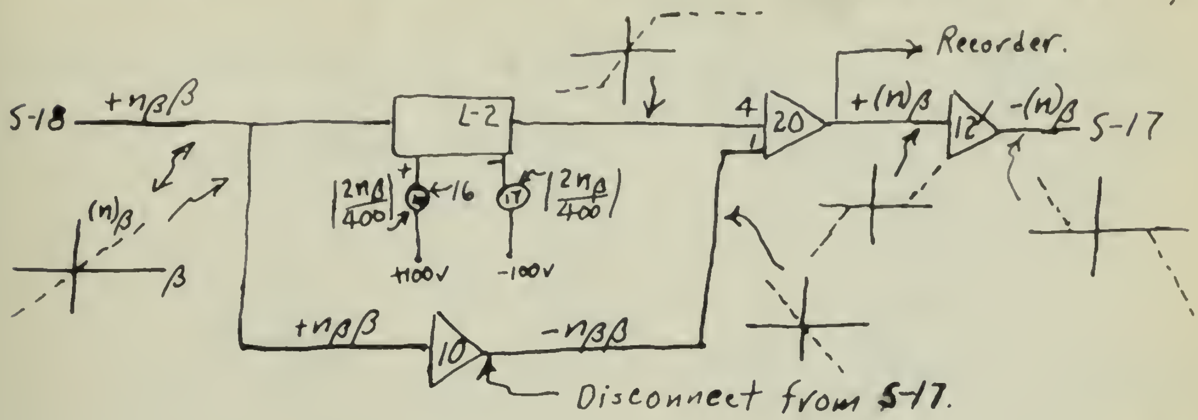

To simulate $n_\beta\beta$ for REAC solution I-1 :-

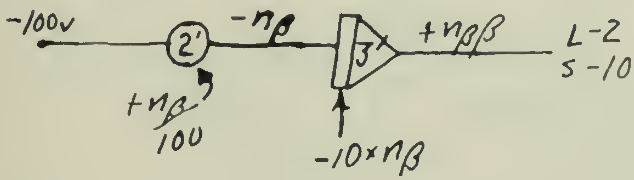

i.e.:- t in seconds is equal to β in degrees.

Above wiring is for Airplane I; Wiring is similar for Airplane II.

REAC Wiring Diagram for Dead Spots in l_r' and n_r :-

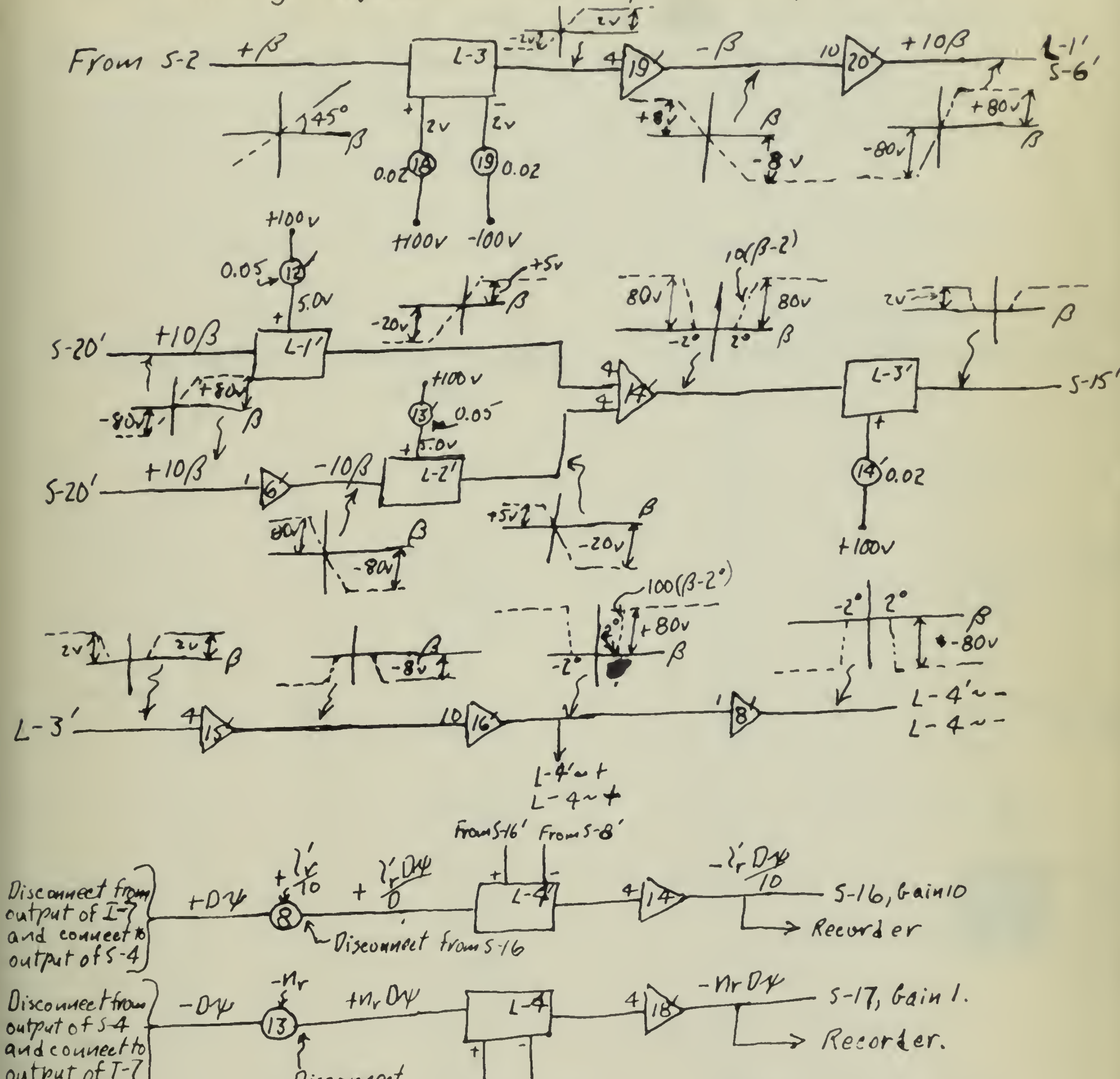

Above wiring is for Airplane I; wiring is similar for Airplane II.

To simulate β for REAC solution I-1:-

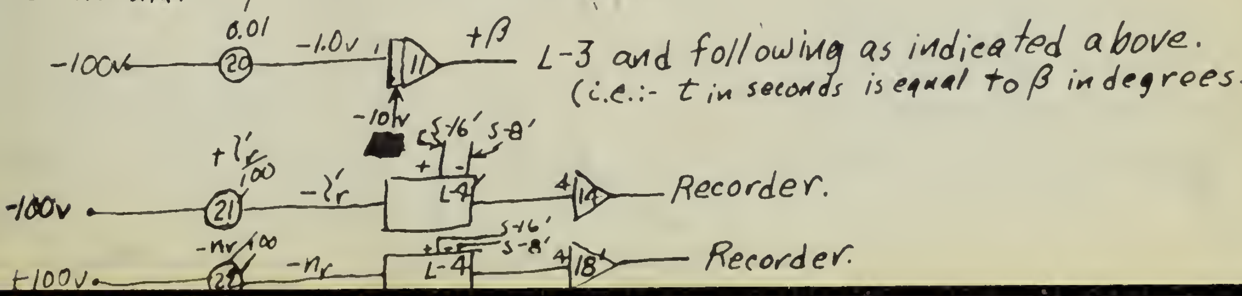

Potentiometer and Initial Condition Settings.

Note that in some cases where dead spot non-linearities are involved, especially in the case of Airplane II, the potentiometer settings are different than would be expected. These settings were determined by trial and error to give proper dead spot limiting.

Settings for All Solutions Except I-1 and II-1.

	Airplane I. Potentiometer No.	Airplane I. Potentiometer Setting	Airplane II. Potentiometer No.	Airplane II. Potentiometer Setting
No non-linearities and also for all non-linearities	1	0.1180	1	0
	2	0	2	0
	3	0.13406	3	0.0428
	4	1.0	4	1.0
	5	0	5	0
	6	0.54036	6	0.710* 0.904**
	7	0.859	7	0.486
	8	0.172	8	0
	9	0	9	0
	10	0.2347	10	0.1871* 0.3435**
	11	0	11	0
	12	0.213	12	0.0183
	13	0.497	13	0.464
Dead Spot in l'_β	14	0.031	14	[redacted] 0.018
	15	0.031	15	0.018
Dead Spot in n_β	16	0.0169	16	0.012
	17	0.0169	17	0.012
Dead spot in l'_r and/or n_r	18	0.02	18	0.04
	19	0.02	19	0.04
	12′	0.05	12′	0.0175
	13′	0.055	13′	0.0175
	14′	0.02	14′	0.04

* Values used with no dead spots in l'_β and n_β, respectively.

** Values used with dead spots in l'_β and n_β, respectively.

For Airplane I:- $5v = 5.0°$

For Airplane II:- $1v = 5.0°$

Therefore:- (Initial conditions on integrator) For Airplane I: $-\beta_0 = -5v$ and $-1v$
For Airplane II: $-\beta_0 = -1v$ and $-0.2v$
for 5° and 1° disturbances, respectively.

Settings for Solutions I-1 and II-1.

Potentiometer or Integrator	Setting for Solution I-1	Setting for Solution II-1.
I-1′	I.C. = +50.45 volts.	I.C. = +66.93 volts
P-1′	0.051	0.066
P-14	0.025	0.032
P-15	0.037	0.042
I-3′	I.C. = -29.00 volts	I.C. = -22.43 volts.
P-2′	0.0265	0.0205
P-16	0.0160	0.0120
P-17	0.251	0.0202
I-11	I.C. = -10.00 volts	-10.00 volts.
P-20	0.009	0.009
P-21′	0.0135	0
P-22′	0.0035	0.0033
P-18	0.010	0.010
P-19	0.0270	0.0270
P-12′	0.0540	0.0540
P-13′	0.040	0.040
P-14′	0.020	0.020

For both solutions I-1 and II-1, time in seconds is equivalent to sideslip angle β in degrees.

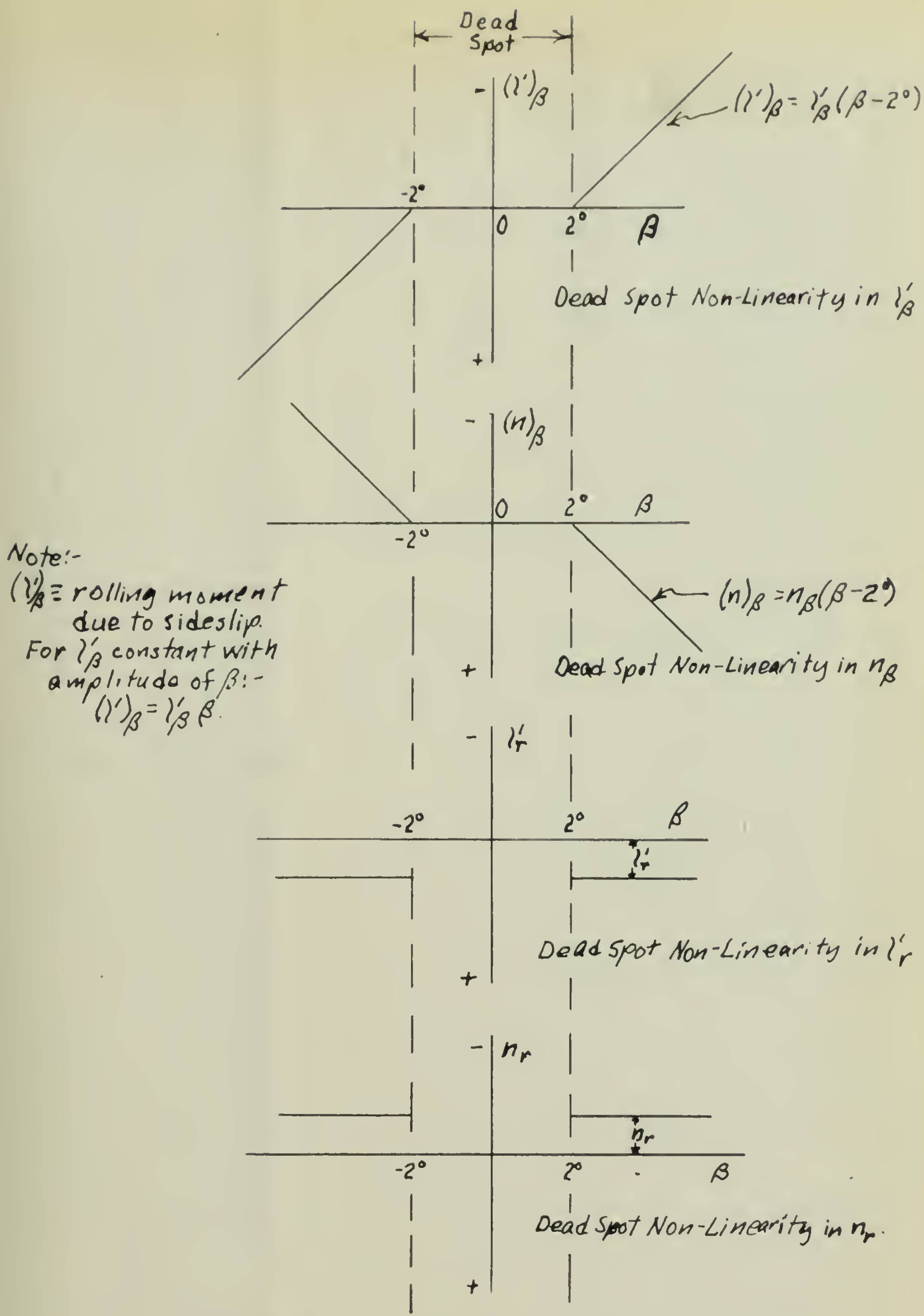

Illustration of the Nature of the Various Assumed Dead Spot Non-Linearities.

Fig. [redacted]1.

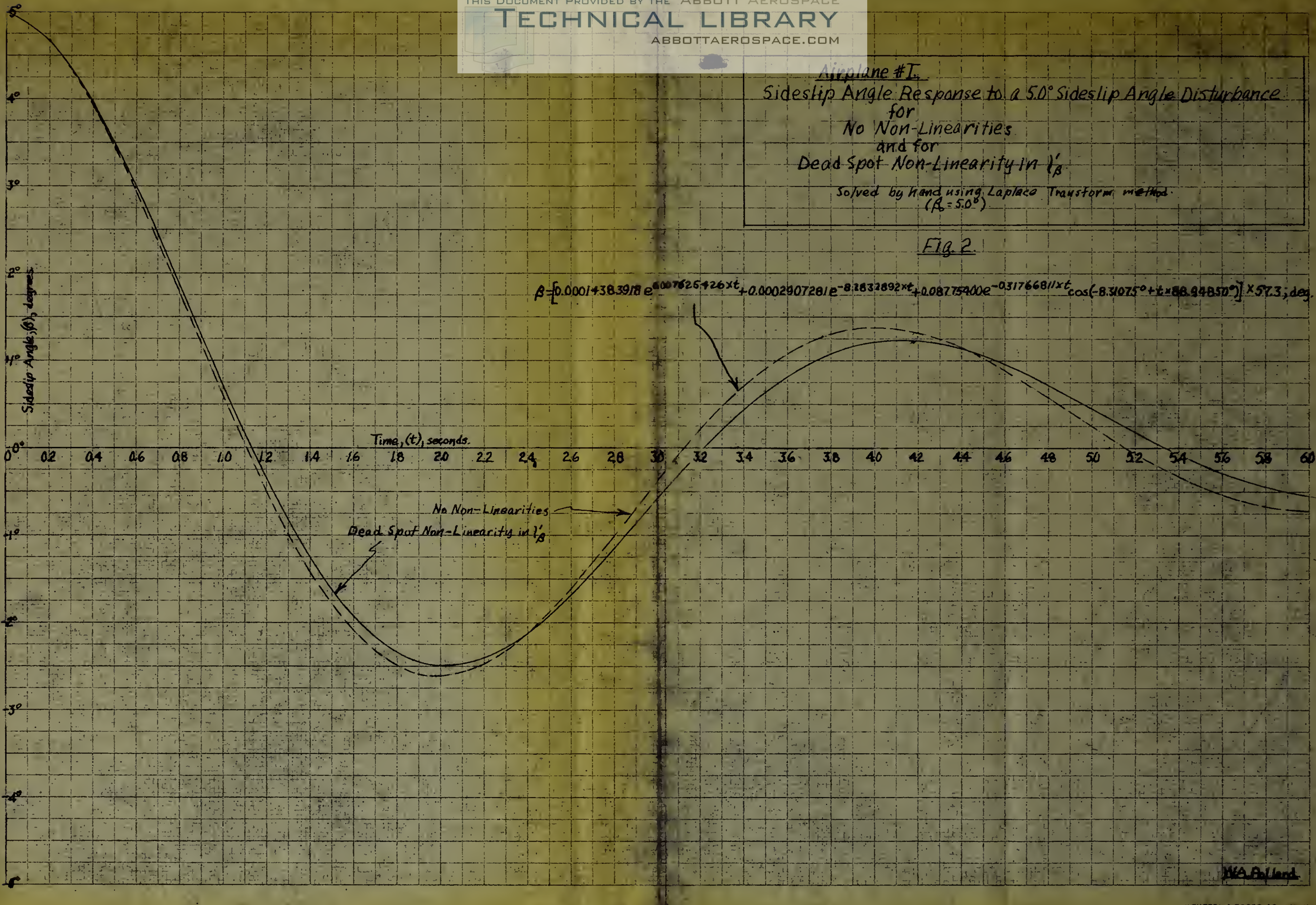
Airplane #I.
Sideslip Angle Response to a 5.0° Sideslip Angle Disturbance
for
No Non-Linearities
and for
Dead Spot Non-Linearity in l'_β
Solved by hand using Laplace Transform method
(β_0 = 5.0°)
$\beta = [0.0001438391\!8\, e^{0.007625426 \times t} + 0.0002907281\, e^{-8.2832892 \times t} + 0.08775400\, e^{-0.3176681 \times t} \cos(-8.31075° + t \times 88.94850°)] \times 57.3$; deg.
Sideslip Angle, (β), degrees
Time, (t), seconds.
No Non-Linearities
Dead Spot Non-Linearity in l'_β
5°
4°
3°
2°
1°
0°
-1°
-2°
-3°
-4°
-5°
0
0.2
0.4
0.6
0.8
1.0
1.2
1.4
1.6
1.8
2.0
2.2
2.4
2.6
2.8
3.0
3.2
3.4
3.6
3.8
4.0
4.2
4.4
4.6
4.8
5.0
5.2
5.4
5.6
5.8
6.0
W.A. Pollard
KEUFFEL & ESSER CO. N.Y.

Fig. 2.

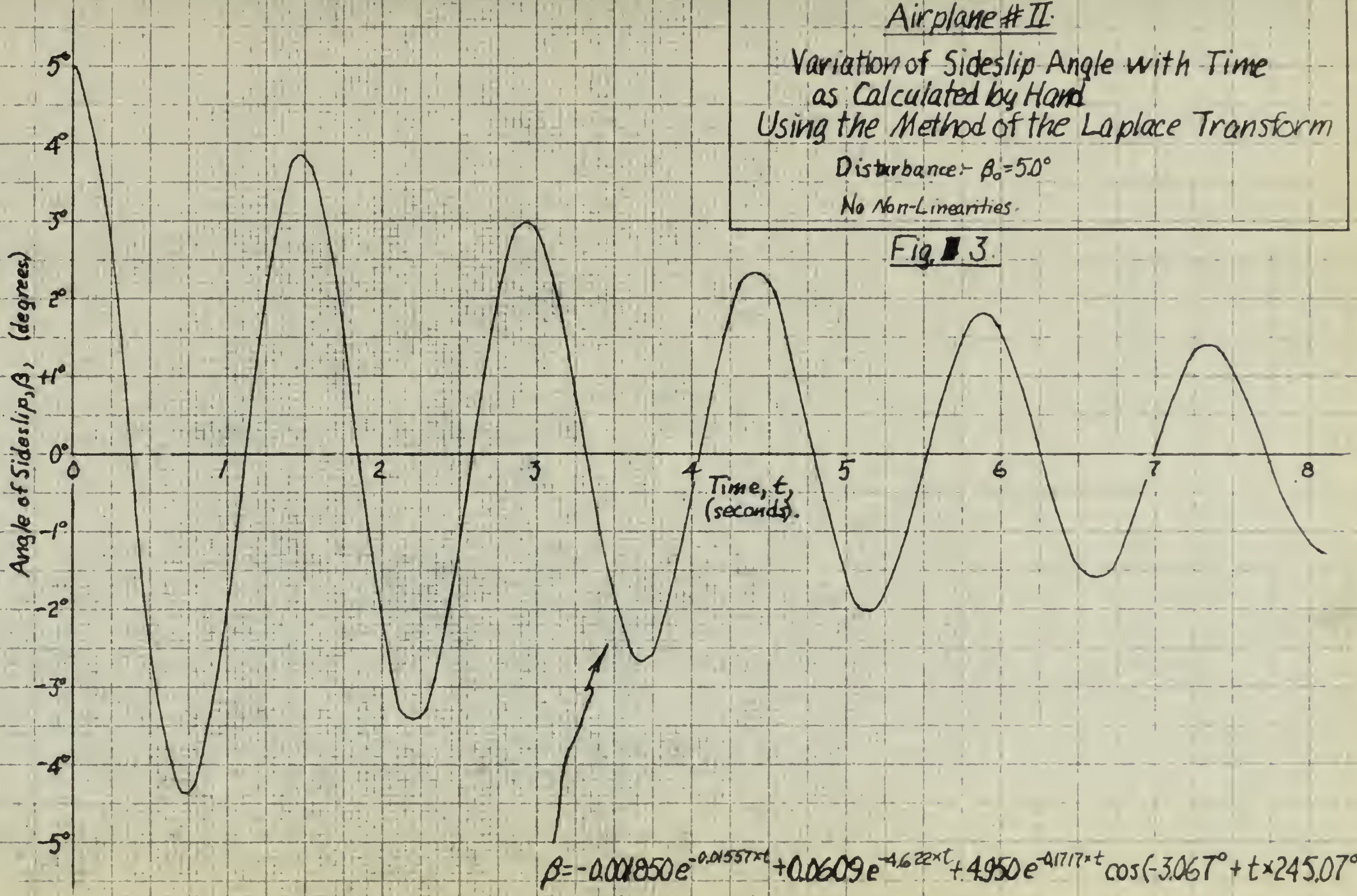

$$\beta = -0.001850 e^{-0.01557 \times t} + 0.0609 e^{-4.622 \times t} + 4.950 e^{-0.1717 \times t} \cos(-3.06T^{\circ} + t \times 245.07^{\circ}), \text{ degrees}$$

Airplane # II.

Variation of Sideslip Angle with Time as Calculated by Hand Using the Method of the Laplace Transform

Disturbance:- $\beta_o = 5.0°$

No Non-Linearities.

Fig. [redacted] 3.

W.A.P.

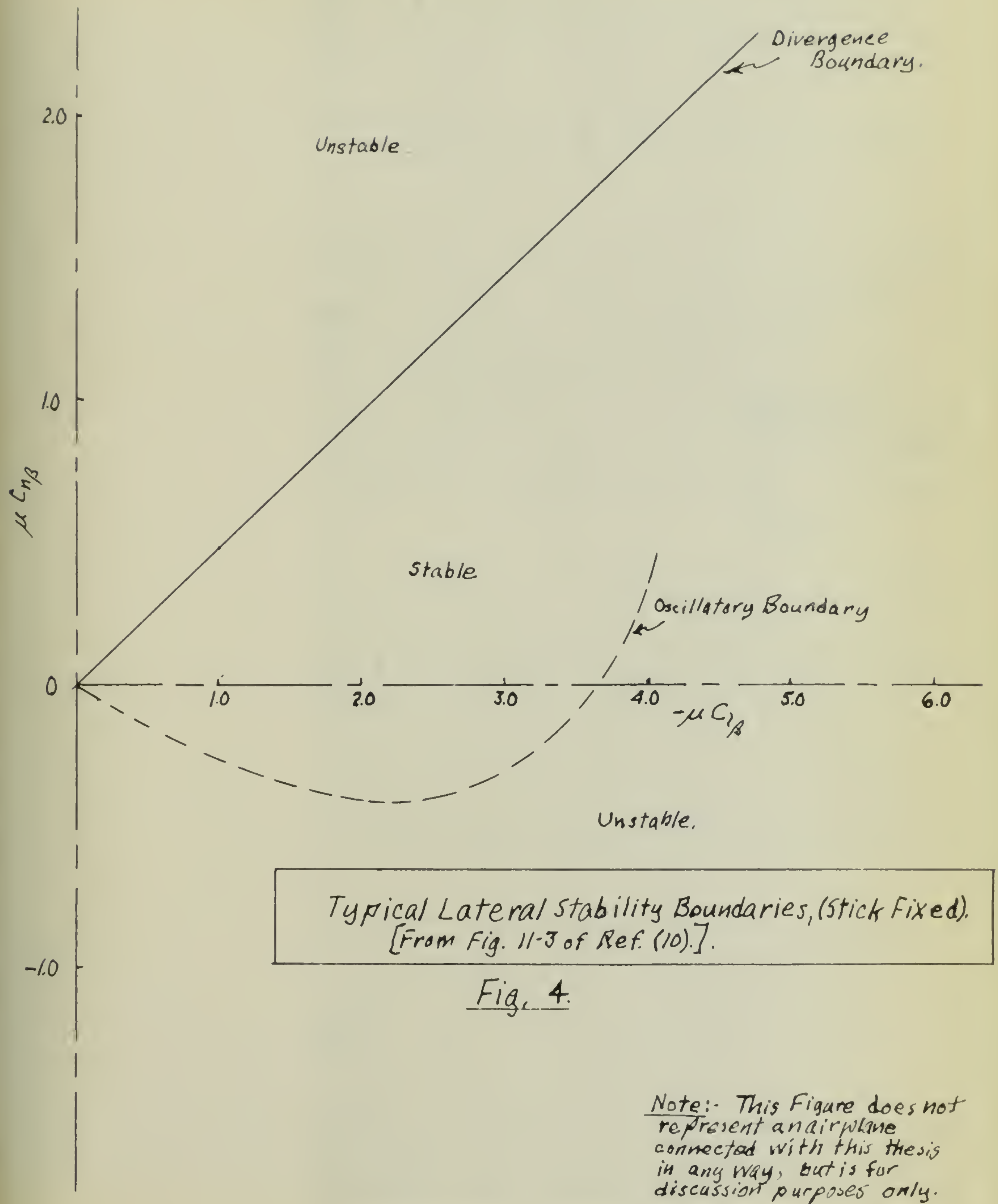

Typical Lateral Stability Boundaries, (Stick Fixed). [From Fig. 11-3 of Ref. (10).].

Fig. 4.

Note:- This Figure does not represent an airplane connected with this thesis in any way, but is for discussion purposes only.

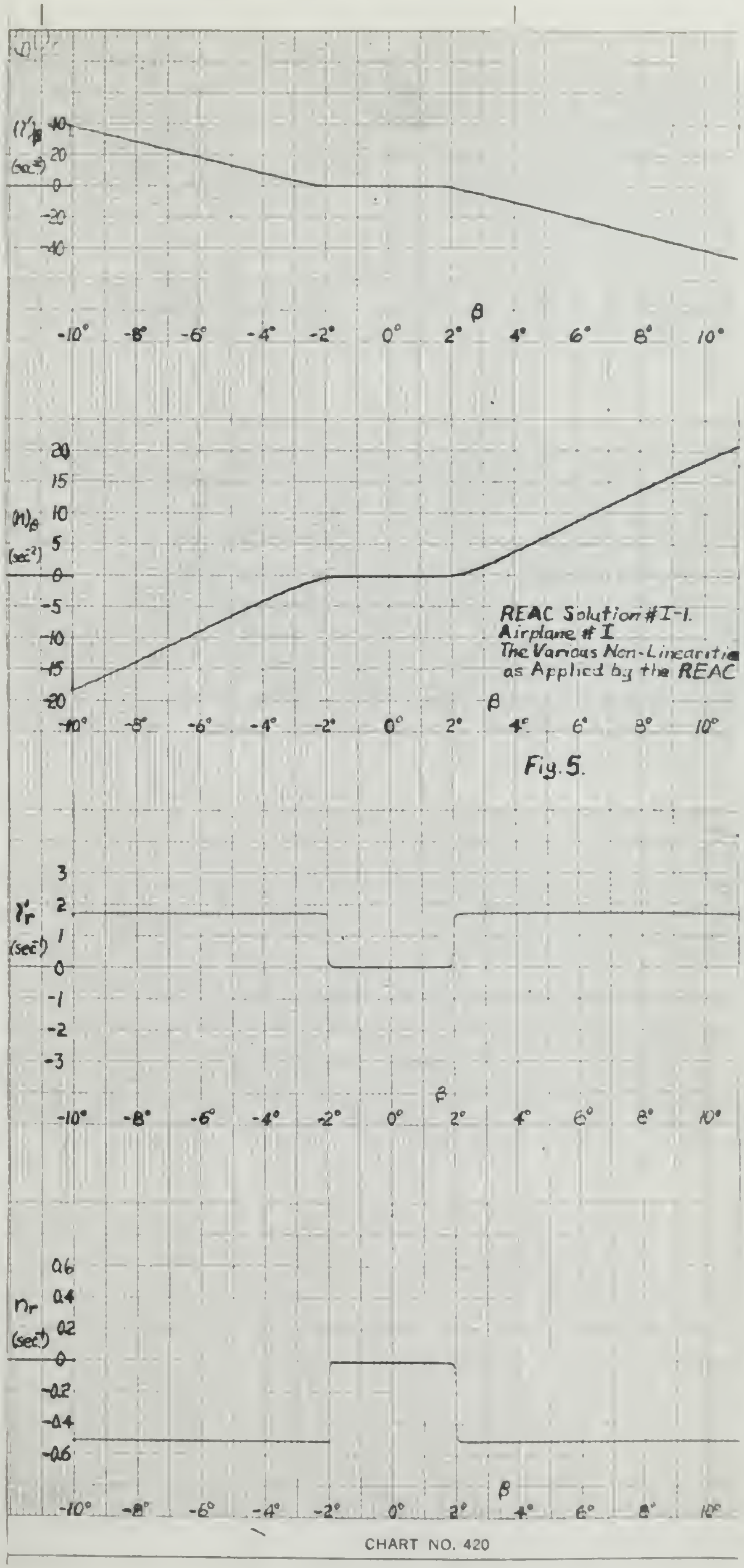

REAC Solution #I-1.
Airplane #I
The Various Non-Linearities as Applied by the REAC

Fig. 5.

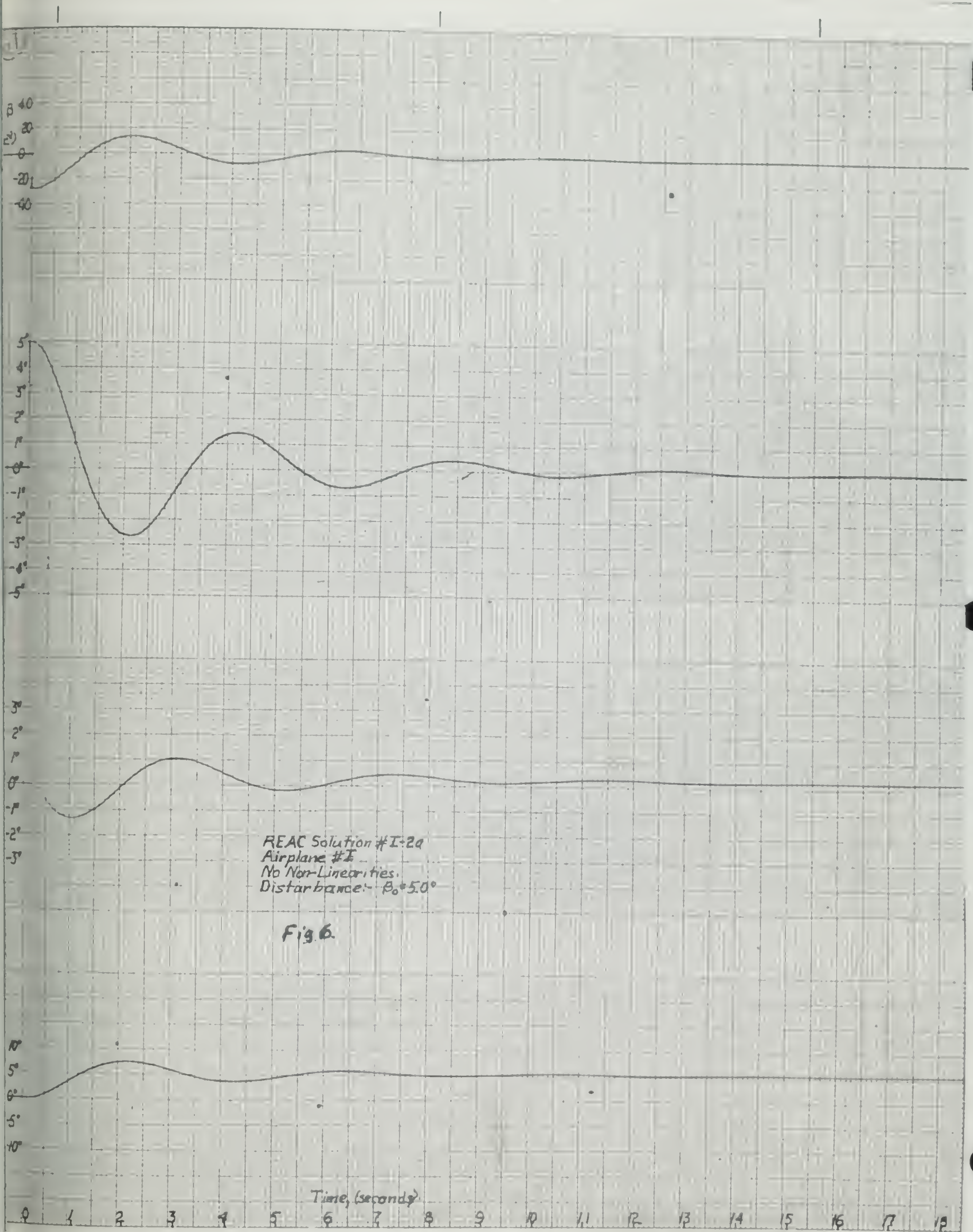
40
20
0
-20
-40
5°
4°
3°
2°
1°
0°
-1°
-2°
-3°
-4°
-5°
3°
2°
1°
0°
-1°
-2°
-3°
REAC Solution #I-2a
Airplane #I
No Non-Linearities.
Disturbance:- β_0=5.0°
Fig. 6.
10°
5°
0°
-5°
-10°
Time, (seconds)
0 1 2 3 4 5 6 7 8 9 10 11 12 13 14 15 16 17 18

CHART NO. 420

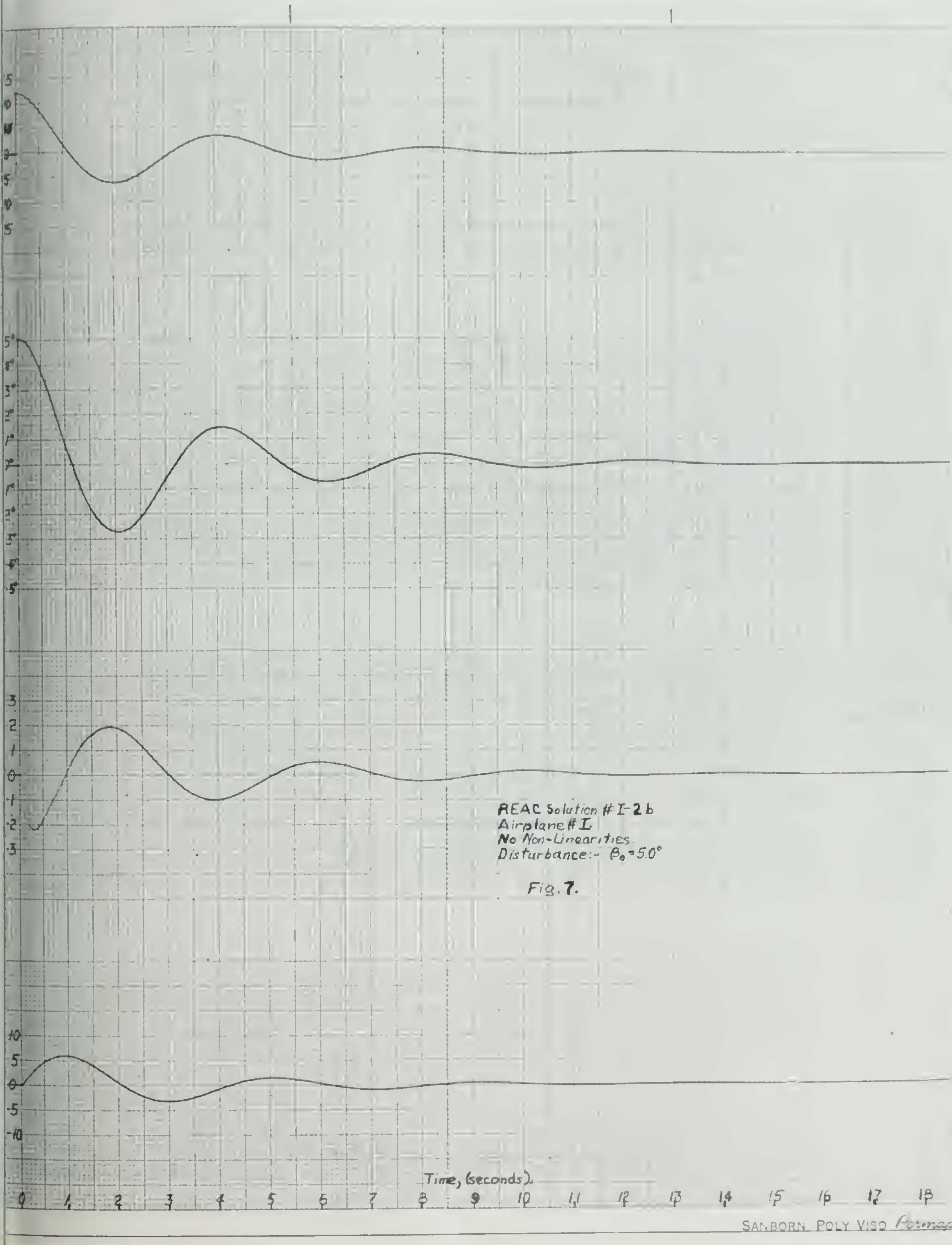
REAC Solution # I-2 b
Airplane # I
No Non-Linearities.
Disturbance:- β_0 = 5.0°
Time, (seconds).
0 1 2 3 4 5 6 7 8 9 10 11 12 13 14 15 16 17 18
SANBORN POLY VISO

Fig. 7.

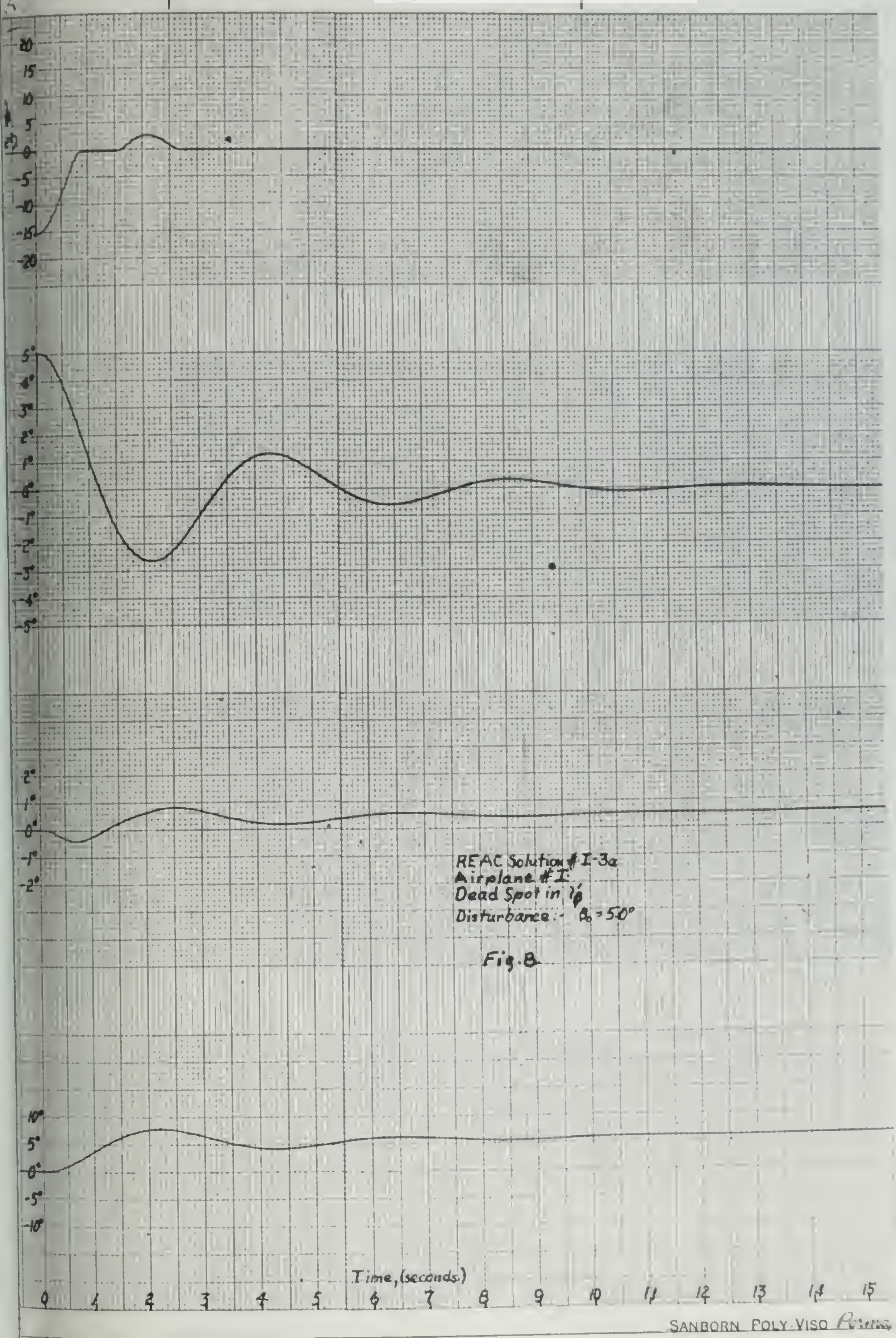
20
15
10
5
0
-5
-10
-15
-20
5°
4°
3°
2°
1°
0°
-1°
-2°
-3°
-4°
-5°
2°
1°
0°
-1°
-2°
REAC Solution # I-3a
Airplane # I
Dead Spot in $\dot{\psi}$
Disturbance: - ϕ_0 = 5.0°
10°
5°
0°
-5°
-10
Time, (seconds)
0
1
2
3
4
5
6
7
8
9
10
11
12
13
14
15
SANBORN POLY-VISO

Fig. 8

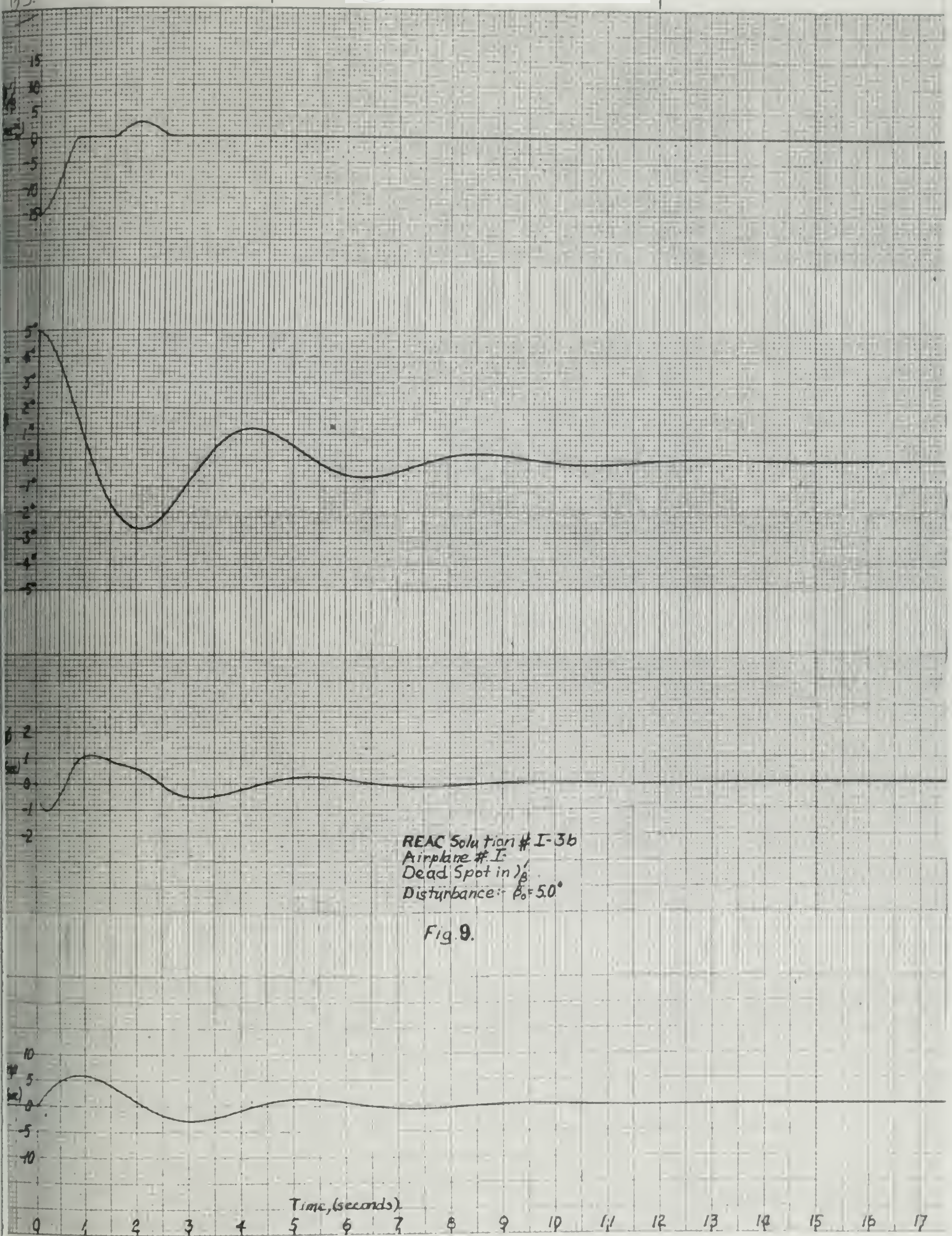

Fig. 9.

CHART NO. 420

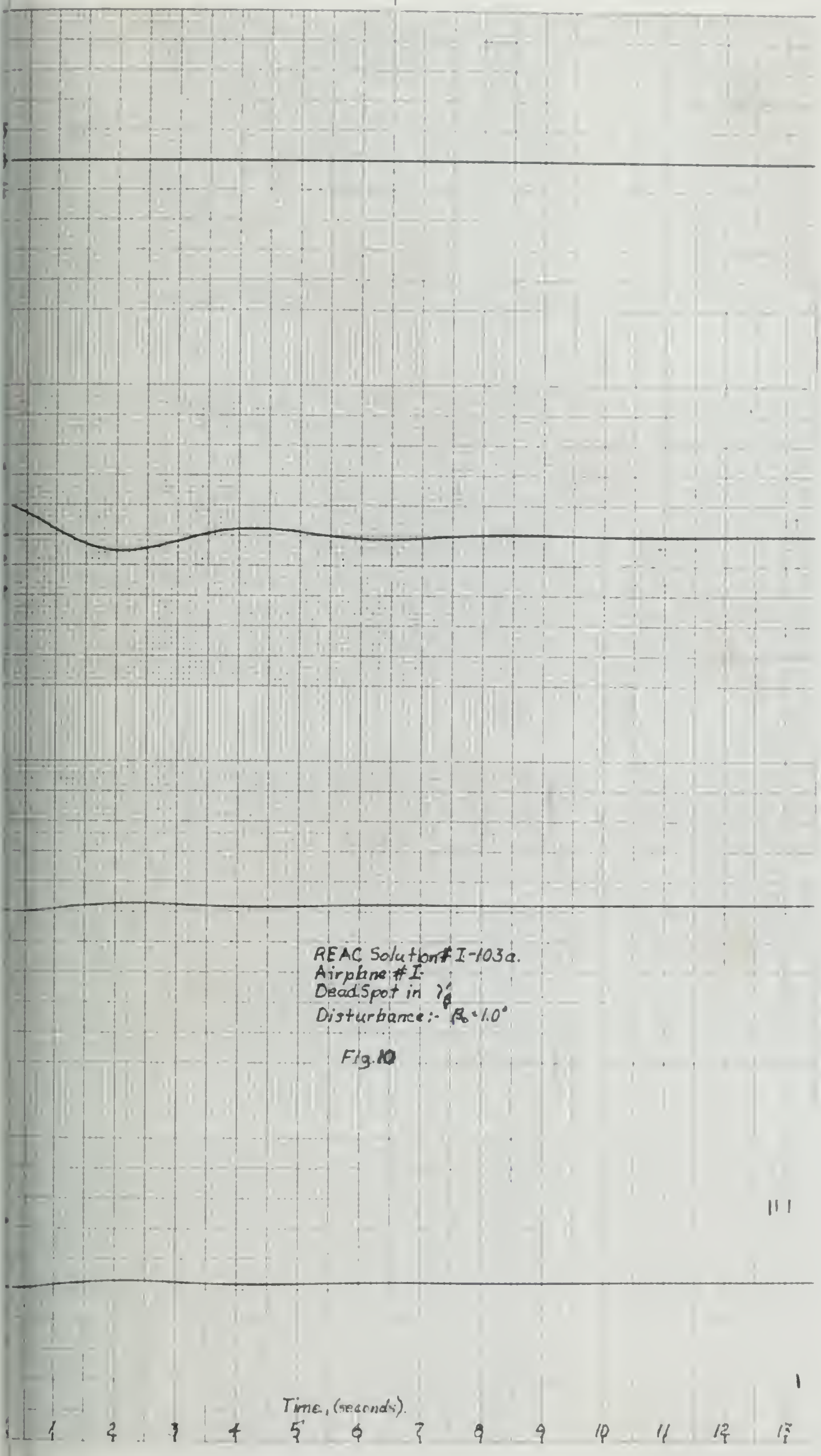
REAC Solution # I-103a.
Airplane # I
Dead Spot in δ_r
Disturbance:- $\beta_0 = 1.0°$
Fig. 10
Time, (seconds).
1 2 3 4 5 6 7 8 9 10 11 12 13

CHART NO. 420

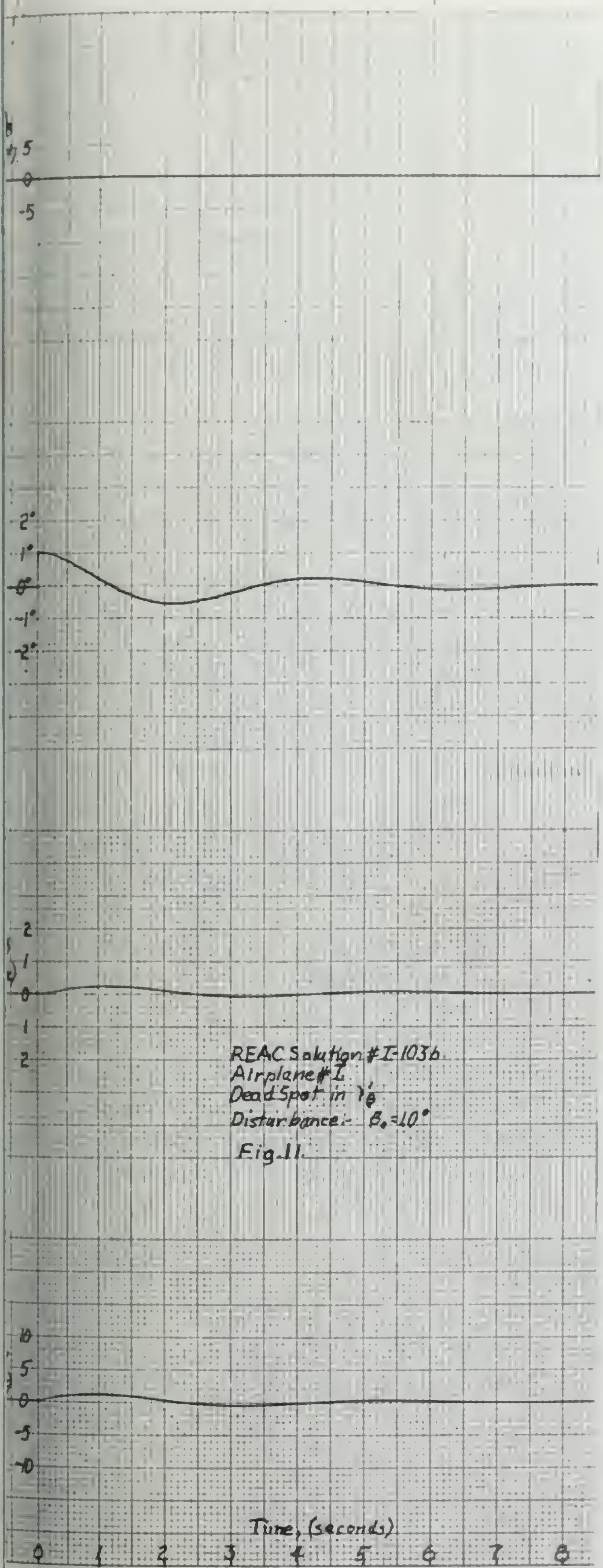
5
0
-5
2°
1°
0°
-1°
-2°
2
1
0
1
2
REAC Solution #I-103b
Airplane #I
Dead Spot in γ_θ
Disturbance - β_0=10°
Fig. 11.
10
5
0
-5
-10
Time, (seconds)
0
1
2
3
4
5
6
7
8

CHART NO. 420

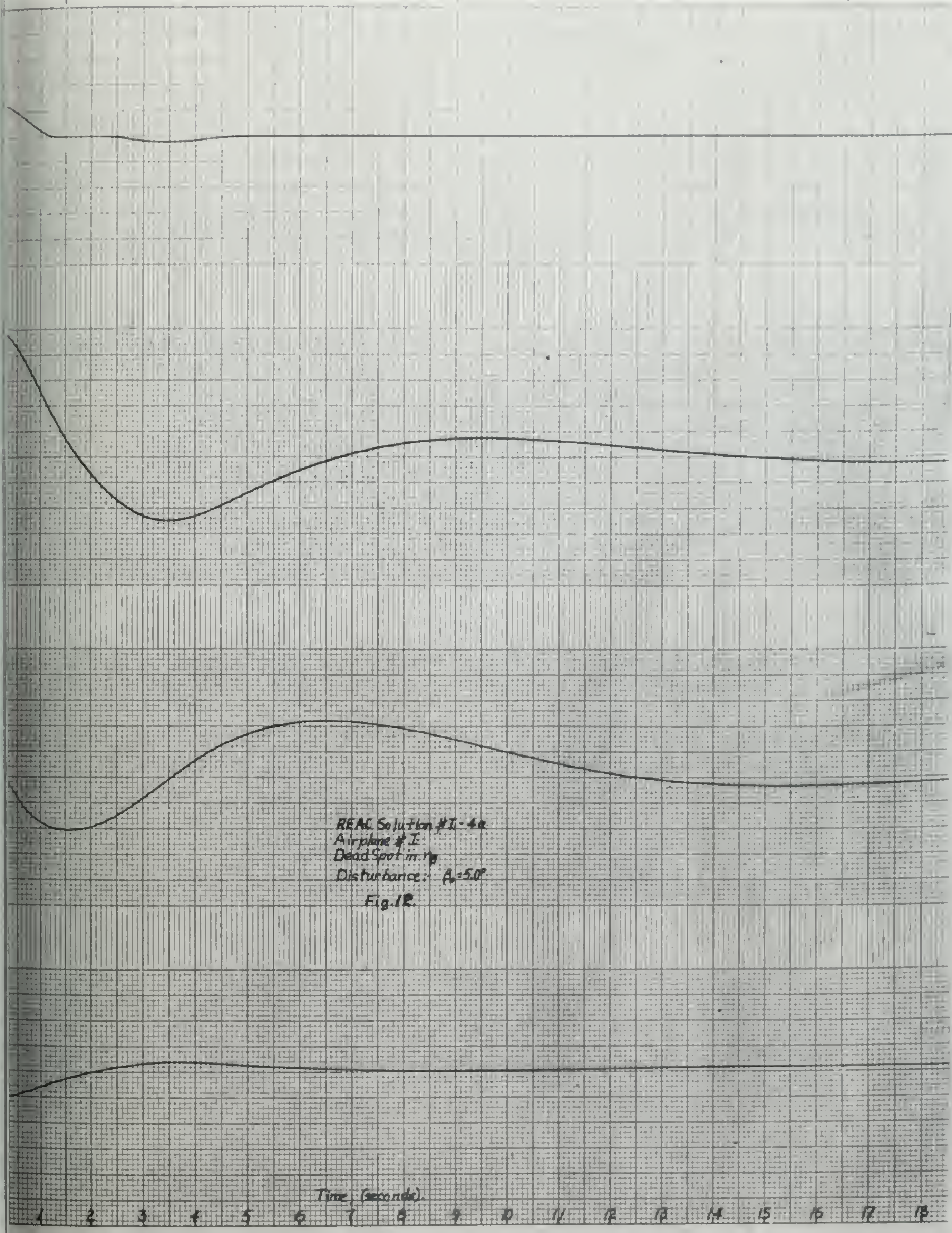

Fig. 12.

CHART NO. 420

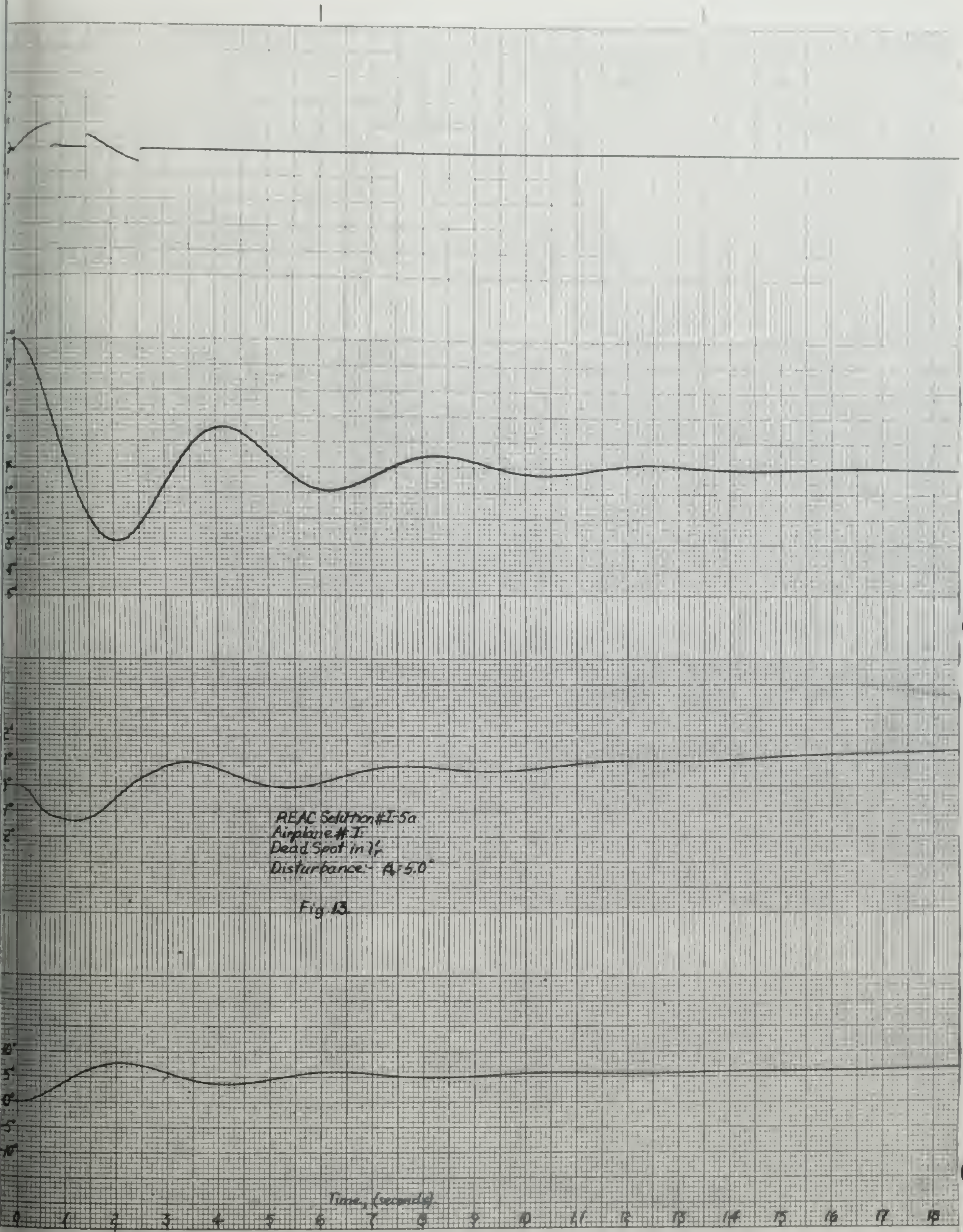

Fig. 13.

SANBORN POLY-VISO *Permapaper* CHART NO. 420

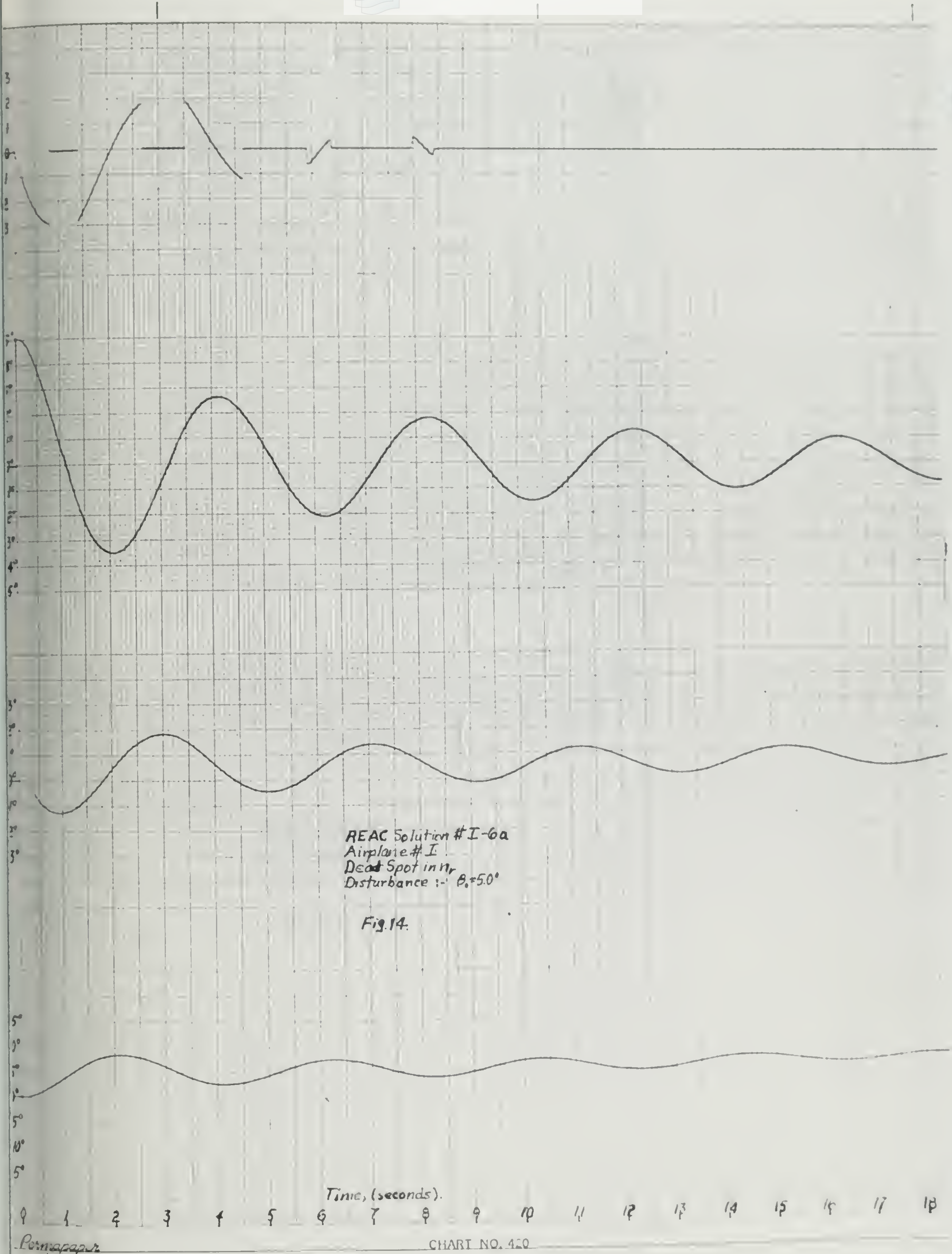
REAC Solution #I-6a
Airplane #I
Dead Spot in n_r
Disturbance :- $\beta_0 = 5.0°$
Time, (seconds).
0 1 2 3 4 5 6 7 8 9 10 11 12 13 14 15 16 17 18
Permapaper
CHART NO. 420

Fig. 14.

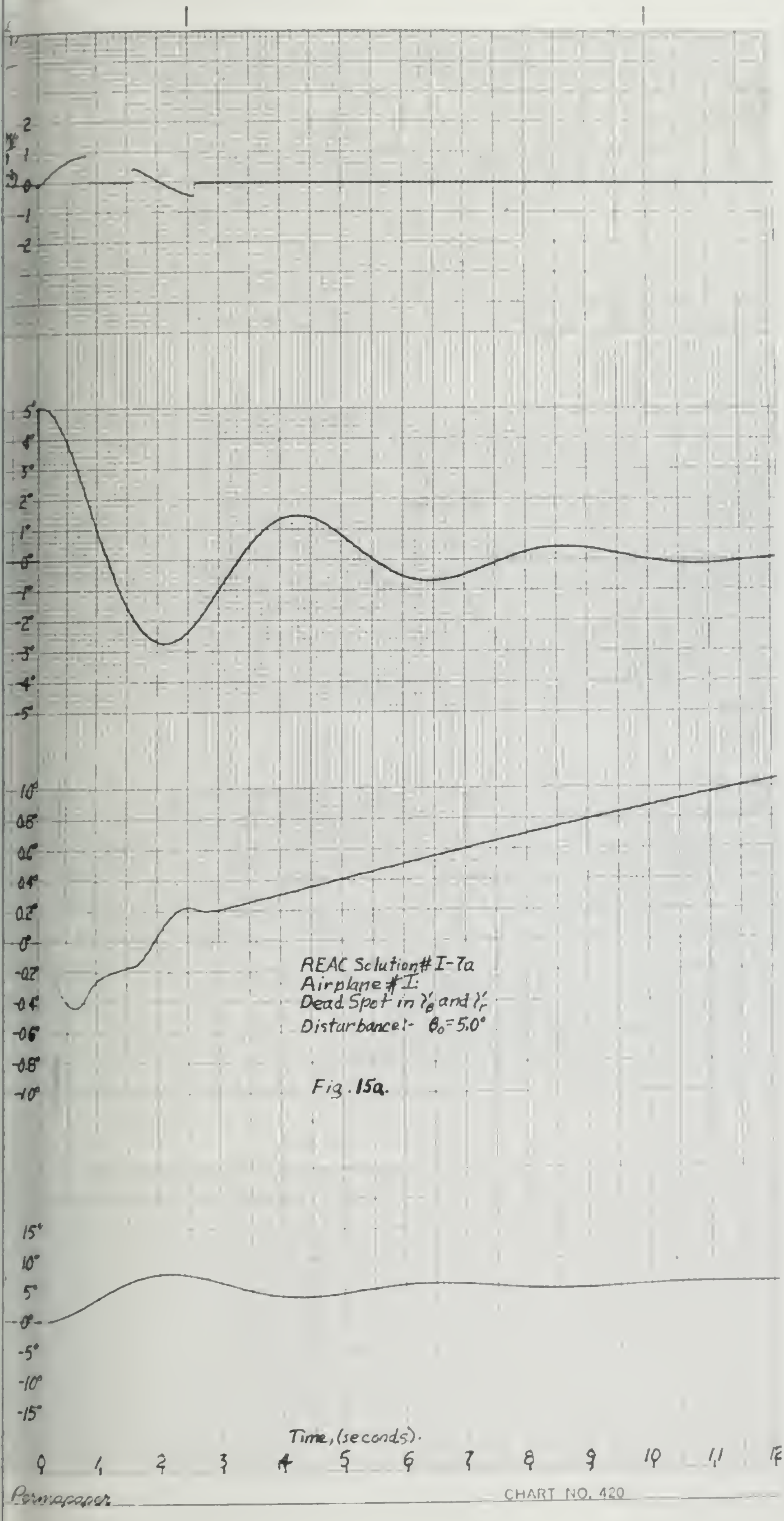
REAC Solution # I-7a
Airplane # I
Disturbance:- θ₀ = 5.0°
Time, (seconds).
0 1 2 3 4 5 6 7 8 9 10 11 12
Permapaper
CHART NO. 420

Fig. 15a.

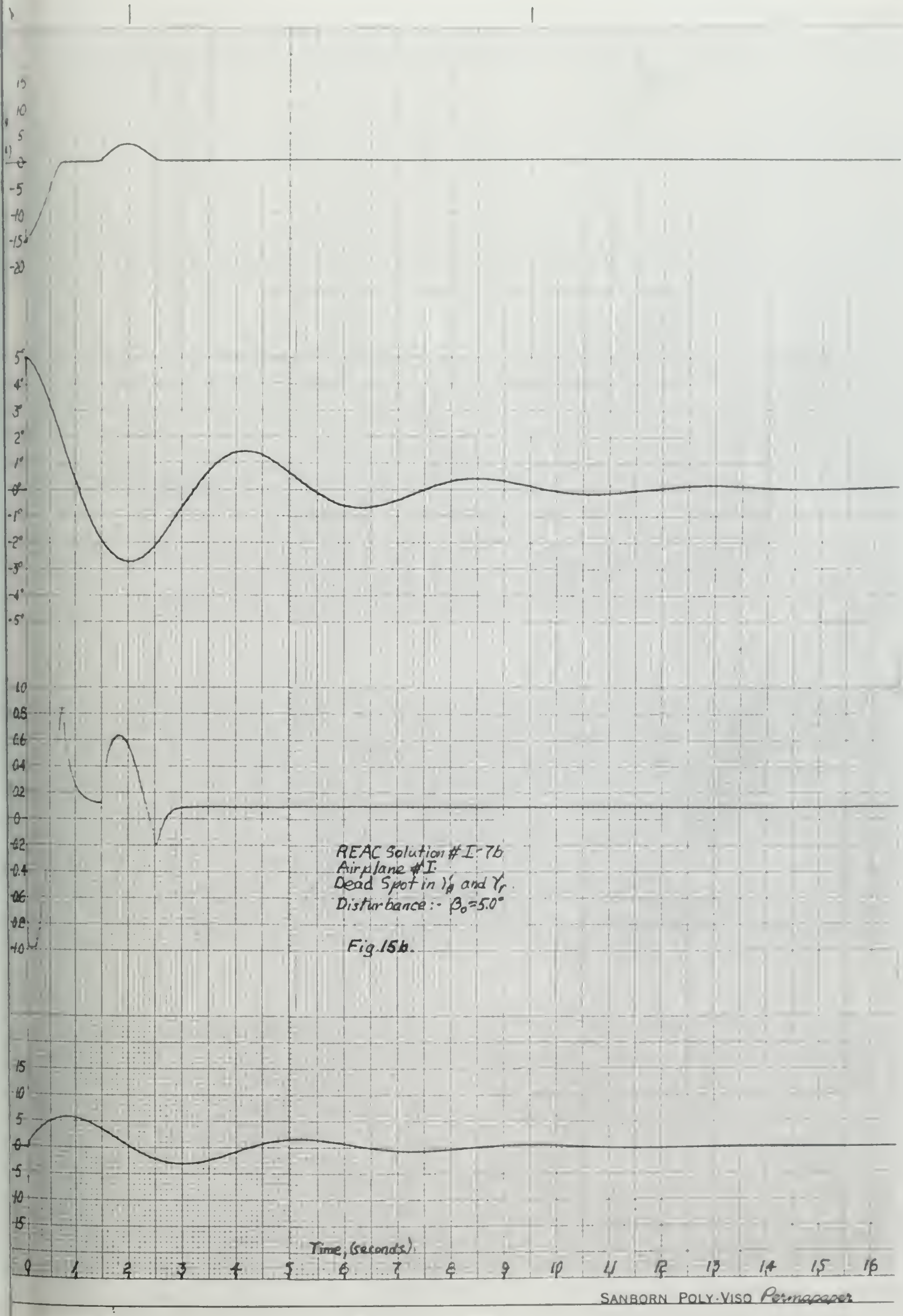
REAC Solution # I-7b
Airplane # I
Dead Spot in γ_a and γ_r
Disturbance :- $\beta_0 = 5.0°$
Time, (seconds)
SANBORN POLY-VISO Permapaper

Fig. 15b.

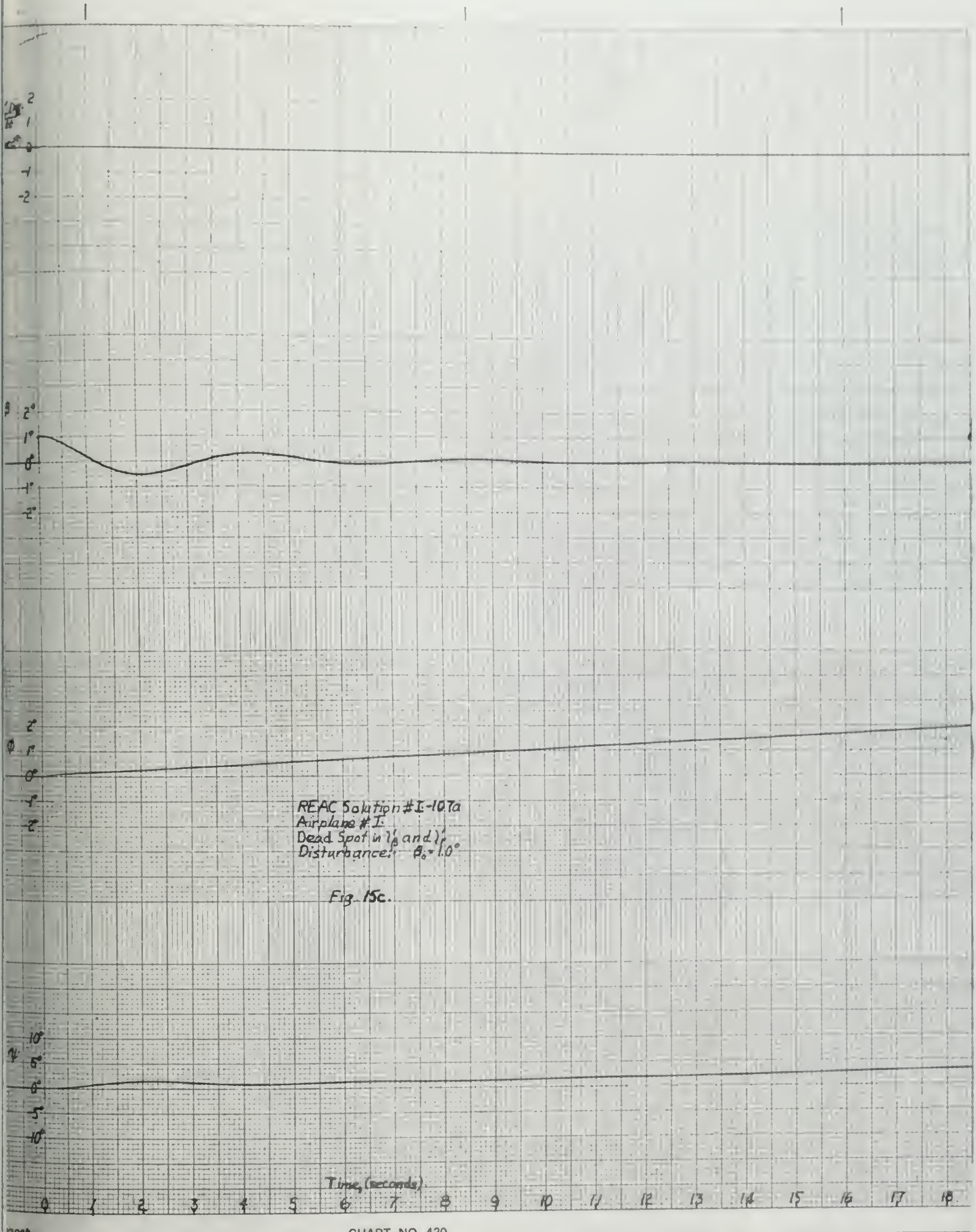
REAC Solution # I-107a
Airplane # I
Dead Spot in $\dot{\psi}_b$ and $\dot{\psi}$
Disturbance: $\theta_0 = 1.0°$
Time, (seconds)
0
1
2
3
4
5
6
7
8
9
10
11
12
13
14
15
16
17
18

Fig. 15c.

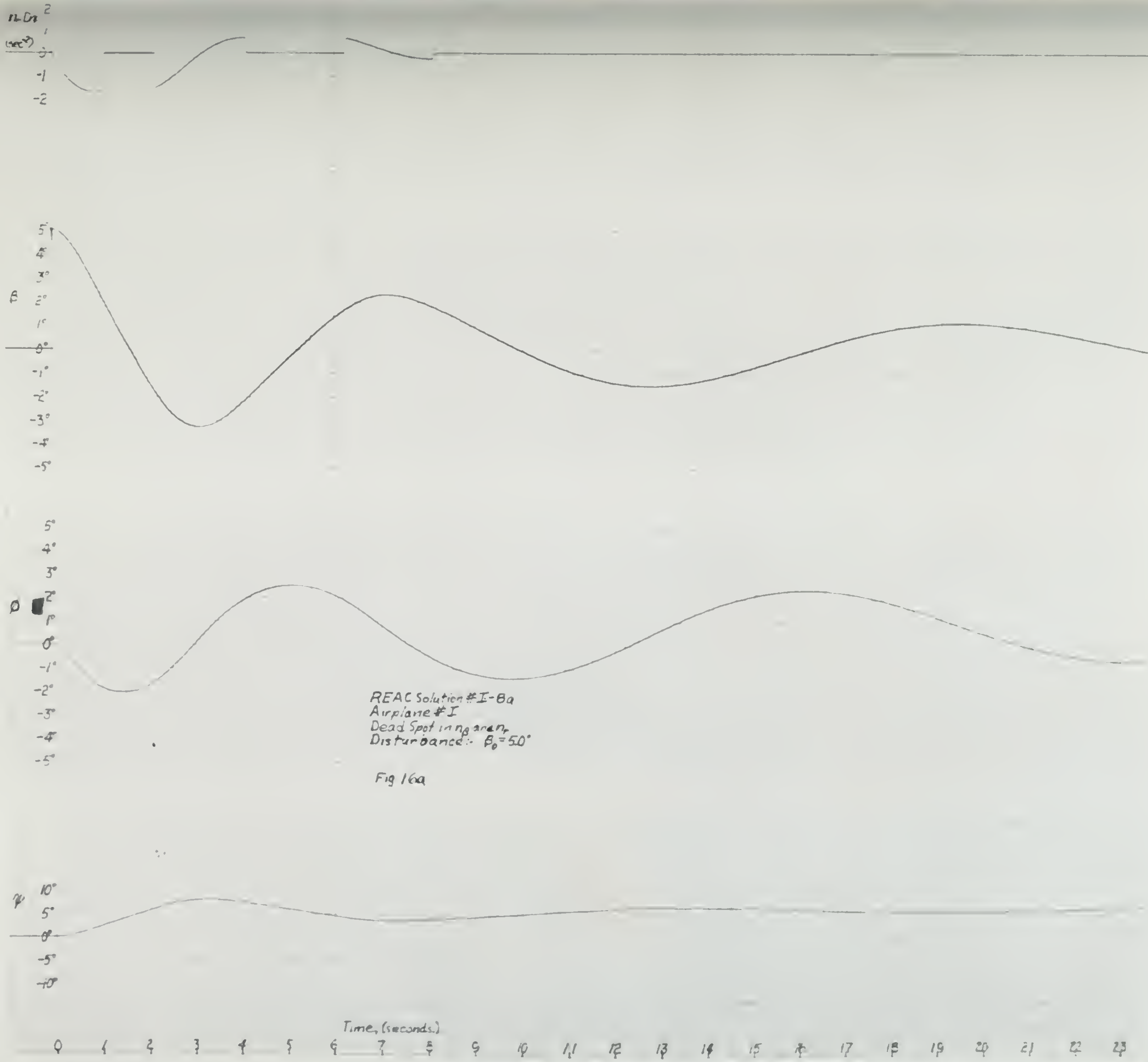
REAC Solution #I-8a
Airplane #I
Dead Spot in n_β and n_r
Disturbance:- $\beta_0 = 5.0°$
Time, (seconds.)

Fig 16a

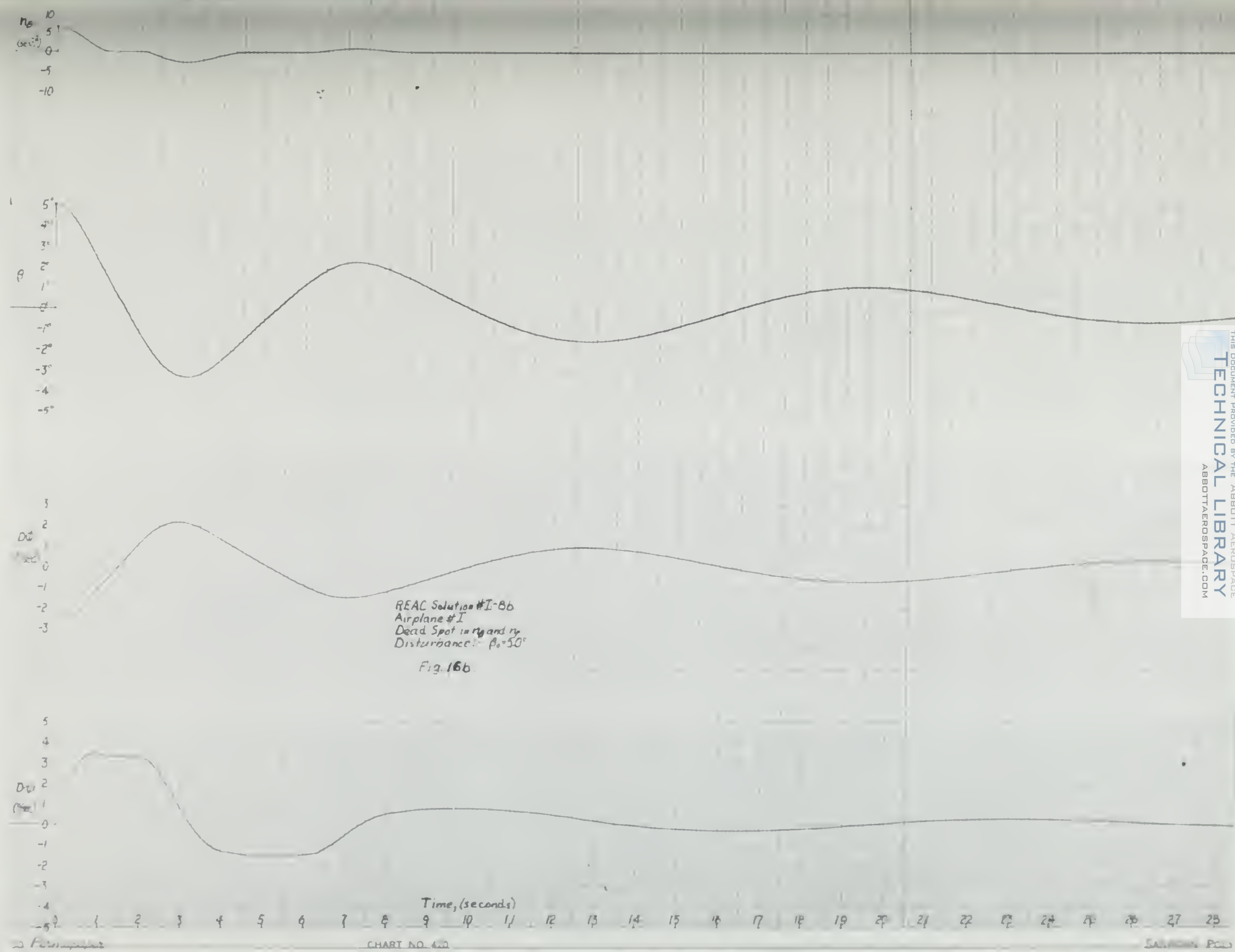
REAC Solution #I-8b
Airplane #I
Dead Spot in r_g and r_y
Disturbance: β_0=5.0°
Time, (seconds)
CHART NO.

Fig. 16b

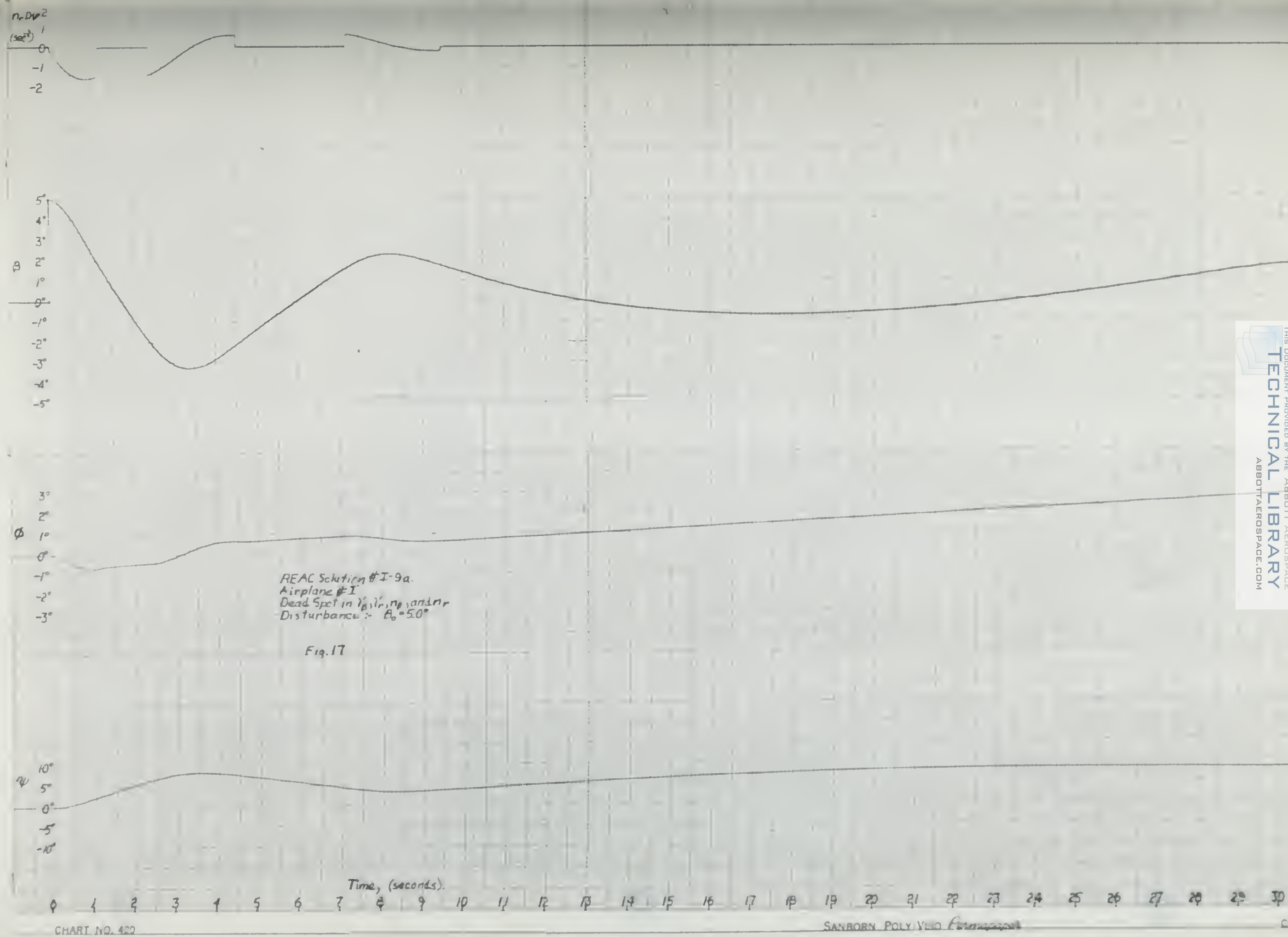
$n_r D\psi^2$ (sec^{-2})
β
φ
ψ
REAC Solution #I-9a.
Airplane #I
Dead Spot in Y_β, l_r, n_β, and n_r
Disturbance :- $\beta_0 = 5.0°$
Time, (seconds).
CHART NO. 422
SANBORN POLY VISO

Fig. 17

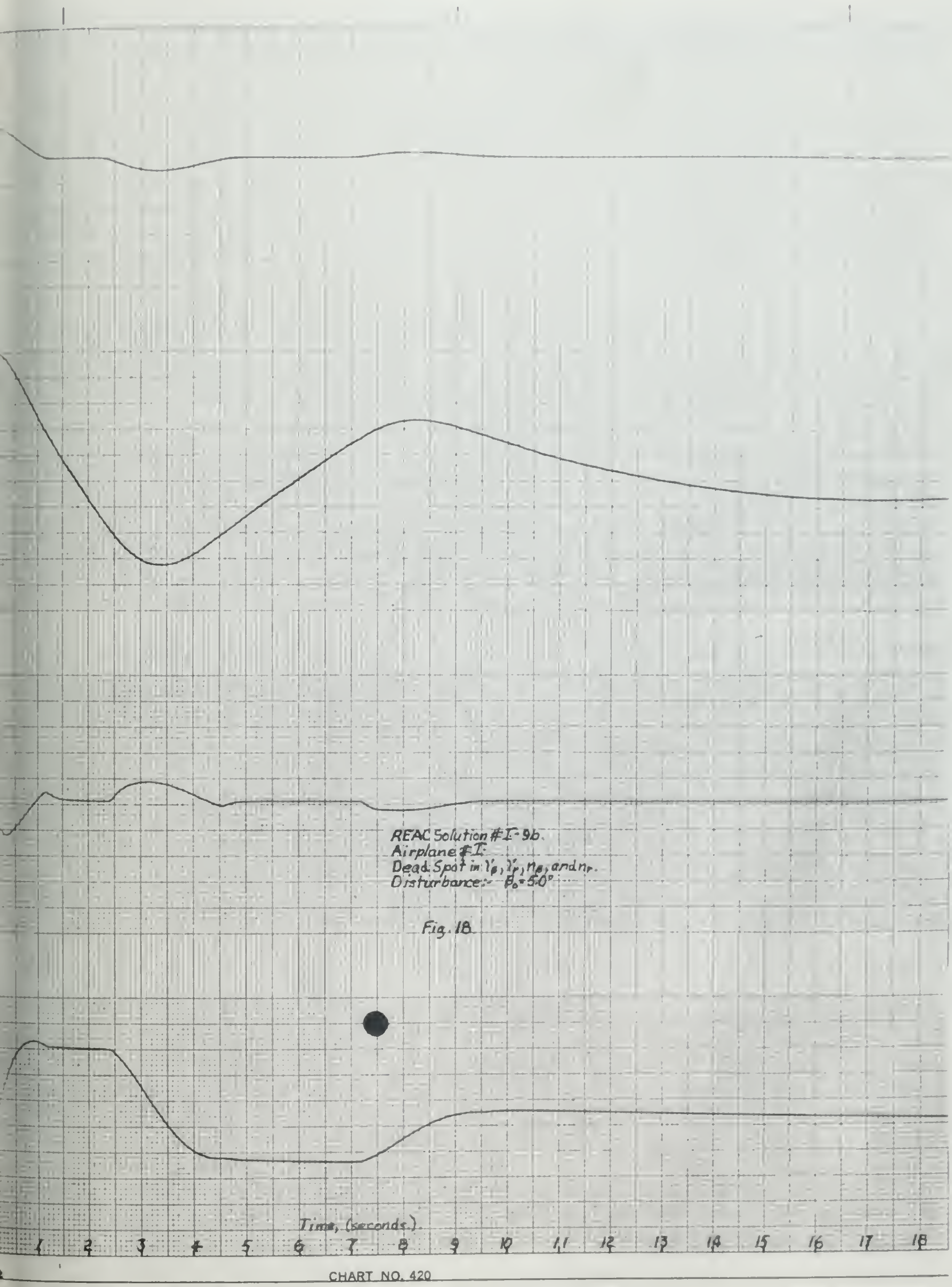

Fig. 18

CHART NO. 420

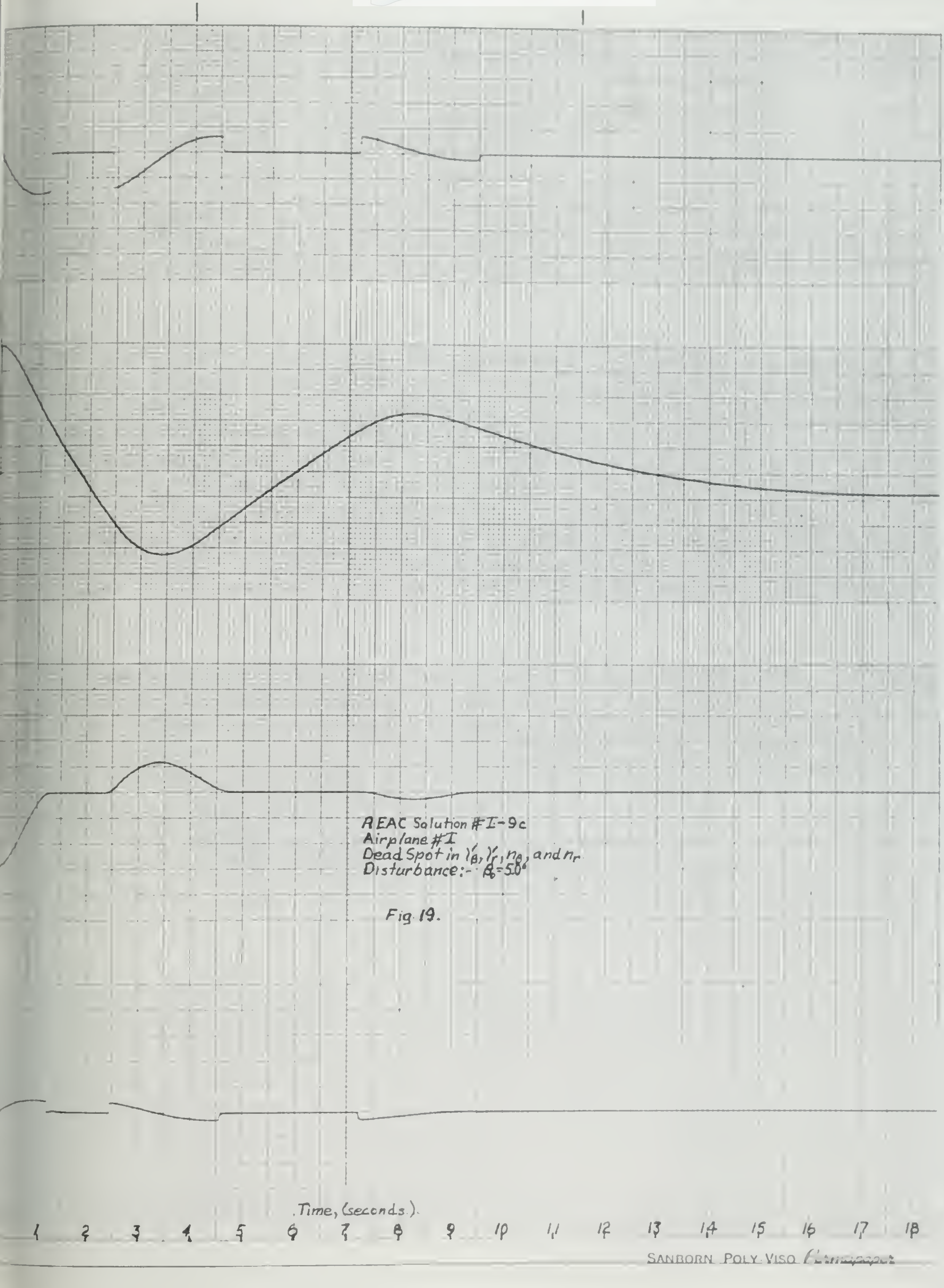
REAC Solution #I-9c
Airplane #I
Dead Spot in Y_β, Y_r, n_β, and n_r
Disturbance:- β_0=5.0°
Time, (seconds).
1 2 3 4 5 6 7 8 9 10 11 12 13 14 15 16 17 18
SANBORN POLY VISO

Fig. 19.

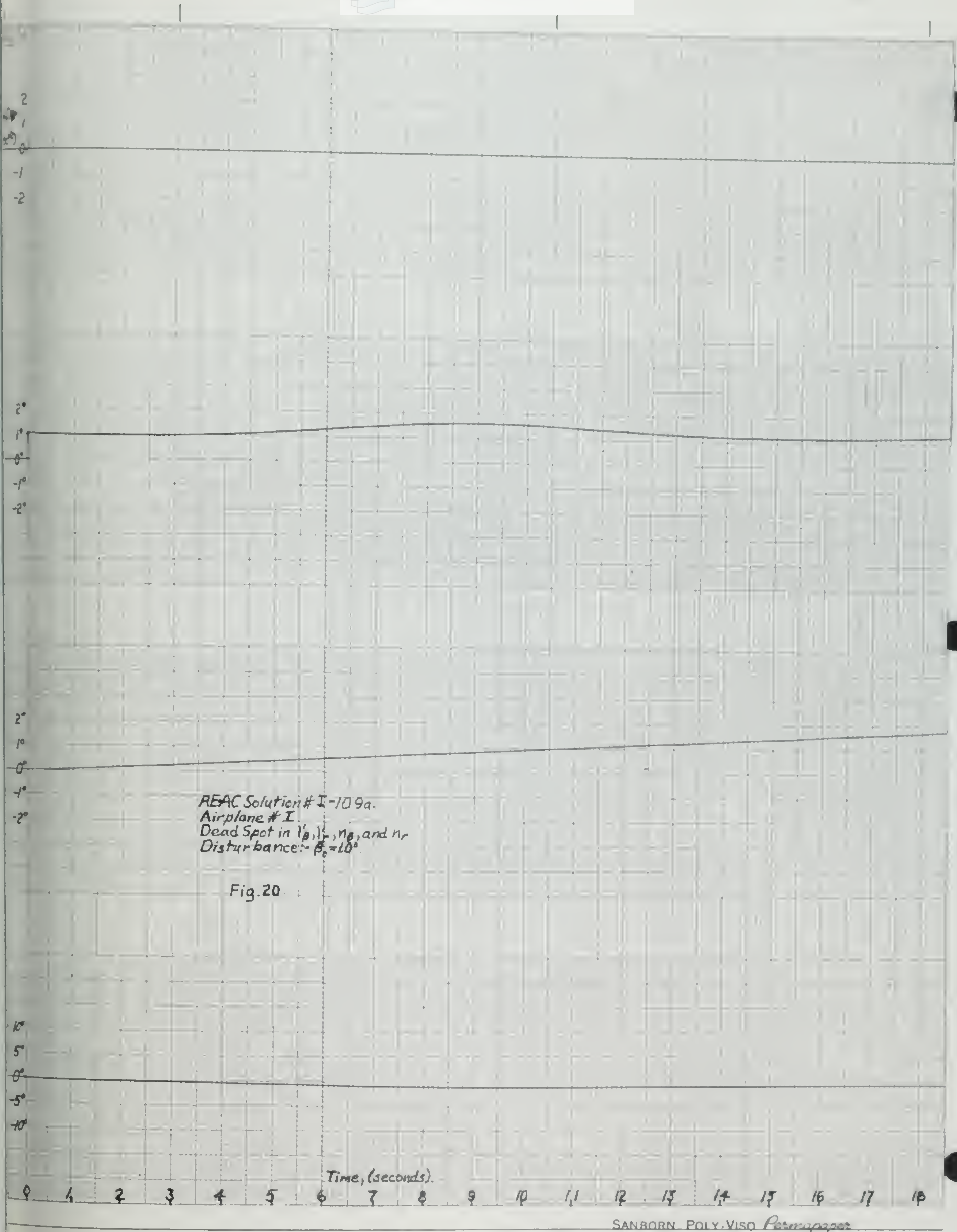
REAC Solution # I-109a.
Airplane # I.
Dead Spot in l'_β, l'_r, n_β, and n_r
Disturbance:- $\beta_0 = 10°$.
Time, (seconds).
0 1 2 3 4 5 6 7 8 9 10 11 12 13 14 15 16 17 18
2° 1° 0° -1° -2°
10° 5° 0° -5° -10°
SANBORN POLY-VISO Permapaper

Fig. 20

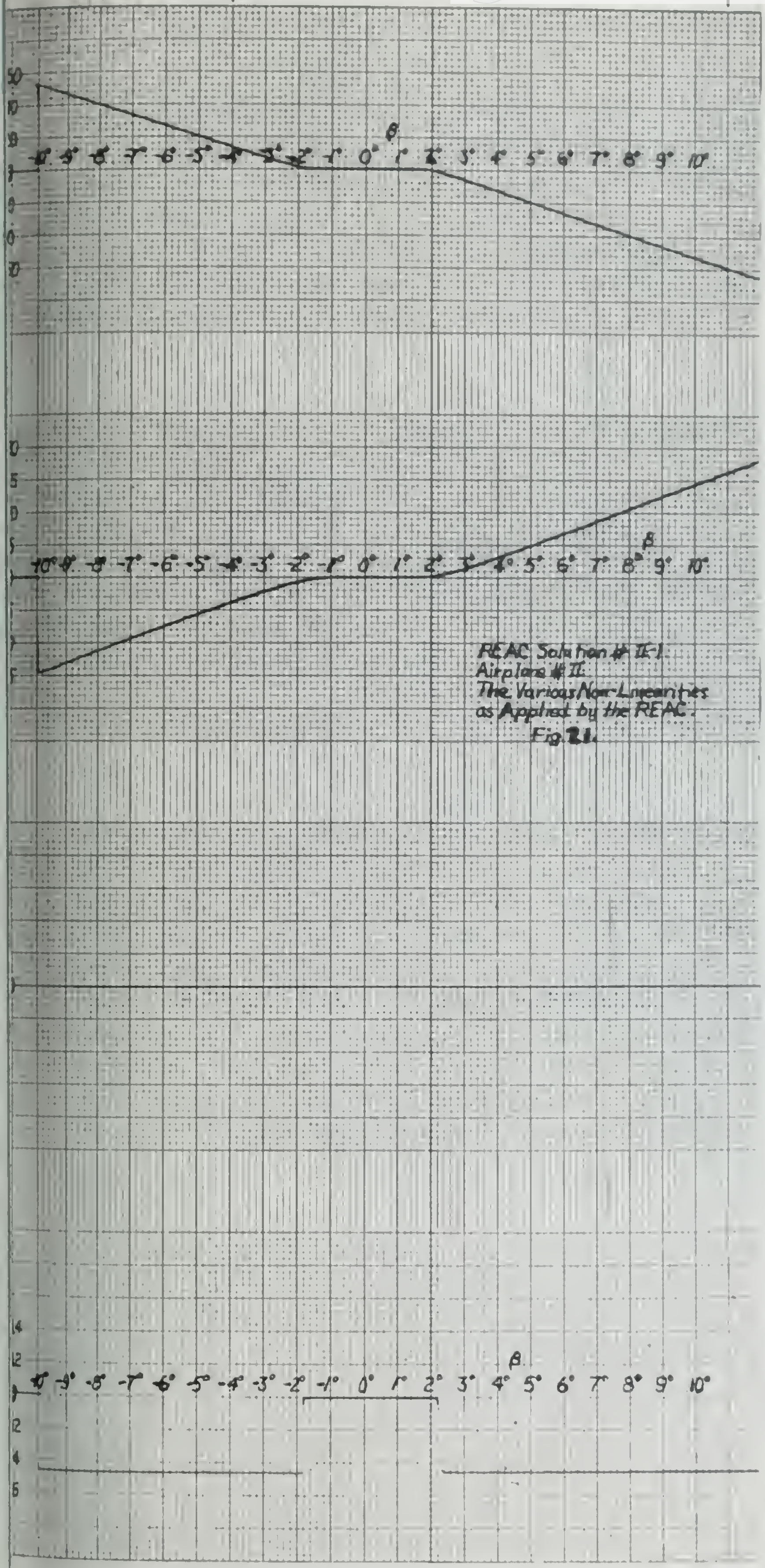

REAC Solution # II-1.
Airplane # II.
The Various Non-Linearities
as Applied by the REAC.
Fig 21.

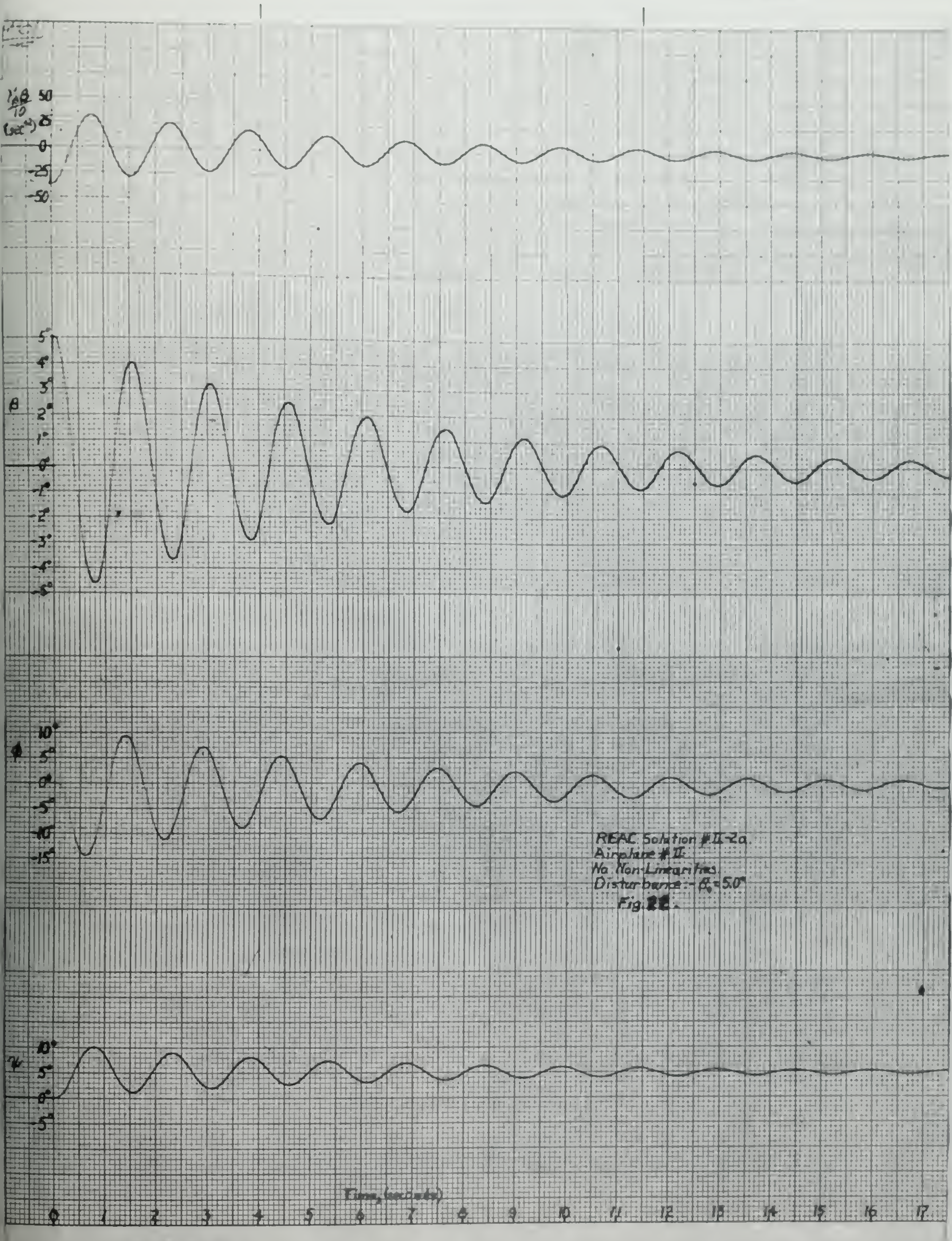
50
25
0
-25
-50
5°
4°
3°
θ
2°
1°
0
-1°
-2°
-3°
-4°
-5°
10°
5°
0°
-5°
-10°
-15°
10°
ψ
5°
0°
-5°
REAC Solution #II-2a
Airplane #II
No Non-Linearities
Disturbance:- β₀ = 5.0°
Fig. 22.
Time, (seconds)
0
1
2
3
4
5
6
7
8
9
10
11
12
13
14
15
16
17

CHART NO. 420

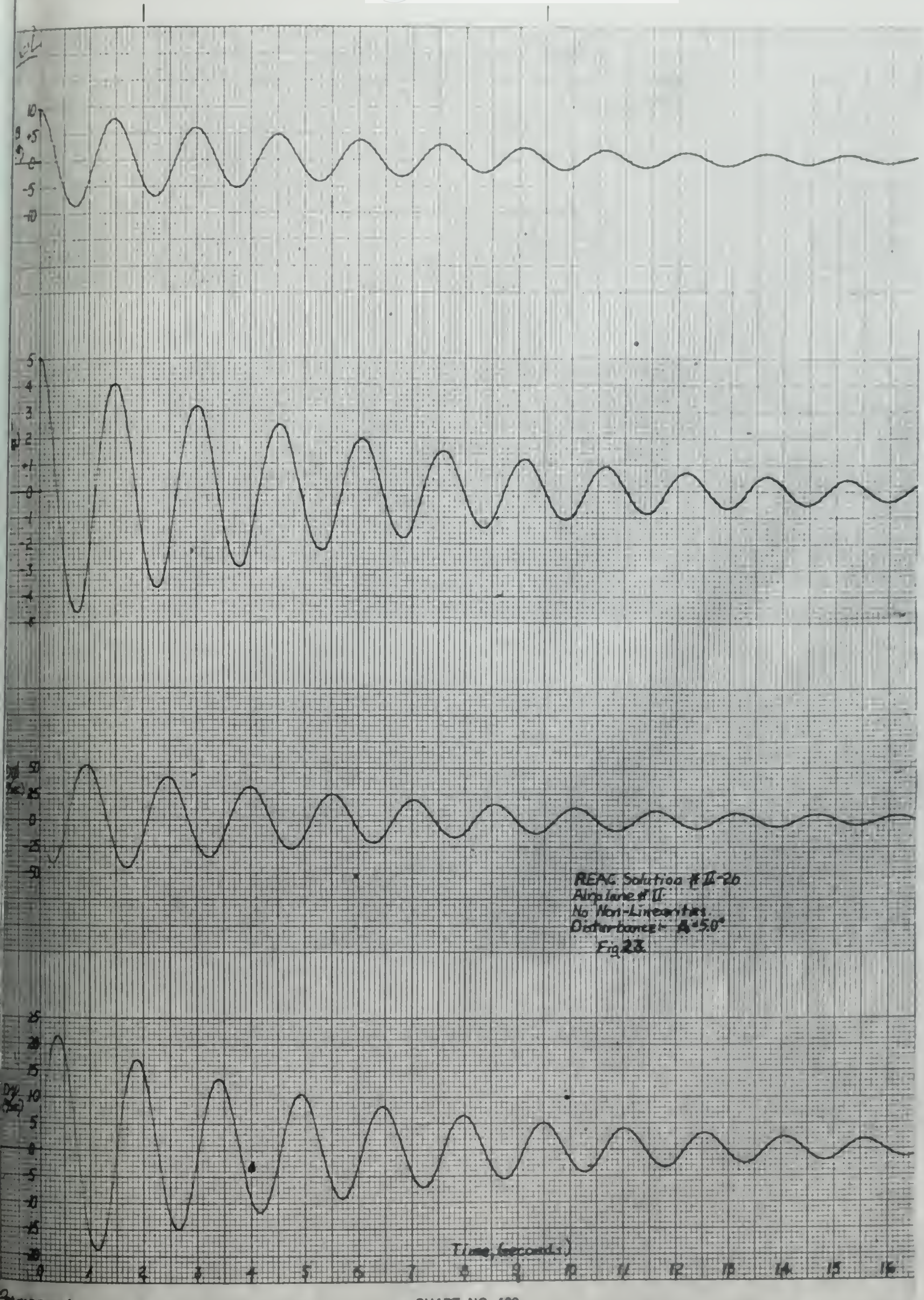

Fig. 23.

Permapaper CHART NO. 420

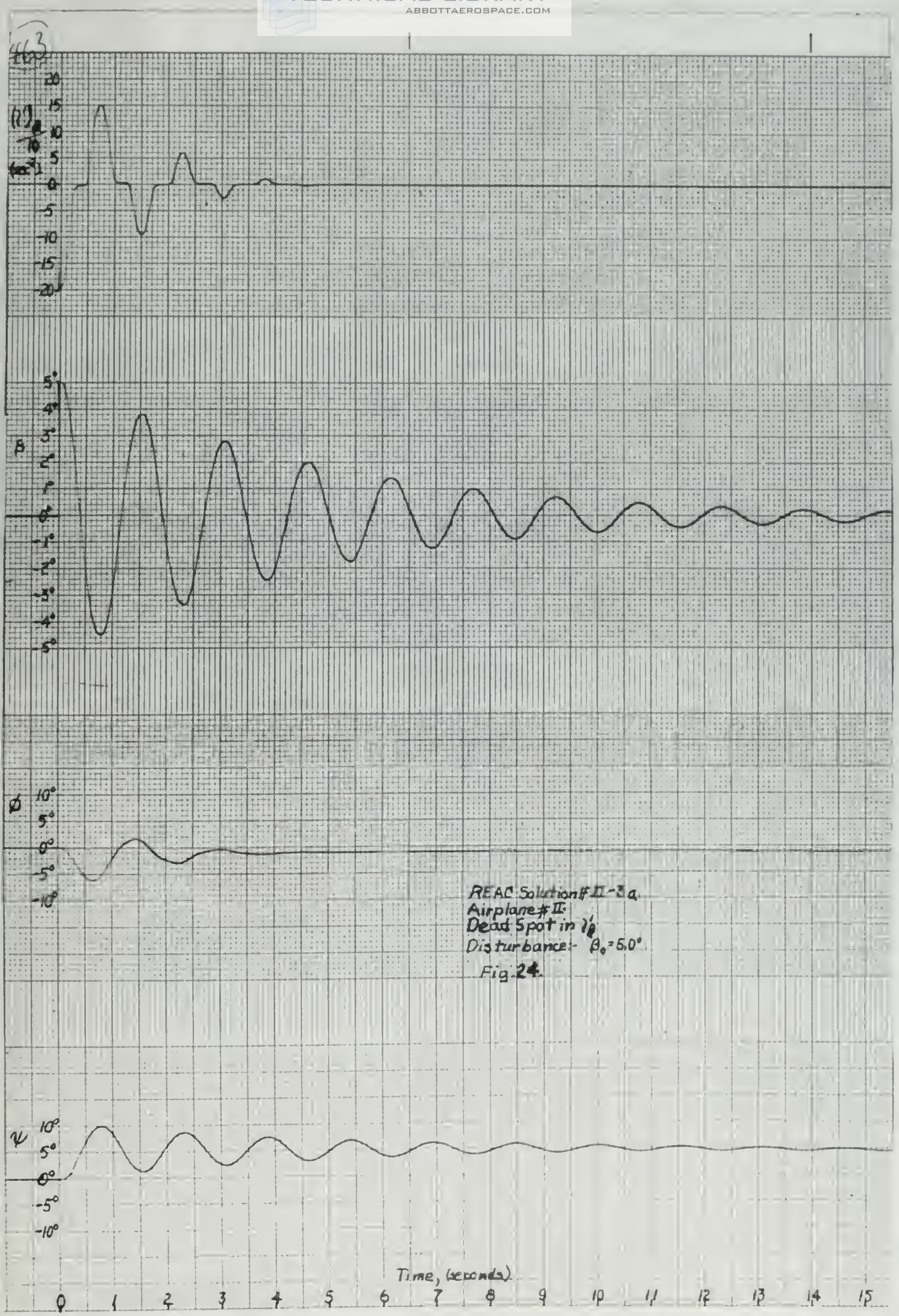
20
15
10
5
0
-5
-10
-15
-20
5°
4°
3°
2°
1°
0°
-1°
-2°
-3°
-4°
-5°
10°
5°
0°
-5°
-10°
10°
5°
0°
-5°
-10°
REAC Solution # II-3a
Airplane # II
Dead Spot in
Disturbance:- β_0 = 5.0°
Fig. 24
Time, (seconds)
0
1
2
3
4
5
6
7
8
9
10
11
12
13
14
15

CHART NO. 420

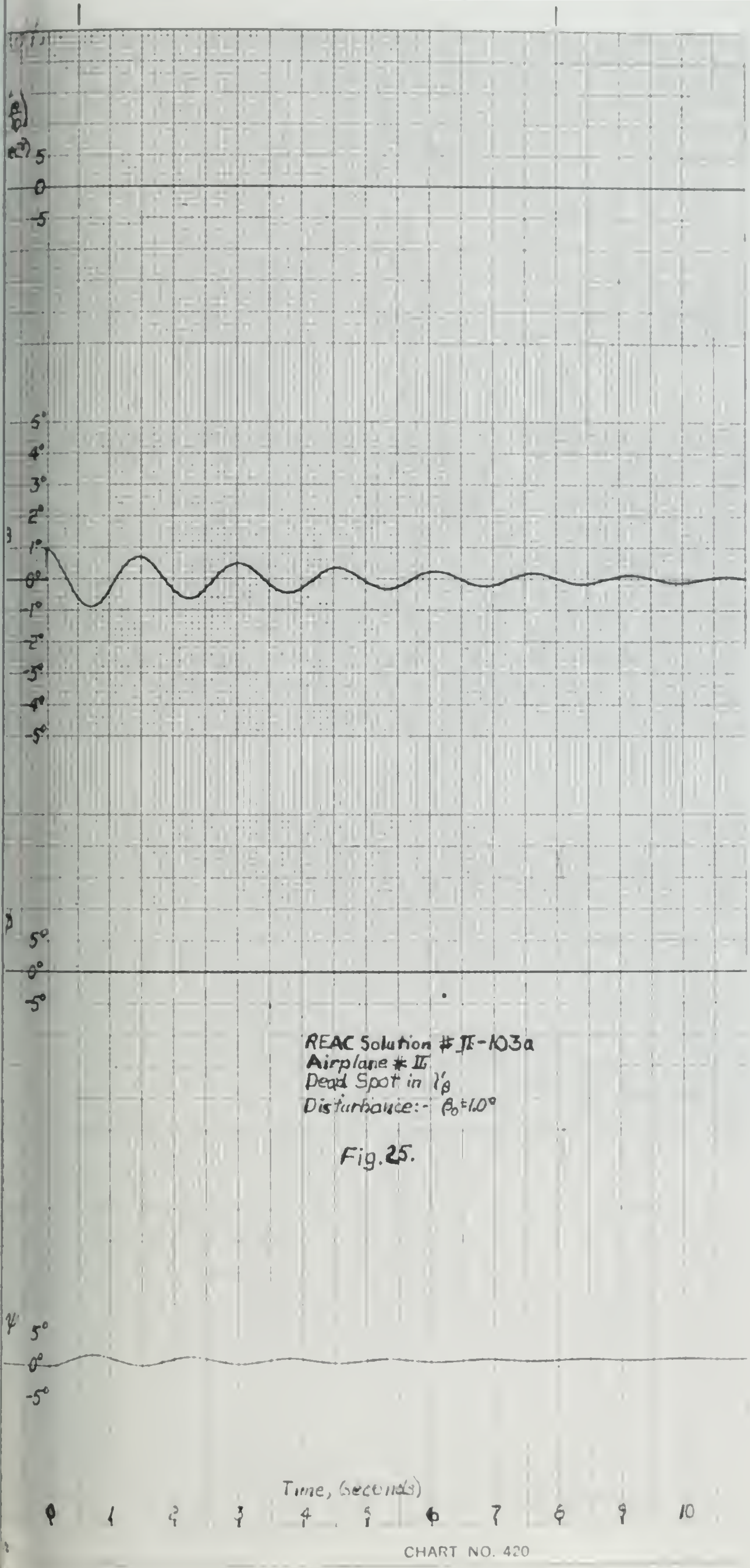
5
0
-5
5°
4°
3°
2°
1°
0°
-1°
-2°
-3°
-4°
-5°
β
5°
0°
-5°
REAC Solution # II-103a
Airplane # II
Dead Spot in Y'_β
Disturbance:- $\beta_0 = 1.0°$
ψ
5°
0°
-5°
Time, (seconds)
0 1 2 3 4 5 6 7 8 9 10
CHART NO. 420

Fig. 25.

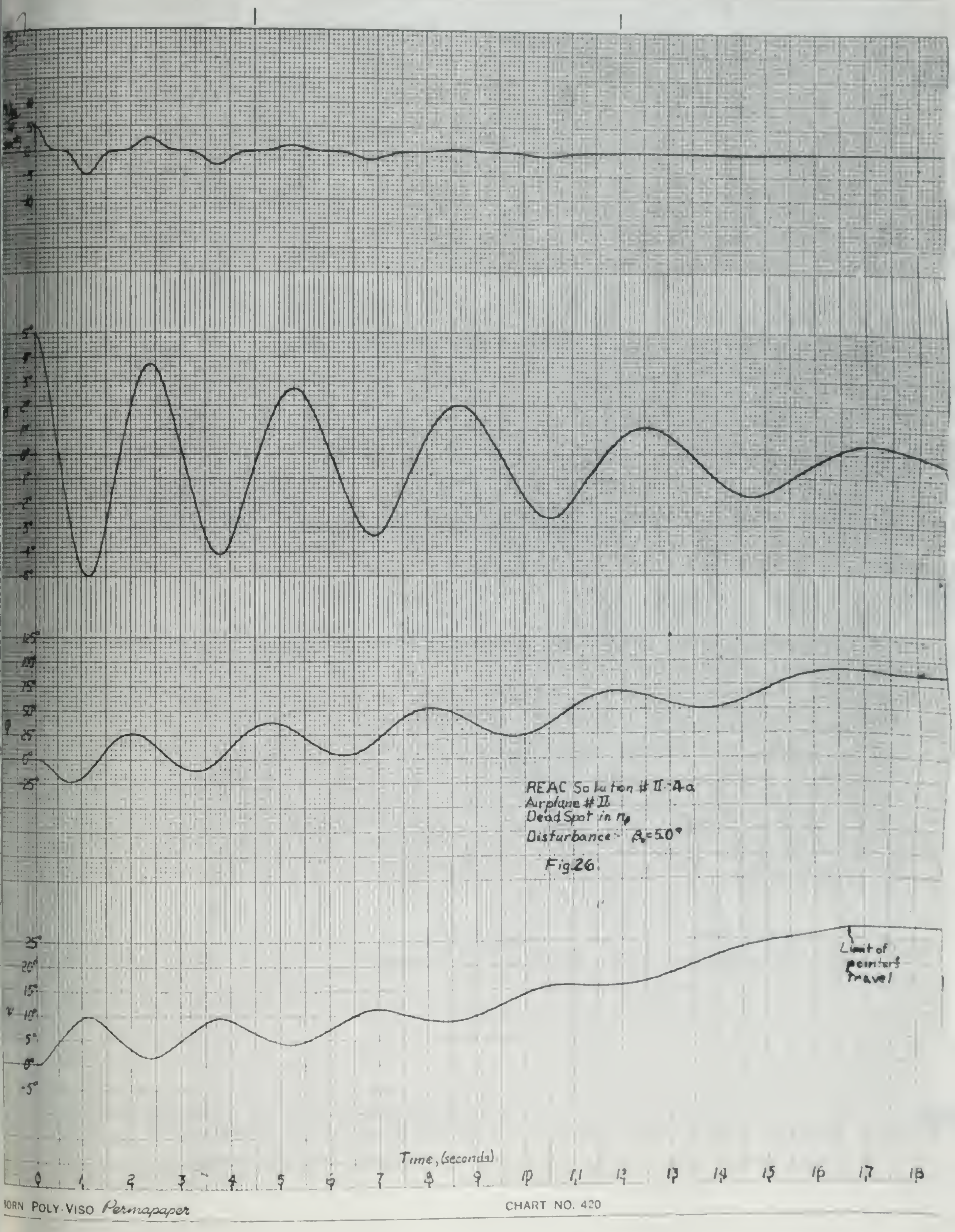
REAC Solution # II-4a
Airplane # II
Dead Spot in η_θ
Disturbance: β_0=5.0°
Limit of pointer travel
Time, (seconds)
0 1 2 3 4 5 6 7 8 9 10 11 12 13 14 15 16 17 18
BORN POLY-VISO Permapaper
CHART NO. 420

Fig. 26.

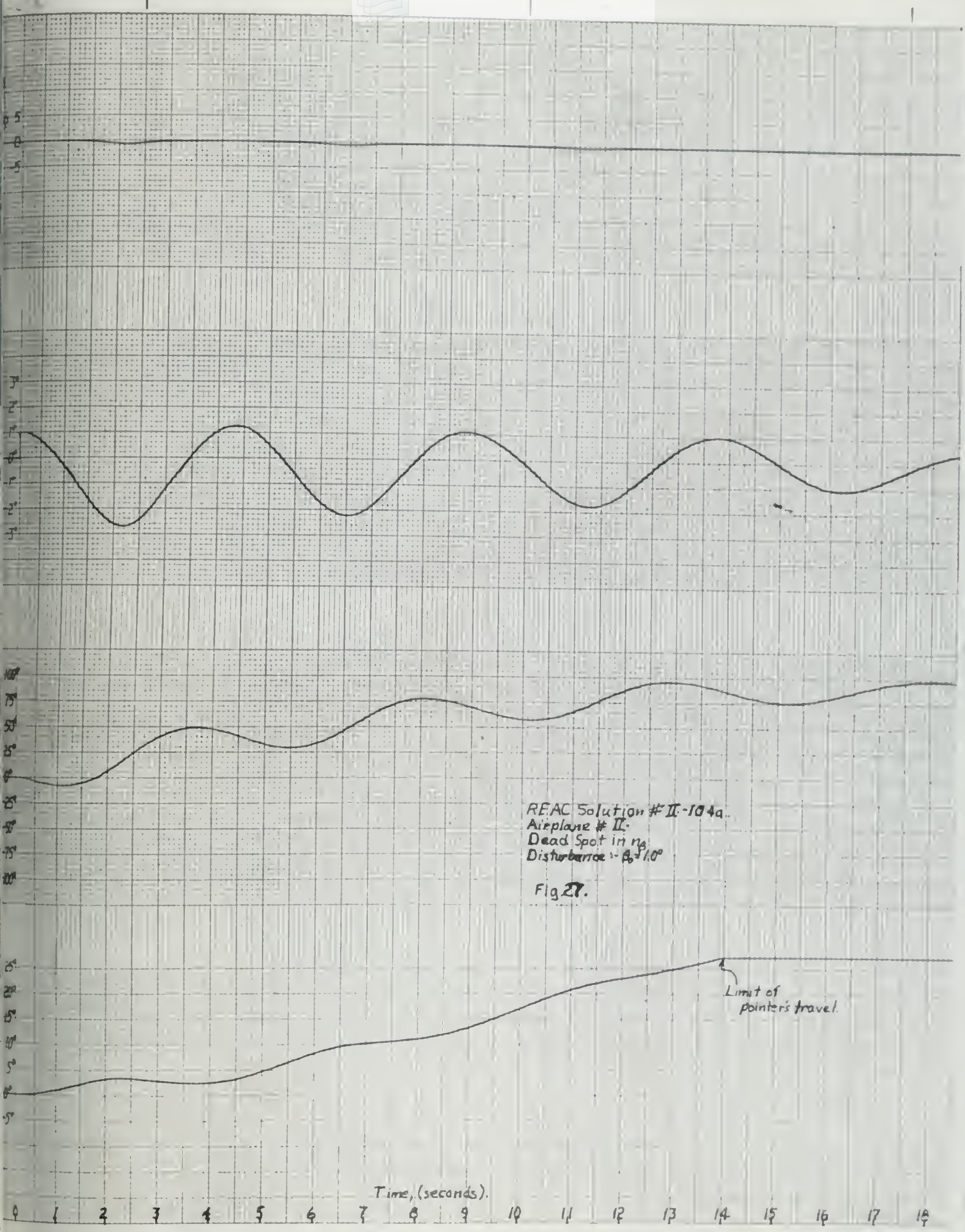

Fig 27.

SANBORN POLY-VISO *Permapaper* CHART NO. 420

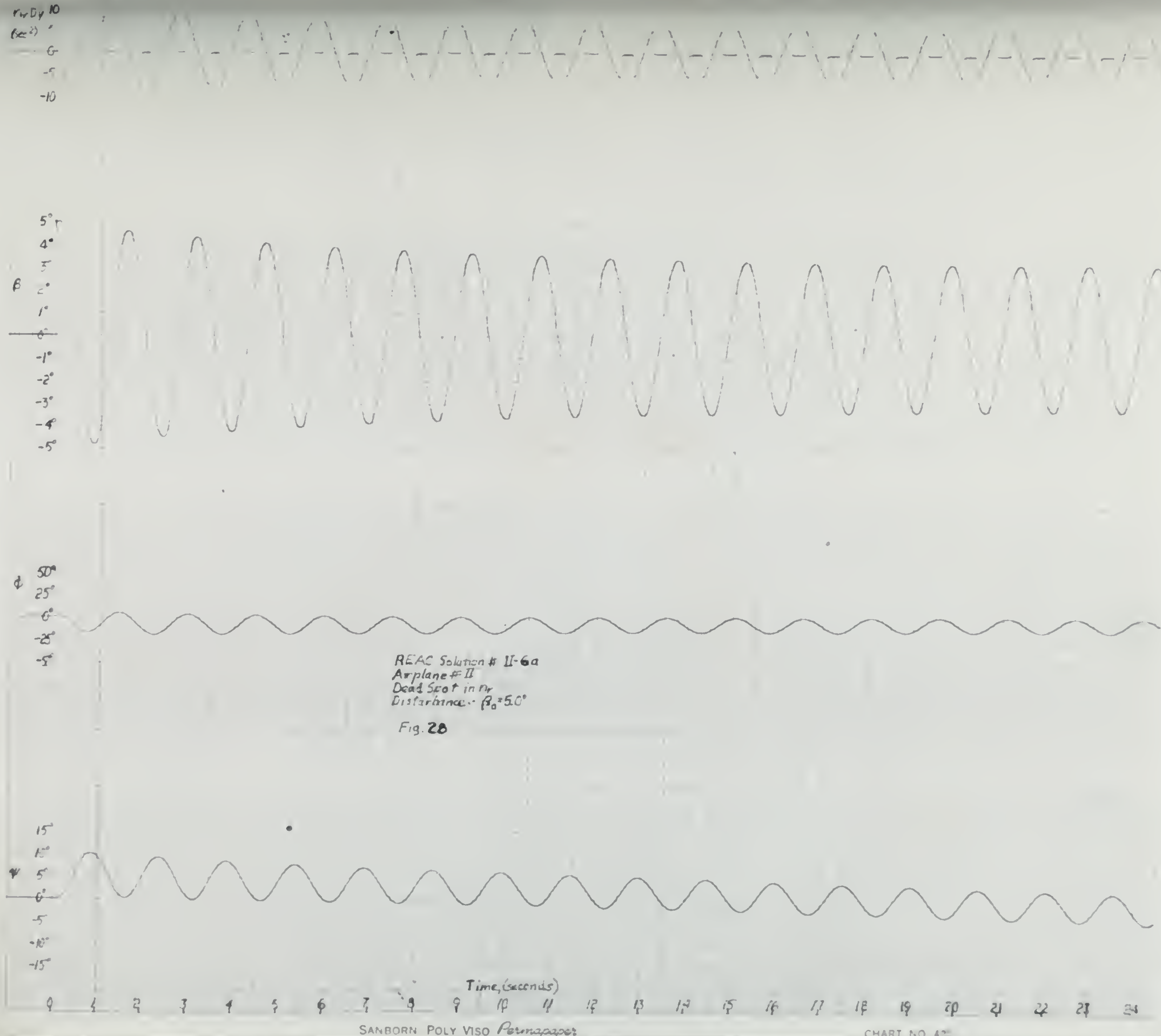

REAC Solution # II-6a
Airplane # II
Dead Spot in n_r
Disturbance: $\beta_0 = 5.0°$
Time, (seconds)
SANBORN POLY VISO Permapaper
CHART NO 42

Fig. 28

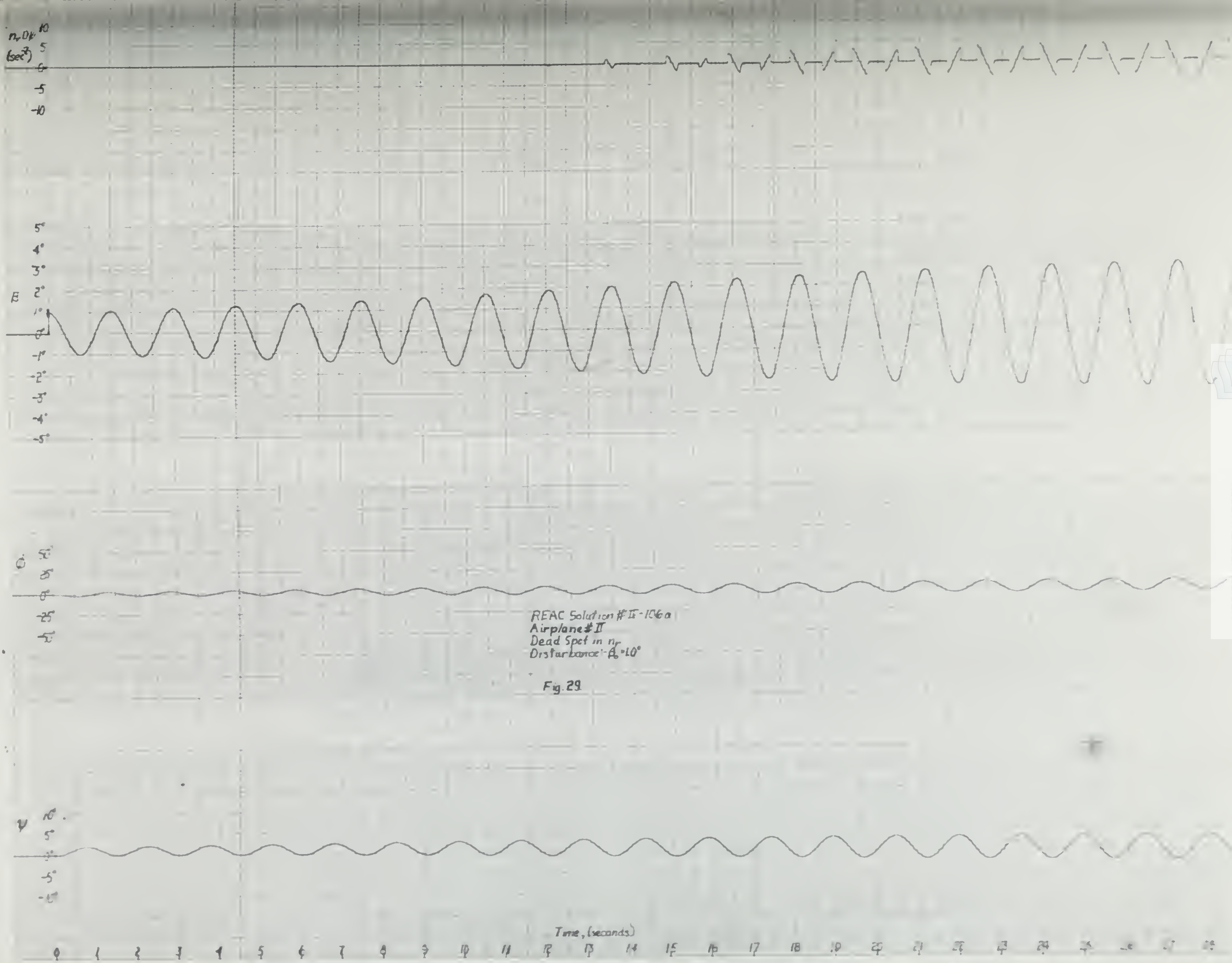
REAC Solution # II - 106a
Airplane # II
Dead Spot in n_r
Disturbance - $\beta_0 = 10°$
Time, (seconds)
SANBORN POLY VISO Permapaper

Fig. 29

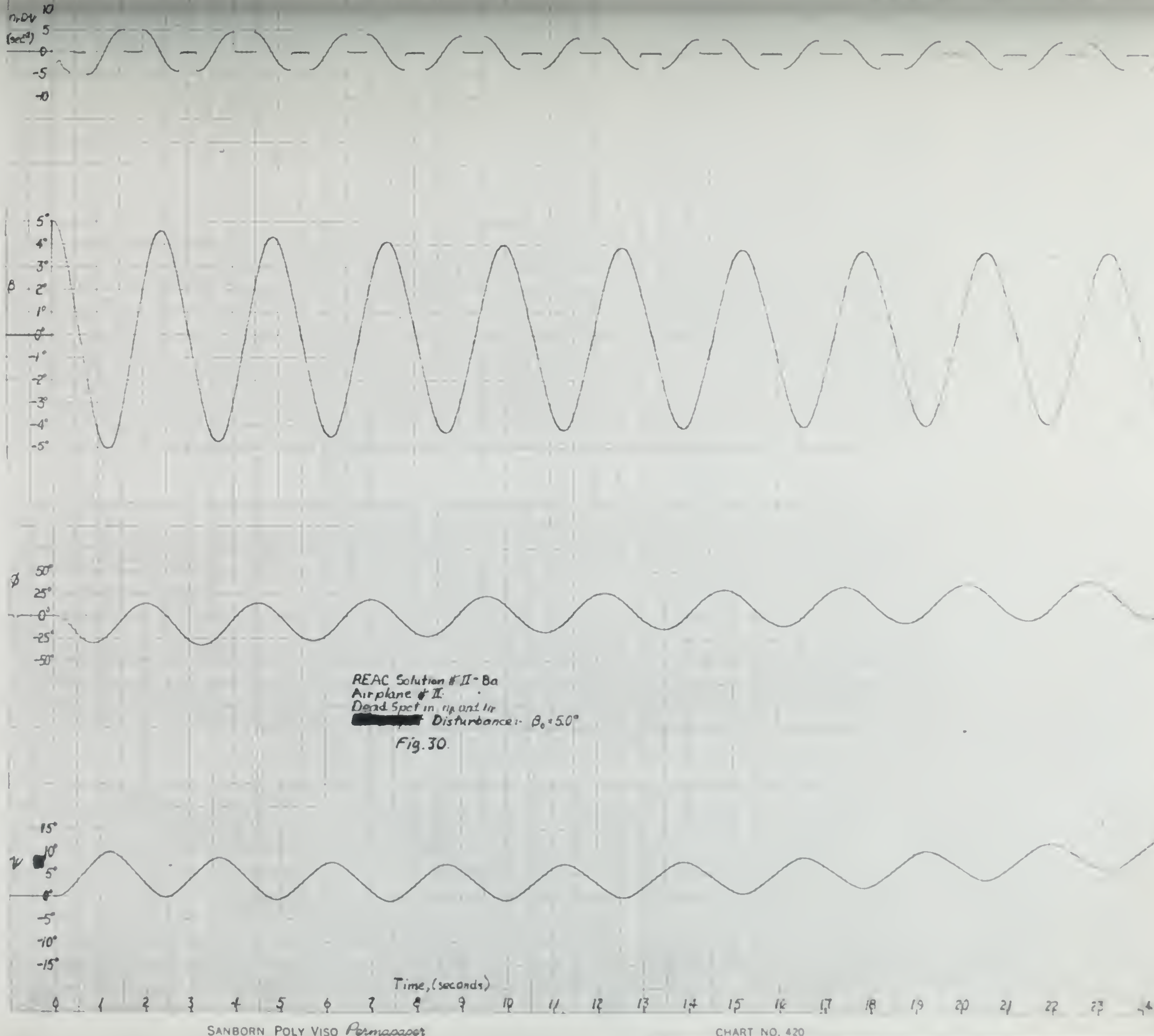

REAC Solution # II - Ba
Airplane # II
Dead Spot in r_p and l_r
[redacted] Disturbance: $\beta_0 = 5.0°$

Fig. 30.

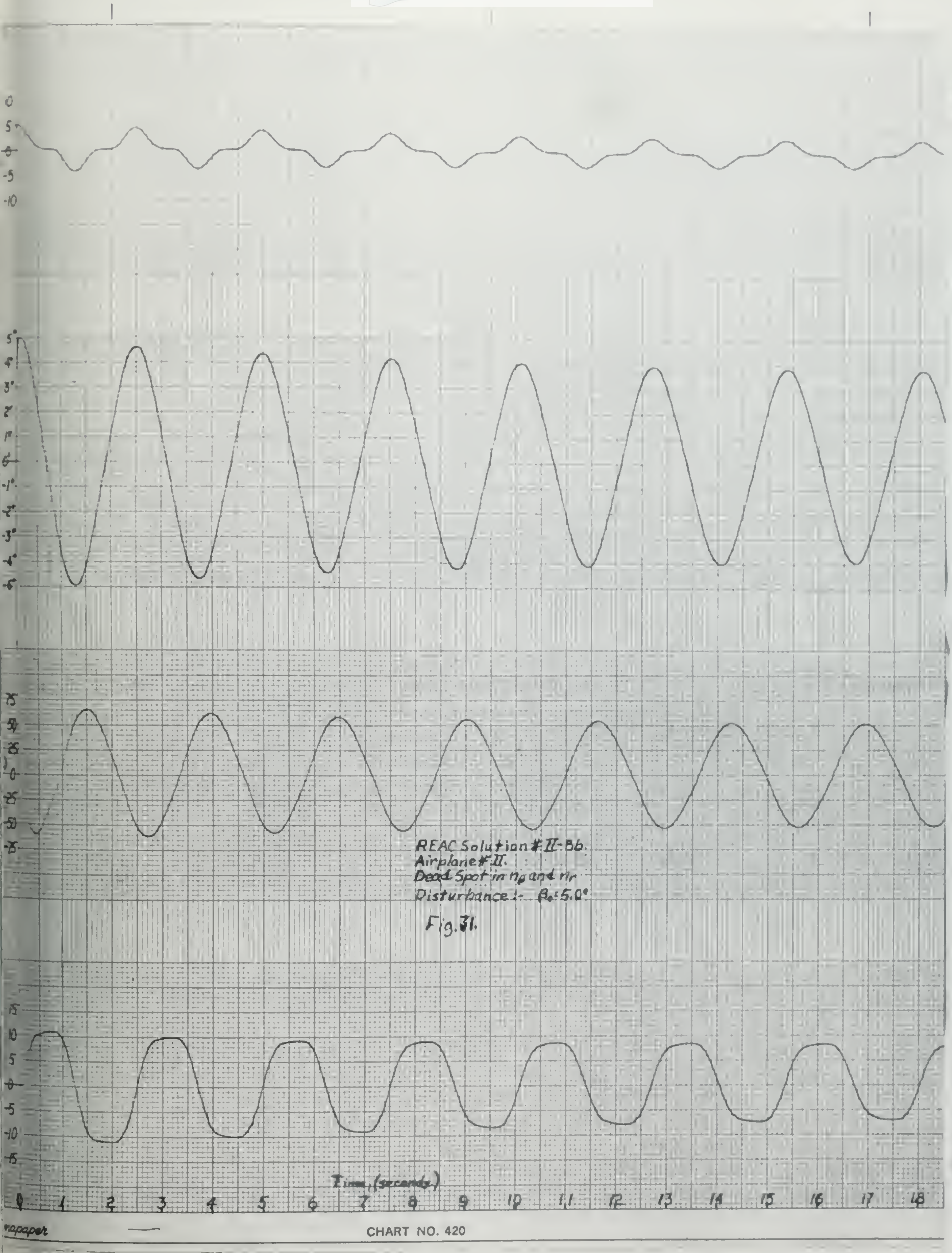
REAC Solution # II-Bb.
Airplane # II.
Dead Spot in n_p and n_r
Disturbance :- β_0 = 5.0°
Time, (seconds)
0 1 2 3 4 5 6 7 8 9 10 11 12 13 14 15 16 17 18
CHART NO. 420

Fig. 31.

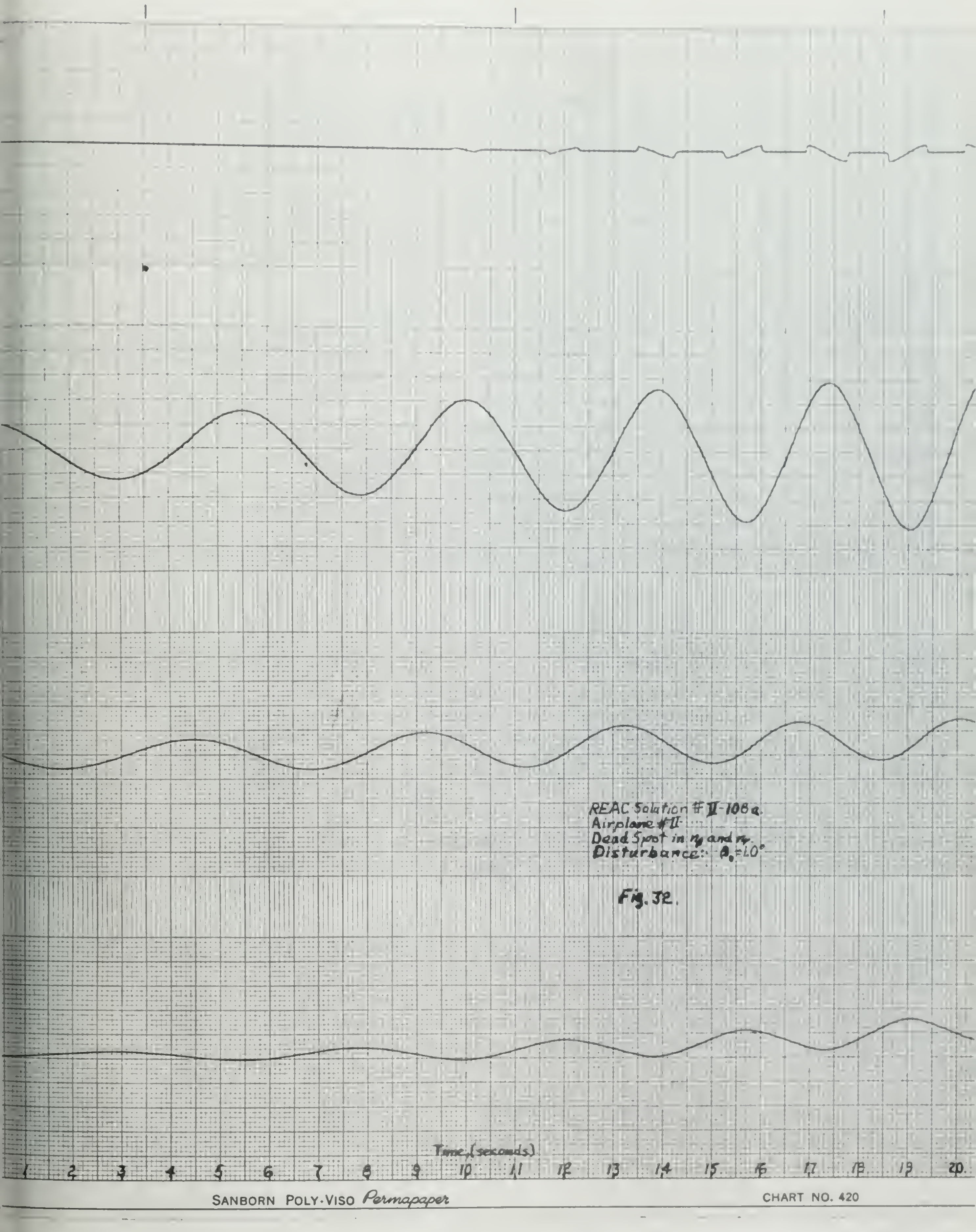
REAC Solution # II-108a.
Airplane # II
Dead Spot in r_y and r_x.
Disturbance: θ_0 = 1.0°
Time, (seconds)
1 2 3 4 5 6 7 8 9 10 11 12 13 14 15 16 17 18 19 20.
SANBORN POLY·VISO Permapaper
CHART NO. 420

Fig. 32.

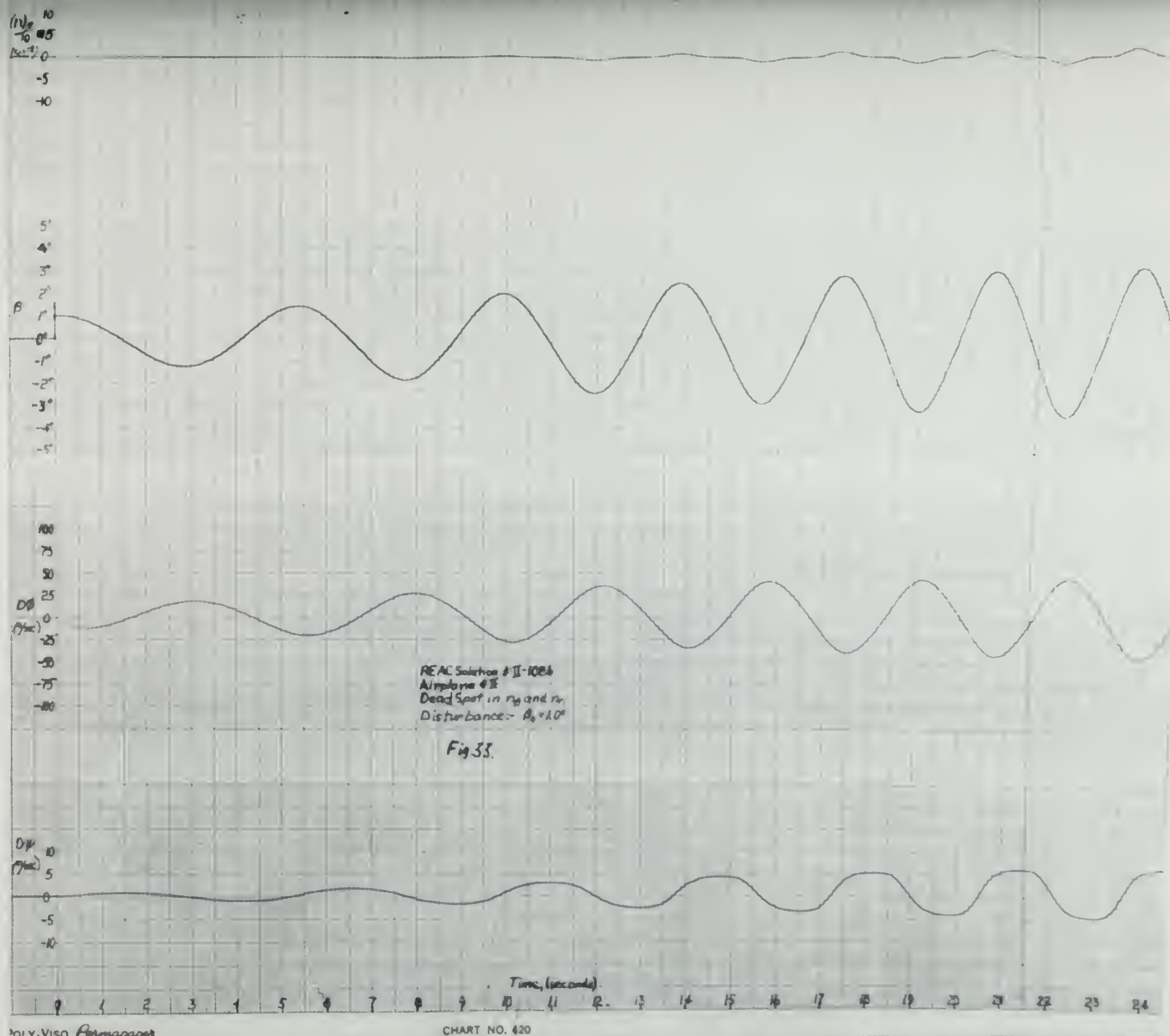
REAC Solution # II-1086
Airplane # II
Dead Spot in n_ϕ and n_r
Disturbance:- $\beta_0 = 1.0°$
Time, (seconds).
β
CHART NO. 420
POLY-VISO Permapaper

Fig 33.

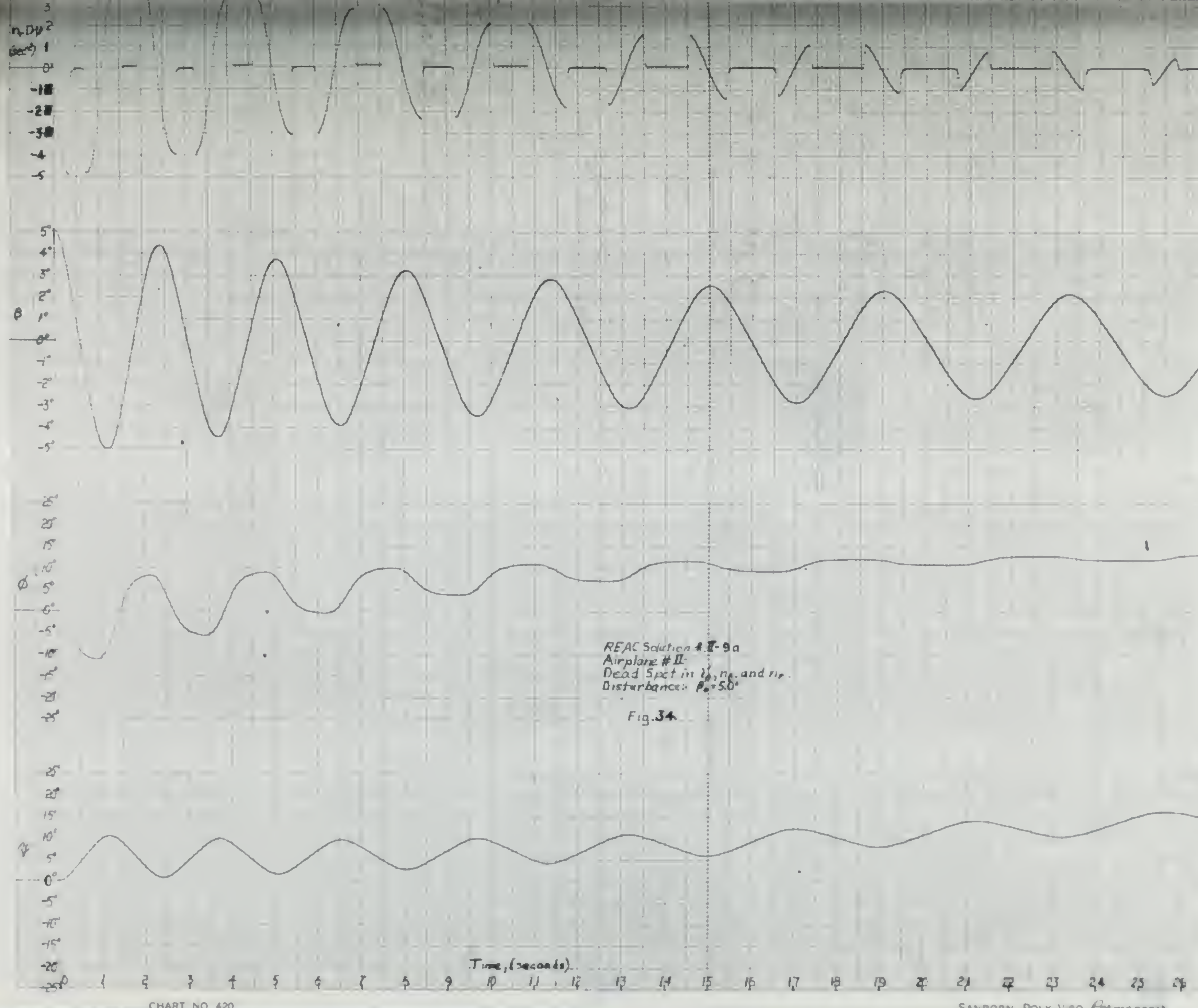

REAC Solution # II-9a
Airplane # II
Dead Spot in i_δ, n_r and n_p
Disturbance: β_0 = 5.0°
Time, (seconds)
CHART NO. 420
SANBORN POLY V 50 Permapaper

Fig. 34

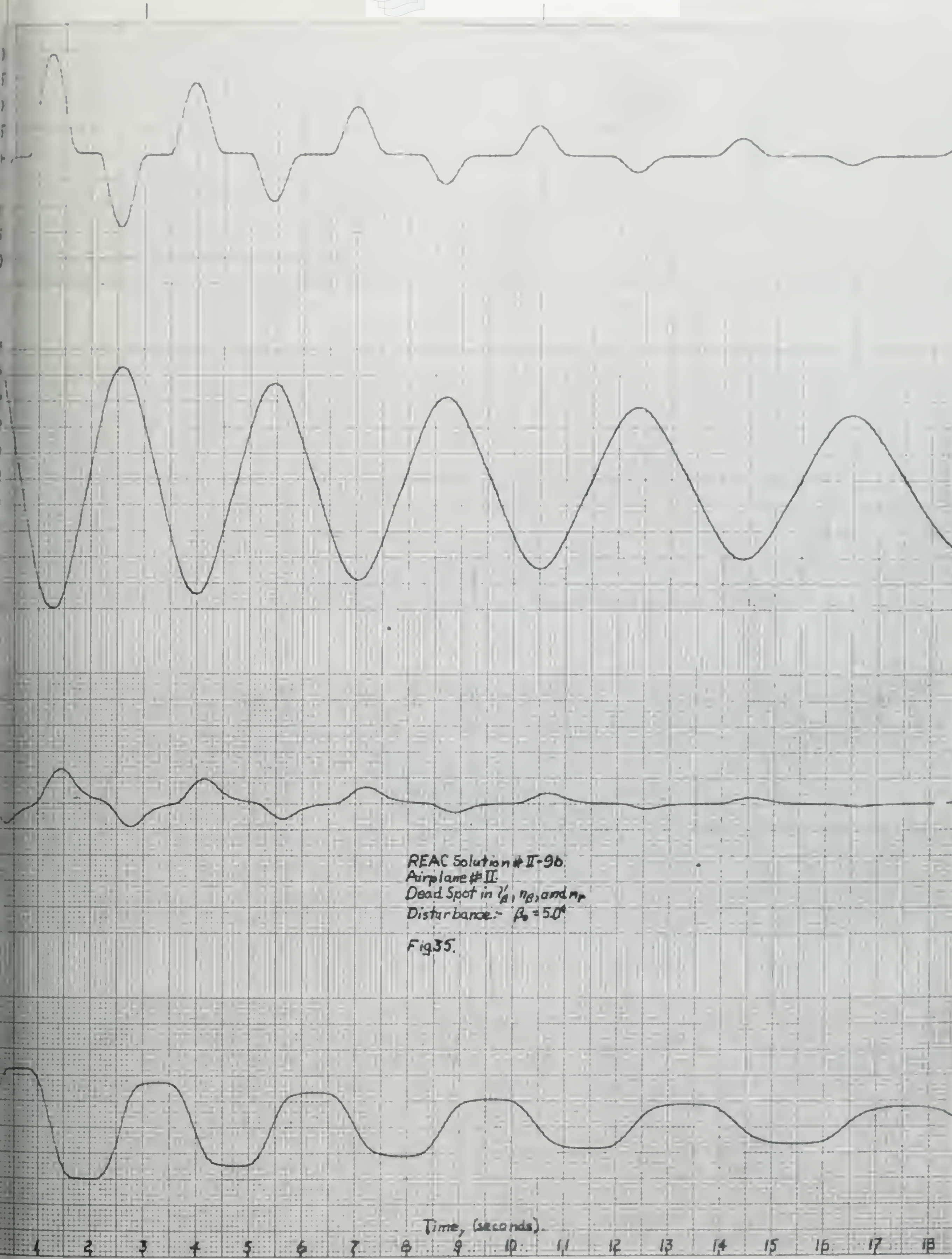

Fig. 35.

SANBORN POLY-VISO *Permapaper* CHART NO. 420

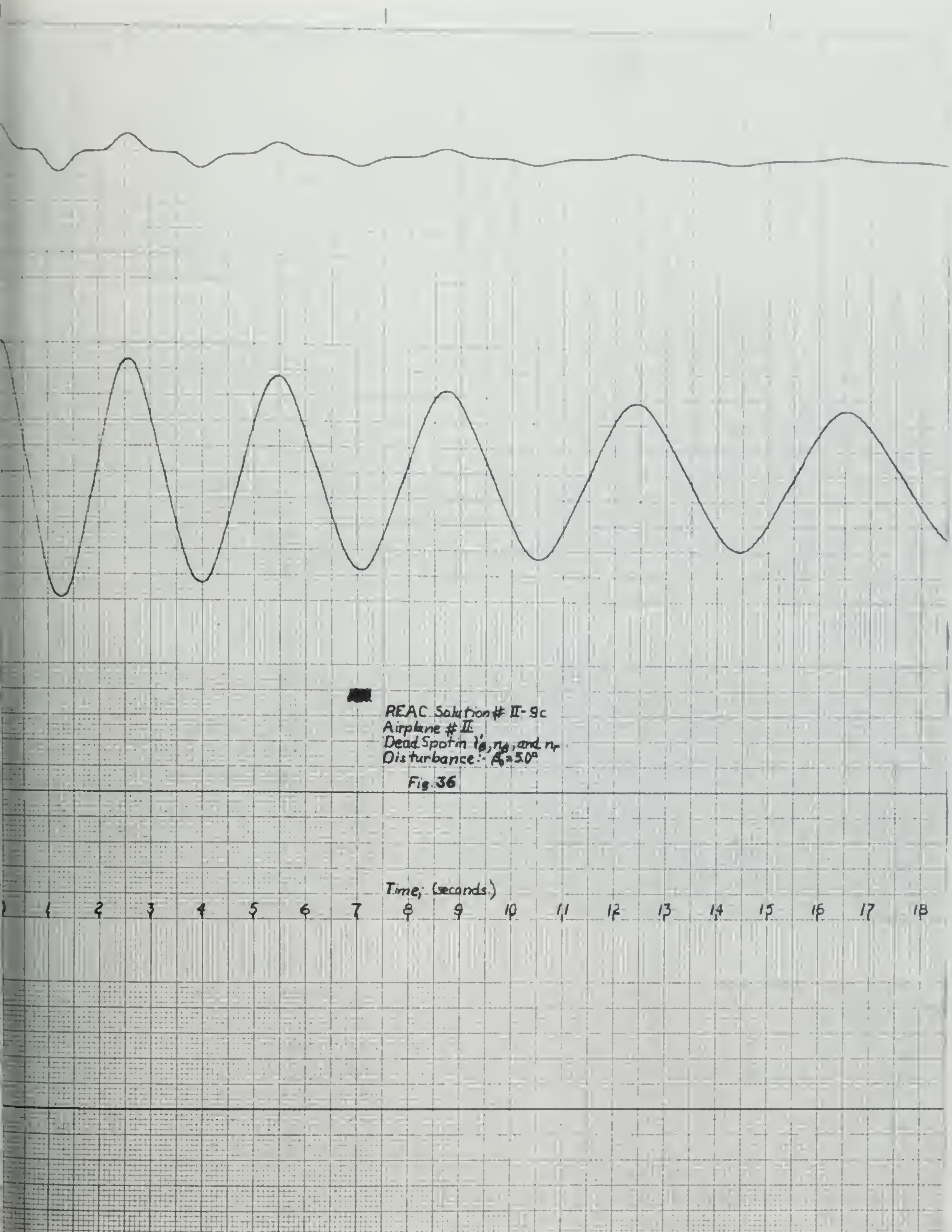
REAC Solution # II-9c
Airplane # II
Dead Spot in Y'β, nβ, and nr
Disturbance:- β0 = 5.0°
Time; (seconds)
1 2 3 4 5 6 7 8 9 10 11 12 13 14 15 16 17 18

Fig. 36

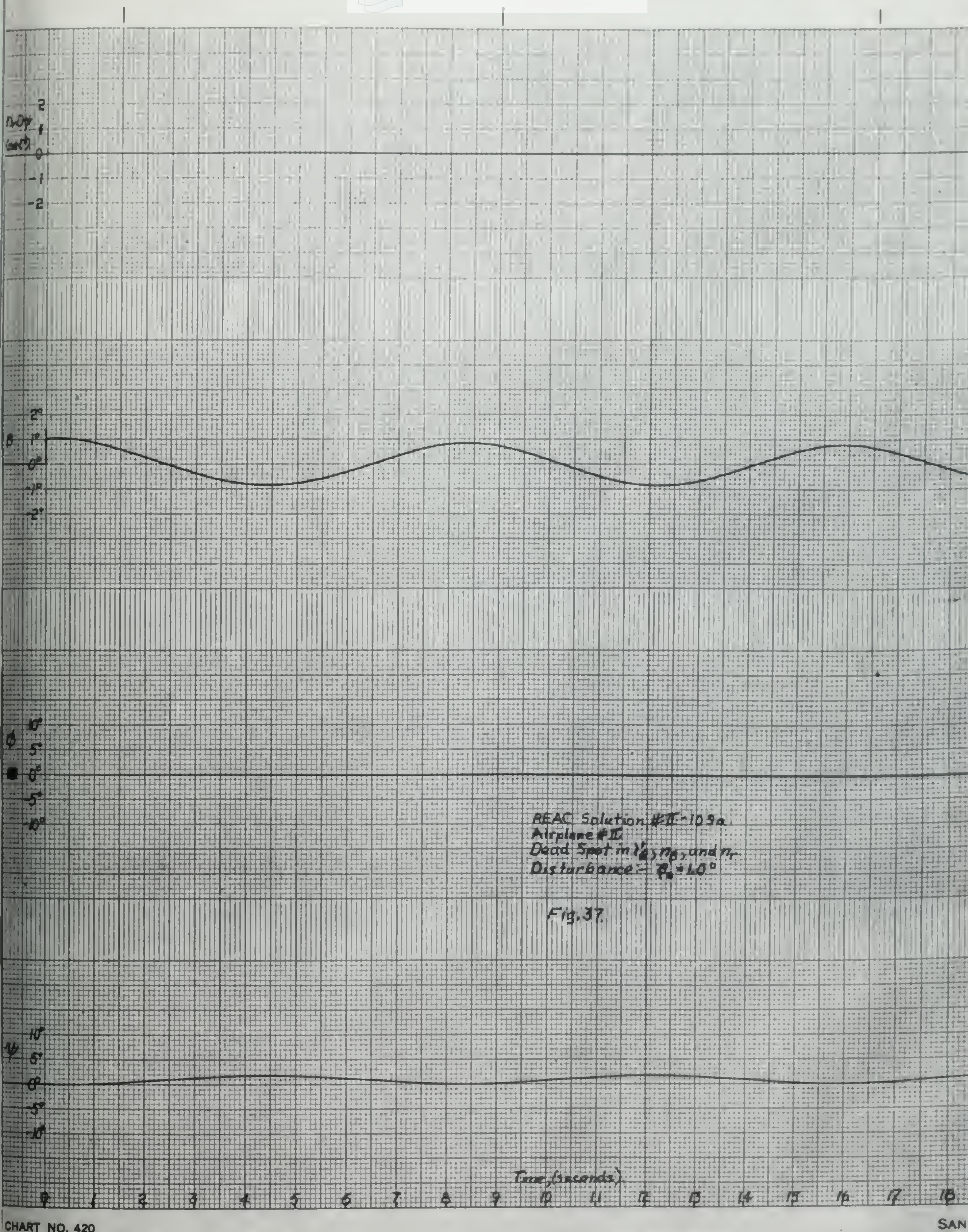
REAC Solution #II-109a
Airplane #II
Disturbance - β_0 = 1.0°
β
φ
ψ
Time (seconds)
0
1
2
3
4
5
6
7
8
9
10
11
12
13
14
15
16
17
18
CHART NO. 420

Fig. 37.

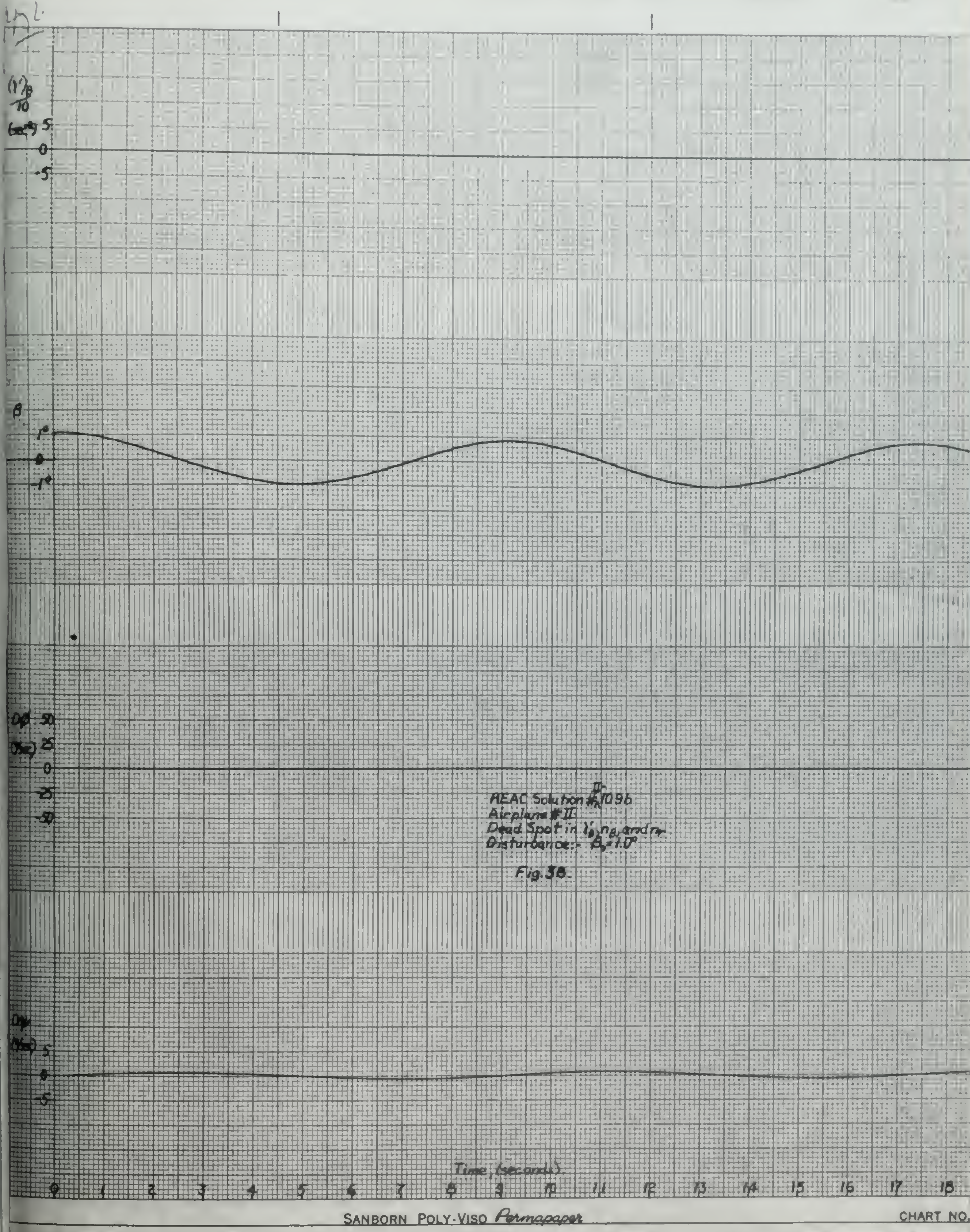
β
1°
0
-1°
5
0
-5
50
25
0
-25
-50
REAC Solution # 1096
Airplane # II
Dead Spot in Y_β, n_β and n_r
Disturbance:- $\beta_0 = 1.0°$
Time, (seconds)
0
1
2
3
4
5
6
7
8
9
10
11
12
13
14
15
16
17
18
SANBORN POLY-VISO Permapaper
CHART NO.

Fig. 38.

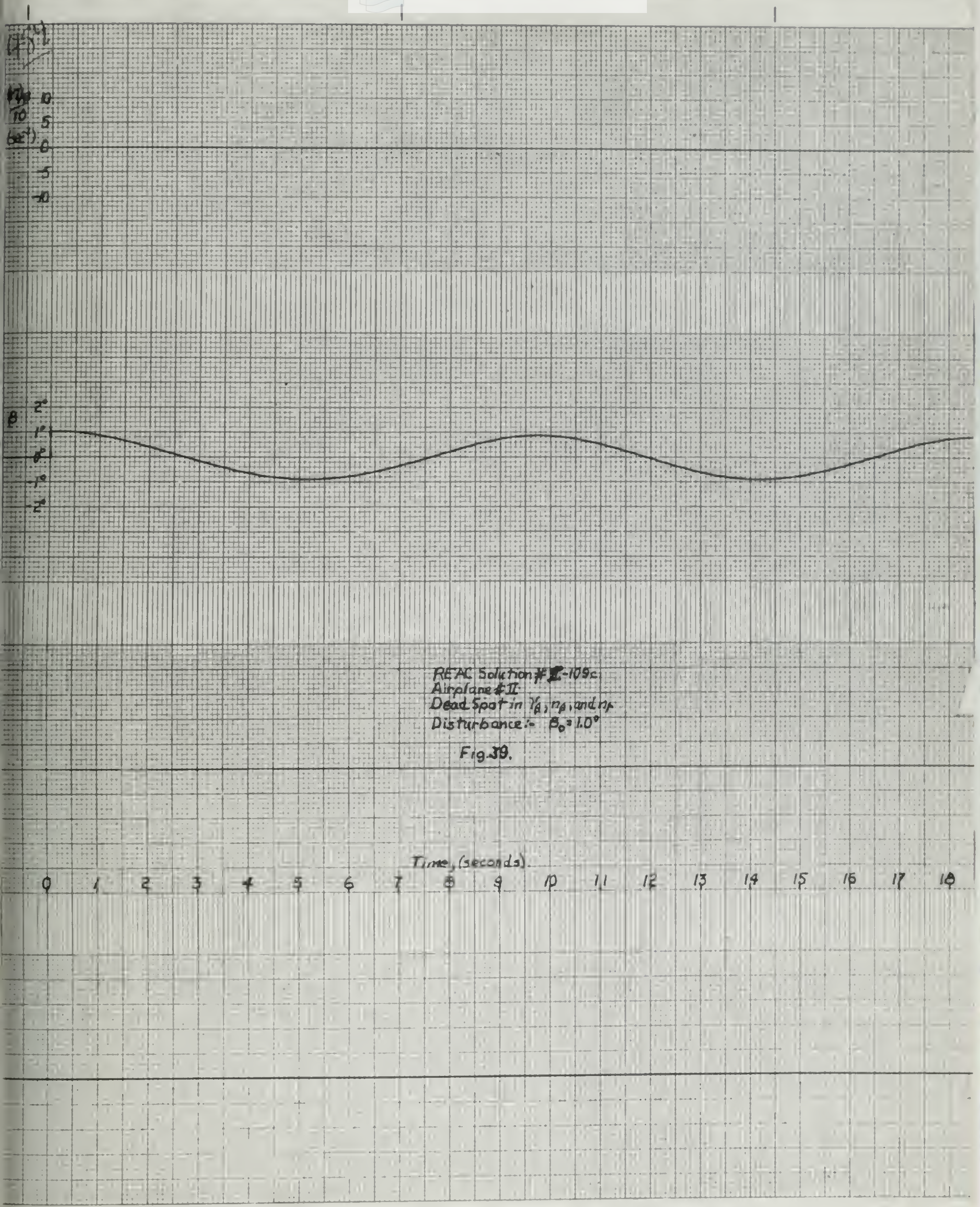
10
5
0
-5
-10
β
2°
1°
0°
-1°
-2°
REAC Solution # II-109c
Airplane # II
Dead Spot in Y_β, n_β, and n_r
Disturbance:- β_0 = 1.0°
Time, (seconds).
0
1
2
3
4
5
6
7
8
9
10
11
12
13
14
15
16
17
18

Fig. 39.

5/9

A study of the effect of some non-linear stability derivatives on the lateral motions of aircraft.

Thesis 16263
P69 Pollard
A study of the effect of some non-linear stability derivatives on the lateral motions of aircraft.

Thesis 16263
P69 Pollard
A study of the effect of some non-linear stability derivatives on the lateral motions of aircraft.